ISBN 978-82-326-4094-2 (printed ver.)
ISBN 978-82-326-4095-9 (electronic ver.)
ISSN 1503-8181

NTNU
Norwegian University of
Science and Technology

Jørgen Blindheim

Doctoral theses at NTNU, 2019:249

NTNU

NTNU
Norwegian University of Science and Technology
Thesis for the Degree of
Philosophiae Doctor
Faculty of Engineering
Department of Mechanical and Industrial
Engineering

Doctoral thesis

Doctoral theses at NTNU, 2019:249

Jørgen Blindheim

On Solid-State Deposition of Metal Structures

Conceptualization of a New Additive Manufacturing Method based on Hybrid Metal Extrusion & Bonding

NTNU
Norwegian University of
Science and Technology

Jørgen Blindheim

On Solid-State Deposition of Metal Structures

Conceptualization of a New Additive Manufacturing Method based on Hybrid Metal Extrusion & Bonding

Thesis for the Degree of Philosophiae Doctor

Trondheim, September 2019

Norwegian University of Science and Technology
Faculty of Engineering
Department of Mechanical and Industrial Engineering

NTNU
Norwegian University of
Science and Technology

NTNU
Norwegian University of Science and Technology

Thesis for the Degree of Philosophiae Doctor

Faculty of Engineering
Department of Mechanical and Industrial Engineering

© Jørgen Blindheim

ISBN 978-82-326-4094-2 (printed ver.)
ISBN 978-82-326-4095-9 (electronic ver.)
ISSN 1503-8181

Doctoral theses at NTNU, 2019:249

Printed by NTNU Grafisk senter

Preface

This doctoral thesis has been submitted to the Norwegian University of Science and Technology (NTNU) for the degree of Philosophiae Doctor (PhD). The work has been carried out at the Department of Mechanical and Industrial Engineering (MTP) under the supervision of Professor Martin Steinert and Professor Torgeir Welo. The research has been funded by NTNU and Napic (NTNU Aluminium Product Innovation Center).

Acknowledgment

I've worked as a whaler on the coast of Spitsbergen and as a seal hunter in the drift ice on Greenland's east coast. I've visited some high altitude summits and climbed a few steep and remote peaks. I thought I knew what voluntary suffering and first world problems were all about. Now, when finishing this thesis, I realize that there were still lessons to be learned in that regard. Luckily, the moments of breakthroughs and new insights easily compensate the suffering - the same mechanism that makes me look for new mountains to climb, despite the fact that it's gonna be exhausting and that my fingers are gonna get frozen, over again. Vanity and striving after wind. Yet, I'm thankful for having gotten the opportunity to walk this road. I feel blessed and privileged!

First of all, a huge thank you to Professor Martin Steinert, who has believed in me and supported and supervised me all the way - first through my master studies - and now also these years of PhD studies. I'm also deeply grateful to Professor Torgeir Welo for taking the time to co-supervise and give important input and guidance during this work.

I'd like to thank Professor Øystein Grong, the inventor of the HYB technology and the founder of Hybond. He has been a valuable resource in sharing his knowledge and, as importantly, giving honest feedback. I would also like to extend my thanks to Tor Austigard for sharing his practical knowledge of the HYB process. Moreover, advice given by Professor Henry Valberg on modelling of metal forming has been a great help in the final stages of the thesis work.

I've also received a lot of inspiration and help from many colleagues at the university. Thanks to Stephanie, Matilde, Carlo, Heikki, Achim, Jørgen, Andreas, Kristoffer, Henrikke, Emil, Steffen, Jan Magnus, Eivind, Sigmund, Kristin, Lise, Christer and all the other good colleagues here at MTP.

Running full-scale experiments for a new invention means that a lot of parts have to be produced. Hence, over the last years, I've got to spend quite a lot of time in the workshop. I did take some shortcuts - and I did break a few taps and mill bits. Still, I got to learn some new practical skills along the way. Thanks to Børge, Agnes, Carl-Magnus, Roar, Aleksander, Kurt, Nils-Inge and the rest of the crew in the workshop for your support.

Thanks to my loved family and my friends for being there for me all the time. And finally - more important than everyone and everything: Thank you Gunilla for your love, patience and support - the seemingly endless study is finally coming to an end. I promise to spend less time at the university and more time with you from now on.

Trondheim, September 2019

Jørgen Blindheim

Abstract

This thesis presents the conceptualization of a new solid-state process for additive manufacturing (AM) of extrudable metals and alloys. The process is based on the Hybrid Metal Extrusion & Bonding (HYB) technology and has been termed HYB-AM.

The main objective of this thesis has been to develop the HYB-AM process through concept evaluation and full-scale experimental testing, hence making it possible to assess the mechanical integrity of a deposited structure and understand the governing mechanisms of the process.

A novel set-based approach for concept evaluation has been developed and applied. The combination of rapid prototyping and physical modelling made it possible to test and evaluate multiple extruder and deposition concepts without having to build full-scale steel prototypes. Plastic models of the different extruder concepts were produced by rapid prototyping and attached to a small CNC-machine. To test the function of each design, plasticine was processed through the different extruders and deposited on the machine bed. Through the evaluation of all the modelled concepts the extruder design for full-scale testing was identified.

Full-scale experiments have been carried out for two different extruder designs. Through the fabrication of samples and the subsequent assessment of the layer bonding, the technical feasibility of the HYB-AM process has been conclusively demonstrated in producing mechanically sound 3D structures. The results from the mechanical testing display an ultimate tensile strength across the bonded layers approaching that of the substrate material, yet at lower elongation prior to fracture. Moreover, inspections of the fracture surfaces show evidence of extensive dimple formation. This indicates that metallic bonding is achieved between the layers. However, regions of kissing-bonds and lack of bonding are also present, thus calling for further process optimization.

A novel method for fabrication of tensile specimens for assessing the bond strength between the layers has been developed and applied. The miniature specimens are machined from the samples using a single thread milling tool. In this way, the specimens can be located such that the interface between separate layers crosses the reduced section of the specimens. This allows the bond strength between the layers to be tested in pure tension.

FEA has been used to study material flow in the extruder, as well as the conditions at the interfaces of the deposited extrudate and the substrate in order to identify and characterize the process parameters involved. Analysis of the material flow, shows that the extrusion pressure is virtually independent of the deposition rate. Furthermore, from the simulations of the material deposition sequence it is visible how the contact pressure at the interface will drop below the bonding threshold if the feed speed becomes too high relative to the material flow through the die.

The results obtained in this work, will be useful in the further development towards industrialization of the process. Although this work has demonstrated the process in full-scale and established an understanding of the process, further research is required prior to industrialization.

List of papers

Paper 1
Hybrid Metal Extrusion & Bonding (HYB) - a new technology for solid-state additive manufacturing of aluminium components.
Published in Procedia Manufacturing.
DOI: 10.1016/j.promfg.2018.07.092

Paper 2
Rapid prototyping and physical modelling in the development of a new additive manufacturing process for aluminium alloys.
Published in Procedia Manufacturing.
DOI: 10.1016/j.promfg.2019.06.212

Paper 3
Concept evaluation in new product development: A set-based method utilizing rapid prototyping and physical modelling.
Submitted to Journal of Engineering, Design and Technology

Paper 4
First demonstration of a new additive manufacturing process based on metal extrusion and solid-state bonding.
Accepted for publication in The International Journal of Advanced Manufacturing Technology.
DOI: 10.1007/s00170-019-04385-8

Paper 5
On the mechanical integrity of AA6082 3D structures deposited by hybrid metal extrusion & bonding additive manufacturing.
Under review in Journal of Materials Processing Technology

Paper 6
Investigating the Mechanics of Hybrid Metal Extrusion & Bonding Additive Manufacturing by FEA
Published in Metals.
DOI: 10.3390/met9080811

List of figures

1.1 The stages of the research project with an overview of the tasks leading to the appended papers. 3

2.1 Overview of single-step AM processing principles for metallic materials according to ISO/ASTM 52900:2015 (ASTM, 2015). 6

2.2 Schematic sketches of the SLA process: (1) ultraviolet rays; (2) mask; (3) solidified layers; (4) liquid photo-hardening polymer; (5) movable plate; (6) receptacle; (7) shutter; (8) optical fiber; (9) XY plotter and; (10) optical lens. Exposure and shift of the movable plate is repeated sequentially, and the solid model is grown on or under the plate (Kodama, 1981). 7

2.3 (a) Schematic illustration of the WAAM process which is a DED process based on the GTAW principle; (b) a near-net-shape structure built using the WAAM process (Williams et al., 2016). 8

2.4 (a) Schematic illustration of DED using laser melting (Frazier, 2014); (b) an example of a 3D-structure produced by laser directed energy deposition (Milewski et al., 1998). 9

2.5 (a) Schematic illustration of the DED process based on electron beam melting; (b) example of an AA2219 structure produced using the same process (M. B. Taminger and Hafley, 2003). . . . 9

2.6 (a) Schematic illustration of a PBF system; (b) photograph of topology optimized Ti-6Al-4V brackets for Airbus A350 before build plate and support structure is removed; (c) the finished part after the support structure is removed (Herzog et al., 2016). 10

2.7 (a) Schematic illustration of the Friction Stir Additive Manufacturing Process. In this case the rotating tool is inserted into the overlapping surfaces of sheets or plates to be joined and traversed along the joint line (Palanivel et al., 2015); (b) cross section of a structure created using the FSAM process (Palanivel et al., 2015). 11

2.8 (a) Schematic illustration of the additive friction stir process with continuous powder feeding (Schultz and Creehan, 2014); (b) a part created using the MELD process, before and after post-processing (Aeroprobe). 11

2.9 (a) Schematic illustration of the Ultrasonic Consolidation process; (b) photograph of a multi-material structure created from this process (Kulakov and Rack, 2009). 12

3.1 Schematic illustrations of different types of extrusion; (a) direct extrusion; (b) indirect extrusion; (c) indirect extrusion where the bottom plate of the container is removed; (d) continuous extrusion (Aakenes, 2013). 15

3.2 Schematic illustration of the journey leading to the current extruder design used for welding. Note that the design process has not followed a straight path, which is characteristic of many innovation processes (Steinert and Leifer, 2012). 16

3.4 Photographs of Prototype 4; (a) the extruder mounted in the experimental rig; (b) the wheel extruder from below, showing the drive shaft and the lower ends of the shoe and the extrusion wheel along with the abutment (Erlien and Grong, 2003). 16

3.5 (a) Schematic illustration of the single arm 45° revolving extruder (Prototype 5); (b) the complete extruder assembly used for experimental testing (Aakenes, 2013). 17

3.6 Illustrations of Version B1 of the HYB screw extruder; (a) section through the rotating extruder head with its moving dies, the stationary shoe and the abutment; (b) partially sectioned 3D-image of the extrusion head (Aakenes, 2013). 18
3.7 Conceptual design of the HYB spindle extruder (Aakenes, 2013). 19
3.8 (a) The HYB PinPoint extruder is built around a rotating pin provided with an extrusion head with a set of moving dies through which the aluminium is allowed to flow; (b) cross section of a HYB weld with a weld reinforcement on the top (Blindheim et al., 2018). 19
3.9 Schematic illustration of the deposition sequence used to test the HYB-AM concept (Blindheim et al., 2018). 21
3.10 Photographs of the layered structure produced using the HYB-AM method (Blindheim et al., 2018). 22
3.11 Deposition rates for HYB-AM compared to UAM and WAAM for aluminium feed stock (Blindheim et al., 2018). 22

4.1 Experimental setup for the physical modelling testing. 24
4.2 Experimental setup for the full-scale testing of the HYB-AM process. A Sieg CNC milling machine was rebuilt for this purpose. 25
4.3 Final version of the extruder prototype; (a) as seen from underneath; (b) the die that also is used to scrape the under-laying surfaces. 25

5.1 Chapter structure and overview of the papers included in the thesis 27
5.2 Deposition strategy based on the use of two separate PinPoint extruders; (a) first the protruding stringer beads are deposited using the first extruder, keeping the spacing between them fixed; (b) then the gaps are filled using the second extruder (Blindheim et al., 2018) 28
5.3 Set of alternative extrusion and deposition concepts (C1 - C4) that have been evaluated during the case study; (a1) C1: PinPoint extruder with flat pin; (a2) C1: PinPoint extruder with protruding pin; (b) C2: wheel extruder; (c) C3: Spindle Extruder (d) C4: Rotating die extruder; all of these extruders are based on the wire fed continuous rotary extrusion process. 31
5.4 Optical macrographs of; (a) a transverse section of a deposited structure; (b) pore formation at the interface between two adjacent stringers; (c) cracks on the interface between the substrate and a stringer. 35
5.5 Illustration of the first version of the extruder. The spindle constitutes the fourth wall of the die and makes for the shortest possible die length of the designs; (a) a possible deposition sequence where the die is used as an oxide scraper; (b) section through the spindle and die. The spindle is tilted to reduce interference with the substrate. 36
5.6 Principal illustrations of the second version of the extruder; (a) the extruder consists of a wheel with a groove surrounded by a stationary housing. The feedstock wire is pressed into the groove, and upon rotation the extrusion pressure is built up as the material is blocked by an abutment close to the die. The die also act as a scraper in order to remove oxides from the substrate prior to bonding with the extrudate; (b) rendering of the extruder and a deposited structure. 38
5.7 Tensile specimens used for testing of the substrate material and the layered structure. 38
5.8 Optical micrographs of; (a) section of a deposited structure along with the superimposed contours of the tensile specimens; (b) the bonding interface between the substrate and the first layer; (c) and (d) voids observed at the interface between two stringers. 39
5.9 SEM fractographs of fracture surfaces from three broken specimens. The corresponding tensile test results are plotted in Figure 5.10; (a) fracture surface of specimen B3; (b) fracture surface of specimen B4; (c) fracture surface of substrate specimen S1; (d) mixed region with kissing-bond and dimple formation in specimen B4; (e) dimpled fracture surface observed in specimen B3, and; (f) dimpled fracture surface observed in specimen S3. 40

5.10 Engineering stress vs. displacement curves for different tensile specimens. Four specimens, B1-B4, crossing two bonded layers, and three specimens representing the substrate material, S1-S3. 40
5.11 Normal pressure in the extrusion grip zone; (a) rotational speed 4 RPM; (b) Rotational speed 50 RPM. 43
5.12 Effective stress during deposition at 500°C; (a) balanced ratio - after 1.2s the die cavity is filled and the feeding has started; (b) balanced ratio - after 5s a pocket is formed in the front section of the die; (c) high ratio - after 1.2s the die cavity is filled. (d) high ratio - after 5s the die cavity is still full and the effective stress has increased. 44
5.13 Normal pressure in a section through the die transverse to the feed direction; (a) balanced speed ratio; (b) high speed ratio, 20% over-extrusion. 44

List of tables

2.1 Overview of AM processes covered in Chapter 2. 6

3.1 Characteristics of Ultrasonic Additive Manufacturing (UAM) and Wire Arc Additive Manufacturing (WAAM) when used for aluminium alloys (Blindheim et al., 2018). 20
3.2 Parameters used for the initial proof-of-concept experiment (Blindheim et al., 2018). 21

4.1 Chemical compositions of AA6082 feedstock wire (F) and substrate plate (S). 26

List of symbols

Abbreviations

AFS	Additive Friction Stir, the former name of MELD
AM	Additive manufacturing
BTF	Buy-to-fly; Blank weight vs. finished part weight
CAD	Computer-Aided Design
CMT	Cold Metal Transfer
CNC	Computer Numerical Control
CPW	Cold Pressure Welding
CRE	Continuous rotary extrusion
DED	Directed Energy Deposition
DLF	Directed Light Fabrication
DMD	Direct Metal Deposition
DMLS	Direct Metal Laser Sintering
EBF^3	Electron Beam Freeform Fabrication
EBM	Electron Beam Melting
FDAM	Friction Deposition Additive Manufacturing
FDM	Fused deposition modelling
FEA	Finite Element Analysis
FEM	Finite Element Method
FSAM	Friction Stir Additive Manufacturing
FSW	Friction Stir Welding
GMAW	Gas Metal Arc Welding
GTAW	Gas Tungsten Arc Welding
HAZ	Heat Affected Zone
HYB	Hybrid Metal Extrusion & Bonding

LBFF	Laser Based Flexible Fabrication
LC	Laser Consolidation
LENS	Laser Engineered Net Shaping
MELD	Name of a solid-state AM process
PAW	Plasma Arc Welding
PBF	Powder Bed Fusion
SEM	Scanning Electron Microscope
SLM	Selective Laser Melting
SLS	Selective Laser Sintering
SL	Sheet Lamination
STL	Stereolithography, A file format used for preparing CAD models for AM
UAM	Ultrasonic Additive Manufacturing
UC	Ultrasonic Consolidation
WAAM	Wire Arc Additive Manufacturing

Symbols

ΔT	Temperature change
η	Efficiency
τ	Frictional stress
c	Specific heat capacity
k	Shear yield stress
M	Torque
m	Friction factor
N	Rotational speed
Q	Heat
s	Distance
W_i	Work
σ_y	Yield strength
$\mathbf{p}$	Contact pressure

Table of contents

Preface I

Acknowledgment III

Abstract V

List of papers VII

List of figures IX

List og tables XII

List of symbols XIII

1 Introduction 1
- 1.1 Background 1
  - 1.1.1 What is additive manufacturing? 1
  - 1.1.2 Melted-state vs. solid-state processing of aluminium alloys 1
  - 1.1.3 The problem 2
- 1.2 Research objectives and methods 2
- 1.3 Scope of work 2

2 Additive manufacturing of metals 5
- 2.1 General 5
- 2.2 Process categorization 5
- 2.3 Early history of additive manufacturing 6
- 2.4 Melted-state processes 7
  - 2.4.1 Directed Energy Deposition based on arc welding 7
  - 2.4.2 Directed Energy Deposition based on laser melting 8
  - 2.4.3 Directed Energy Deposition based on electron beam melting 9
  - 2.4.4 Powder Bed Fusion based on laser welding 10
- 2.5 Solid-state processes 10
  - 2.5.1 Friction Stir AM 10
  - 2.5.2 MELD 11
  - 2.5.3 Ultrasonic Consolidation AM 12
  - 2.5.4 Friction Deposition AM 12

3 The Hybrid Metal Extrusion & Bonding process 13
- 3.1 General 13
- 3.2 Bonding mechanisms 13
- 3.3 Extrusion principle 14
- 3.4 HYB technology development 15

3.4.1 Wheel extruder . . . 15
3.4.2 Screw extruder . . . 17
3.4.3 Spindle extruder . . . 18
3.4.4 PinPoint extruder . . . 18
3.5 The feasibility of using the HYB process for additive manufacturing . . . 19
3.5.1 Benchmarking . . . 19
3.5.2 Proof-of-concept . . . 21
3.5.3 Potentials . . . 22

4 Research method and equipment 23
4.1 General . . . 23
4.2 Methods . . . 23
4.3 Experimental setup for concept evaluation . . . 23
4.4 Experimental setup for full-scale testing . . . 24
4.5 Filler wire and substrate material . . . 26
4.6 Microscopy analysis . . . 26

5 Present contributions 27
5.1 General . . . 27
5.2 Paper 1 . . . 28
5.3 Paper 2 . . . 30
5.4 Paper 3 . . . 33
5.5 Paper 4 . . . 34
5.6 Paper 5 . . . 37
5.7 Paper 6 . . . 42

6 Conclusions and suggestions for future work 47
6.1 Conclusion on the main objective . . . 47
6.2 Task-based conclusions . . . 47
6.3 Industrial and academic implications . . . 48
6.4 Recommendations for further work . . . 48

Bibliography 51

Appendix 55

1. Introduction

1.1 Background

1.1.1 What is additive manufacturing?

Additive manufacturing (AM) can be defined as the process of joining materials to make 3D structures, usually layer upon layer, as opposed to subtractive manufacturing methodologies (ASTM, 2015). AM is also known under terms like additive fabrication, solid freeform fabrication, additive layer manufacturing and 3D-printing. The last-mentioned is probably the term most people are familiar with and is a general term covering both manufacturing and rapid prototyping.

Over the past years AM of metals has seen massive research interest along with a gradual adoption by the industry. The use of this technology is claimed to enable new ways of designing products as well as opening for mass customization of parts at reduced energy consumption and with less material waste compared to subtractive processes. A wide range of AM processes exists, each with its individual characteristics when it comes to parameters like feedstock materials, part complexity, deposition rates, form of feedstock material, source of fusion or state of fusion (solid-state or melted-state). State of fusion is of particular interest regarding processing of aluminium alloys.

1.1.2 Melted-state vs. solid-state processing of aluminium alloys

In the melted-state category, the use of aluminium has been limited to only a few alloys due to the resulting microstructure from melting. Furthermore, many melted-state processes suffer from reduced deposition rates due to limitations in the melt pool size. In addition, the contractions occurring during solidification and subsequent cooling can lead to build-up of residual stresses in the structure, hence, causing global deformations and distortions (Blindheim et al., 2018).

Solid-state processes, on the other hand, have no such limitations in deposition rates, as long as the processing temperature is kept below the melting temperature of the material. This makes solid-state processes attractive for manufacturing of larger components. In addition, it enables the use of the advanced aluminium alloys.

In the solid-state category, we find processes based on ultrasonic consolidation of sheets and foils, as first demonstrated by White (2003). Lately, ultrasound has also been used for joining of wire feedstock material (Deshpande and Hsu, 2018). Another solid-state process used for AM purposes is Friction stir welding (FSW), which has been demonstrated for joining of stacked metal plates (Palanivel et al., 2015). Also, a modified FSW process, where the feedstock is added through a rotating stirring tool, has been developed by Aeroprobe (Schultz and Creehan, 2014). In addition, a process based on friction welding, where the material is deposited onto the substrate using a rotating consumable rod has been developed (Dilip et al., 2011). Among these processes, currently no high-deposition-rate solid-state process that uses wire feedstock material does exist.

1.1.3 The problem

Hybrid Metal Extrusion & Bonding (HYB) technology is a solid-state welding process for joining of aluminium plates and profiles (Grong, 2006, 2012). Because the HYB technology involves the use of filler metal additions, it also has the potential of being used for AM of near-net-shape structures. In the work presented herein, the industrial potential of developing such a process, termed HYB-AM, has been explored through concept evaluation and full-scale testing.

1.2 Research objectives and methods

The main objective of the thesis is as follows:

> To develop the HYB-AM process through concept evaluation and full-scale experimental testing, making it possible to assess the mechanical integrity of a deposited structure and understand the governing mechanisms of the process.

In order to target the main objective, the work has been divided into the following tasks:

- To provide an overview of the current additive processes for metals (Chapter 2);
- To review the HYB-technology and its related earlier work (Chapter 3);
- To assess the industrial potential of developing the HYB-AM process (Chapter 3, Paper 1);
- To evaluate possible extruder designs (Paper 2);
- To conduct full-scale experimental testing (Paper 4, Paper 5);
- To assess the mechanical integrity of deposited samples (Paper 5);
- To investigate the material flow of the process (Paper 6).

These tasks are approached through concept evaluation using rapid prototyping and physical modelling, full-scale experiments, mechanical testing and numerical simulations. The results of this work are provided in six scientific articles. Each individual paper furthermore has its own defined objectives that contribute to the main objective of this thesis.

1.3 Scope of work

The main focus of this thesis has been the conceptualization of this new material deposition method. The range of technical challenges in this project is large and only the most important challenges have therefore been subjected to investigation. The main stages of the project have been: (1) Concept evaluation and development; (2) Full-scale testing and; (3) Optimization and interpretation of the governing mechanisms. Figure 1.1 provides an overview of the present contributions and the progress leading up to the individual papers.

A total of four different extruder concepts have been evaluated. This has been done through a novel approach based on the combination of physical modelling and rapid prototyping. Rapid prototyping was used to produce low-cost plastic models for the different concepts, and plasticine feedstock material was subsequently used to model the metal flow during operation.

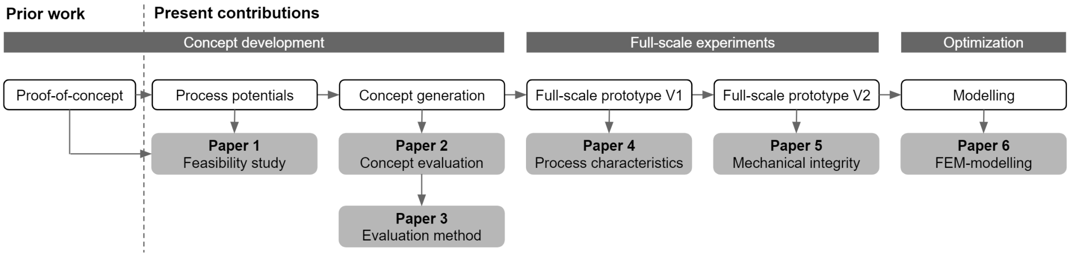
Prior work
Present contributions
Concept development
Full-scale experiments
Optimization
Proof-of-concept
Process potentials
Concept generation
Full-scale prototype V1
Full-scale prototype V2
Modelling
Paper 1
Feasibility study
Paper 2
Concept evaluation
Paper 4
Process characteristics
Paper 5
Mechanical integrity
Paper 6
FEM-modelling
Paper 3
Evaluation method

Figure 1.1: The stages of the research project with an overview of the tasks leading to the appended papers.

Full-scale experiments have been conducted for two extruder designs, and samples produced by the process have been subject for visual inspection and mechanical testing through a novel tensile test method.

One of the most important still remaining challenges after this work is to further improve upon the layer-to-layer bonding. The preliminary mechanical testing has displayed variable bond quality, ranging from lack of bonding to full metallic bonding. Still, for the process to be widely adopted by the industry, the bond quality needs to be fully consistent. Moreover, the use of other feedstock materials as well as post-processing strategies need to be addressed in future studies. The thesis is organized as follows:

Chapter 2	aims at mapping the current landscape of AM-processes for metals;
Chapter 3	introduces the HYB welding technology and discusses the feasibility and potential of using HYB technology for AM purposes;
Chapter 4	presents the methods and experimental equipment;
Chapter 5	provides an overview of the most important results and contributions derived from the appended papers;
Chapter 6	presents the overall conclusions and recommendations for further work;
Appendix	contains the six papers which this thesis is built upon:

Paper 1
Hybrid Metal Extrusion & Bonding (HYB) - a new technology for solid-state additive manufacturing of aluminium components.

Paper 2
Rapid prototyping and physical modelling in the development of a new additive manufacturing process for aluminium alloys.

Paper 3
Concept evaluation in new product development: A set-based method utilizing rapid prototyping and physical modelling.

Paper 4
First demonstration of a new additive manufacturing process based on metal extrusion.

Paper 5
On the mechanical integrity of AA6082 3D structures deposited by hybrid metal extrusion & bonding additive manufacturing.

Paper 6
Investigating the Mechanics of Hybrid Metal Extrusion & Bonding Additive Manufacturing by FEA.

2. Additive manufacturing of metals

2.1 General

This chapter provides an overview of current AM processes. The overview is not complete, yet it is included to display the diversity of processes and also show that there are still undiscovered areas within this field.

AM technology can be applied to a wide range of materials, including metals, ceramics, polymers and composites. In this chapter, the focus will be on the processes used for metals and alloys in accordance with the ASTM categorization illustrated in Figure 2.1. These are processes that use metal feedstock either in the form of powder, wire or sheets, and where the feedstock is fused together to create a 3D structure (ASTM, 2015). There are also AM processes that use metal powder and a binder material to create green-bodies that need to be heated and compressed to sinter into solid components. However, these processes are not included in this overview.

2.2 Process categorization

AM of metals is by ASTM divided into three distinct categories when it comes to process; Powder Bed Fusion (PBF), Directed Energy Deposition (DED) and Sheet Lamination (SL) (ASTM, 2015), see Figure 2.1.

In PBF the part is created by fusing metal powder together, where the heat is supplied from a laser beam or an electron beam (Murr et al., 2012). During processing, the part is supported by the unconsolidated powder, thus giving great design freedom and the possibility to create detailed and complex shapes that are otherwise impossible to manufacture. However, the deposition rate is low, and the part size is limited by the powder bed size.

DED processes use heat sources like plasma, electric arc, laser or electron beam to fuse the feedstock material. However, for these processes, the material is supplied continuously at the point of fusion. When using an electron beam to melt the feedstock, the process needs to run in a low-pressure environment, and the part size will thus be limited to that of the build chamber. Other heat sources typically use shielding gas to protect the molten metal, and in these cases, the part size is only limited by the motion range of the robotic system being used. Parts created from DED usually require post-processing in terms of milling to obtain the final shape.

SL processes, unlike the formerly mentioned processes, are based on solid-state bonding of the feedstock material. The bonding is typically created from ultrasound or friction stirring. Since these processes operate at temperatures below the melting point of the material, they provide the potential of depositing material at higher rates without risking melt-down of the deposited structure. The SL-processes permit manufacturing of larger components and do not require the use of shielding gas or a vacuum environment.

In the remainder of this chapter, a description of some of the individual processes will be given. An overview of the processes included in this chapter is given in Table 2.1. However, before going into the details a brief

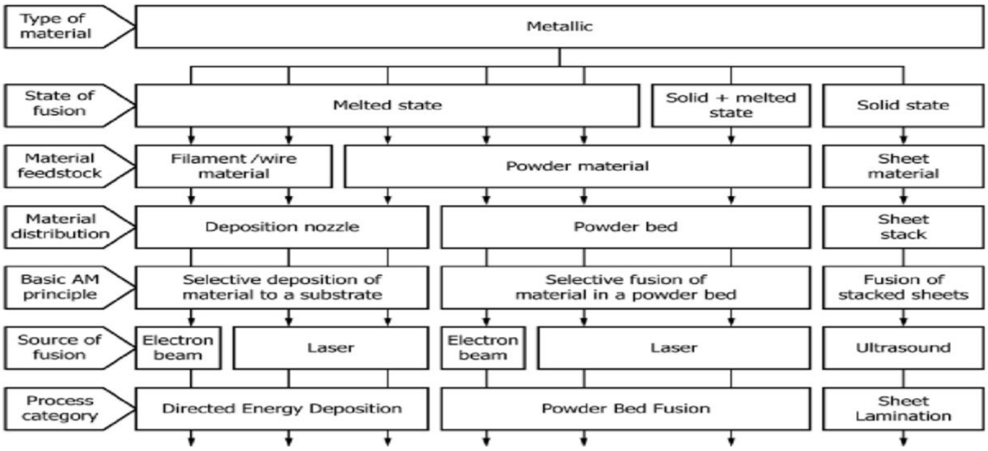
Type of material
Metallic
State of fusion
Melted state
Solid + melted state
Solid state
Material feedstock
Filament /wire material
Powder material
Sheet material
Material distribution
Deposition nozzle
Powder bed
Sheet stack
Basic AM principle
Selective deposition of material to a substrate
Selective fusion of material in a powder bed
Fusion of stacked sheets
Source of fusion
Electron beam
Laser
Electron beam
Laser
Ultrasound
Process category
Directed Energy Deposition
Powder Bed Fusion
Sheet Lamination

Figure 2.1: Overview of single-step AM processing principles for metallic materials according to ISO/ASTM 52900:2015 (ASTM, 2015).

history of additive manufacturing will be presented in the following section.

Table 2.1: Overview of AM processes covered in Chapter 2.

Category	Process name	Source of fusion	Feedstock	Ref
DED	WAAM	GMAW GTAW PAW	Wire	(Ding et al., 2015)
	LC	Laser	Powder	(McGregor et al., 2003)
	LENS	Laser	Powder	(Atwood et al., 1998)
	DMD	Laser	Powder	(Mazumder et al., 1997)
	LBFF	Laser	Powder	(Jiang and Molian, 2002)
	DLF	Laser	Powder	(Lewis et al., 1994)
	EBF	Electron Beam	Wire	(M. B. Taminger and Hafley, 2003)
PBF	SLM	Laser	Powder	(Louvis et al., 2011)
	DMLS	Laser	Powder	(Fulcher et al., 2014)
	EBM	Electron Beam	Powder	(Murr et al., 2012)
SL	UC	Ultrasound	Sheet	(White, 2003)
	FSW	Friction stir	Sheet	(Palanivel et al., 2015)
	FDAM	Friction welding	Sheet	(Dilip et al., 2011)
	MELD	Friction stir	Powder or bar	(Schultz and Creehan, 2014)

2.3 Early history of additive manufacturing

The first publication of an AM process dates back to 1981 when Hideo Kodama of Nagoya Municipal Industrial Research Institute (Kodama, 1981) presented a way to create a solid model by using UV-light to harden a photo-hardening liquid polymer layer by layer. The principle is shown in Figure 2.2. He writes that the operations are simple and can be easily automated.

In 1984, the French inventors Alain Le Méhauté, Olivier de Witte, and Jean Claude André filed a patent based on the same process. However, the application was rejected by the French General Electric Company because of lack of business perspective.

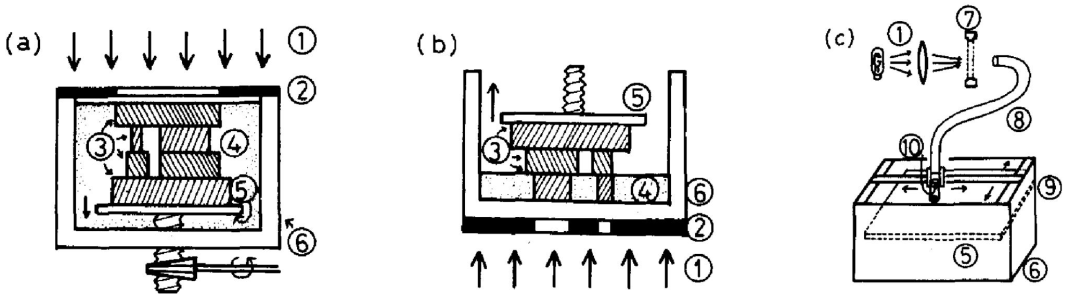

Figure 2.2: Schematic sketches of the SLA process: (1) ultraviolet rays; (2) mask; (3) solidified layers; (4) liquid photo-hardening polymer; (5) movable plate; (6) receptacle; (7) shutter; (8) optical fiber; (9) XY plotter and; (10) optical lens. Exposure and shift of the movable plate is repeated sequentially, and the solid model is grown on or under the plate (Kodama, 1981).

Charles Hull had better luck when he filed his patent based on the same process three weeks later (Hull, 1986). Hull's contribution was the Stereolithography (STL) file format and a way to create slices and infill strategies for the automated fabrication process. The STL file format is still being used today to provide geometrical input to many AM-processes.

The AM technology that most people are familiar with today is the fused deposition modelling (FDM) process for polymers which is widely available also on the consumer market. The FDM process was developed in 1988 and later commercialized by Stratasys, who started to market their first machines in 1992 (Crump, 1992).

AM-processes for metals have gradually been developed over the same time period. The first metal AM processes were based on laser fusion or sintering of powder bed layers. The first patent for a metal process was issued in 1997 for Selective Laser Sintering (SLS) (Deckard). In the same period, the similar processes, Selective Laser Melting (SLM) and Direct Metal Laser Sintering (DMLS), were developed and patented.

2.4 Melted-state processes

Most of the current AM technologies for building larger components are based on DED. Both the feedstock and the substrate are heated above their melting temperature and bonding is achieved upon solidification. For manufacturing of smaller and more complex parts, PFB processes are used. Here the feedstock is provided as a powder layer, and sequentially fused to the previous layer. In the following sections, the principles behind the most common DED and PBF processes will be presented.

2.4.1 Directed Energy Deposition based on arc welding

Bonding of metals has been researched for decades for welding technologies, and this knowledge has also been utilized when AM processes have been developed later on. Processes based on arc welding and wire feedstock are being investigated for AM purposes by several research groups around the world (Ding et al., 2015). These processes typically use off-the-shelf equipment for Gas Metal Arc Welding (GMAW), Gas Tungsten Arc Welding (GTAW) or Plasma Arc Welding (PAW), and are often referred to as Wire Arc Additive Manufacturing (WAAM). CNC machines are used to control the position of the welding tip.

For GMAW, the wire feedstock is usually oriented perpendicular to the substrate. There are different strategies to deposit the feedstock, e.g. globular, short-circuiting, spray or pulsed-spray transfer. Another com-

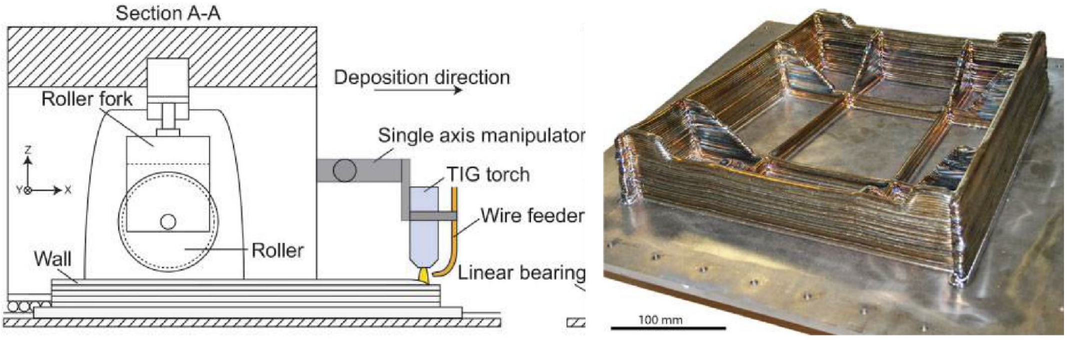

Figure 2.3: (a) Schematic illustration of the WAAM process which is a DED process based on the GTAW principle; (b) a near-net-shape structure built using the WAAM process (Williams et al., 2016).

monly used deposition strategy is Cold Metal Transfer (CMT), which benefits from lower heat input and thus higher deposition rates (Ding et al., 2015). Differently from GMAW, which uses the wire feedstock as the electrode, GTAW and PAW use a tungsten electrode to produce the arc. The control of these processes is more complex because the feedstock has to be aligned in the feed direction. Problems related to these processes are residual stresses and distortions that are induced due to thermal gradients during processing. The latest deposited stringer bead is deposited in a melted state, and upon cooling the contraction of the metal will induce strains in the under-laying structure, causing distortions (Ding et al., 2015). To reduce distortions in the built parts, high-pressure inter-pass rolling or back-to-back building is often used (Williams et al., 2016). An illustration of the WAAM process is shown in Figure 2.3, including an example of a near-net-shape structure being built using this process.

2.4.2 Directed Energy Deposition based on laser melting

DED processes based on laser welding operate under different names like Laser Powder Forming, Directed Light Fabrication (DLF) (Lewis et al., 1994), Laser Engineered Net Shaping (LENS) (Atwood et al., 1998), Direct Metal Deposition (DMD) (Mazumder et al., 1997), Laser Consolidation (LC) (McGregor et al., 2003) and Laser Based Flexible Fabrication (LBFF) (Jiang and Molian, 2002).

A focused laser beam is used to melt the metal powder being supplied through the deposition head. The laser beam typically travels through the centre of the head and is focused to a small spot by one or several lenses. The deposition head deposits the material, stringer by stringer, adding up to layers.

The metal powder is either distributed by a pressurized carrier gas or by gravity. Inert shielding gas is used to protect the melt pool from the atmosphere for control of properties and to promote the layer-to-layer adhesion by providing better surface wetting.

The process can produce parts in a wide range of alloys, including titanium, stainless steel, aluminium, as well as composites and functionally graded materials. The part size for such processes is only limited by the movement system since it does not operate inside a vacuum chamber. The process is also used for cladding of components and for repair of damaged components. A schematic illustration of directed energy deposition using laser melting is shown in Figure 2.4 along with an example of a 3D-structure built using this process.

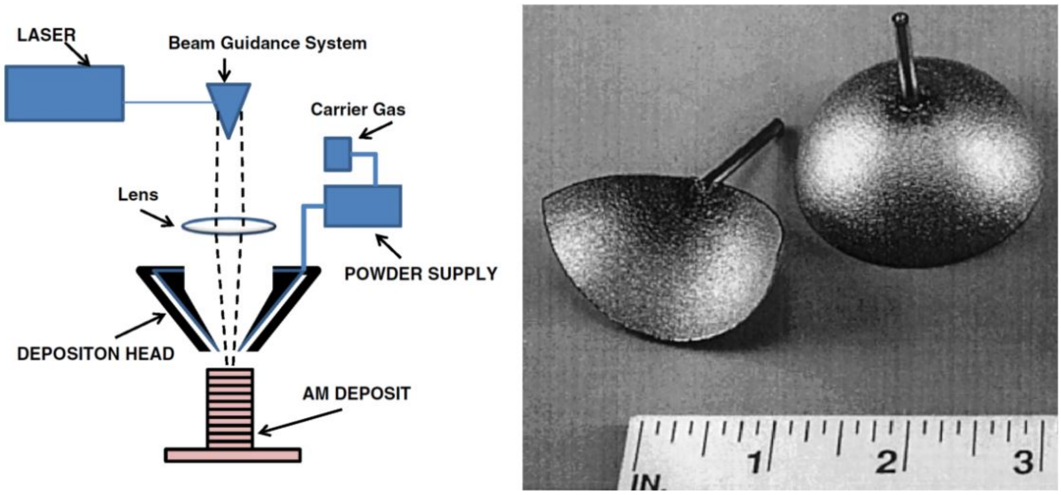
LASER
Beam Guidance System
Carrier Gas
Lens
POWDER SUPPLY
DEPOSITON HEAD
AM DEPOSIT
IN.
1
2
3

Figure 2.4: (a) Schematic illustration of DED using laser melting (Frazier, 2014); (b) an example of a 3D-structure produced by laser directed energy deposition (Milewski et al., 1998).

2.4.3 Directed Energy Deposition based on electron beam melting

A third variant of DED is based on the EDM process, where an electron beam is used as the source of fusion. This process is also known under the name Electron Beam Freeform Fabrication EBF^3. In this case, a focused electron beam is used to create a molten pool on the substrate. The metal is supplied to the molten pool through wire feedstock. The beam is then translated with respect to the surface to control the shape of the part. The sequence is repeated stringer-by-stringer and layer-by-layer to produce a near-net-shape part.

The electron beam requires a high vacuum environment and typically operates at pressures of $1.3 \cdot 10^{-3}$ mbar or lower. Therefore, the size of the vacuum chamber restricts the size of the parts that can be produced.

Deposition rates up to 2500 cm^3 per hour can be achieved using this process. Previous research has focused on aluminium and titanium alloys as feedstock material (M. B. Taminger and Hafley, 2003). Fig 2.5 illustrates the EB DED process and a near-net-shape structure that has been created using the process.

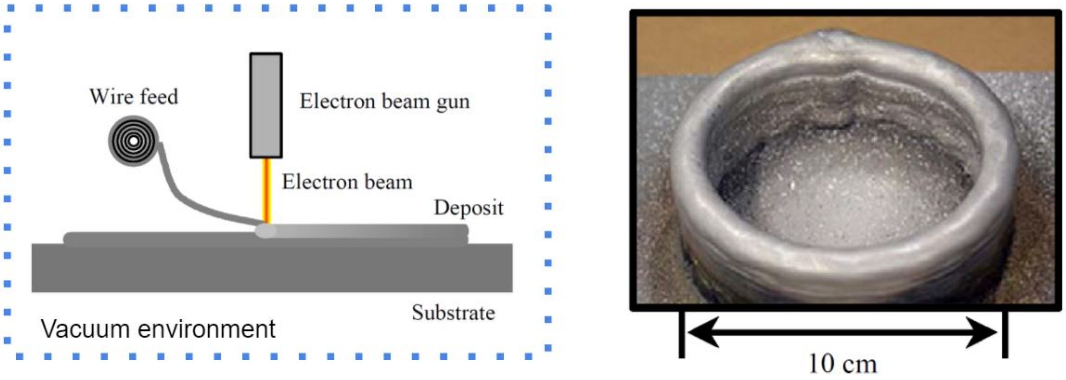
Wire feed
Electron beam gun
Electron beam
Deposit
Substrate
Vacuum environment
10 cm

Figure 2.5: (a) Schematic illustration of the DED process based on electron beam melting; (b) example of an AA2219 structure produced using the same process (M. B. Taminger and Hafley, 2003).

2.4.4 Powder Bed Fusion based on laser welding

In PBF processes, a thin layer of metal powder is distributed over the build area, and a heat source is used to selectively melt the area of the layer that intersects with the part being produced. When a layer is finished, the build platform is lowered a distance equal to the layer thickness, and a new layer of metal powder is supplied. During processing, the part is attached to the build plate by a support structure which has to be removed during post-processing. The part is also supported by the unconsolidated powder, thus making it possible to create thin-walled structures having internal voids and channels integrated into the part.

The temperature of the build platform is typically kept at approximately $90^\circ C$, and the laser beam scanning speed can approach 1,200 mm/s (Murr et al., 2012).

PBF processes based on laser melting are most commonly known under the proprietary name Selective Laser Melting (SLM) (Meiners et al., 1998) and Direct Metal Laser Sintering (DMLS). The latter name is somewhat misleading as the part is actually melted during processing, and not sintered. The SLM process is schematically illustrated in Fig 2.6 along with pictures of parts being produced by the process.

Analogous to the PFB processes based on laser melting, an electron beam can be used to melt the metal powder. The EBM process operates under vacuum at pressures below $1.3 \cdot 10^{-4}$ mbar. However, helium gas is supplied at the build area to enhance the heat conduction and the cooling of the component cooling during processing, thus increasing the pressure up to $1.3 \cdot 10^{-2}$ mbar (Murr et al., 2012).

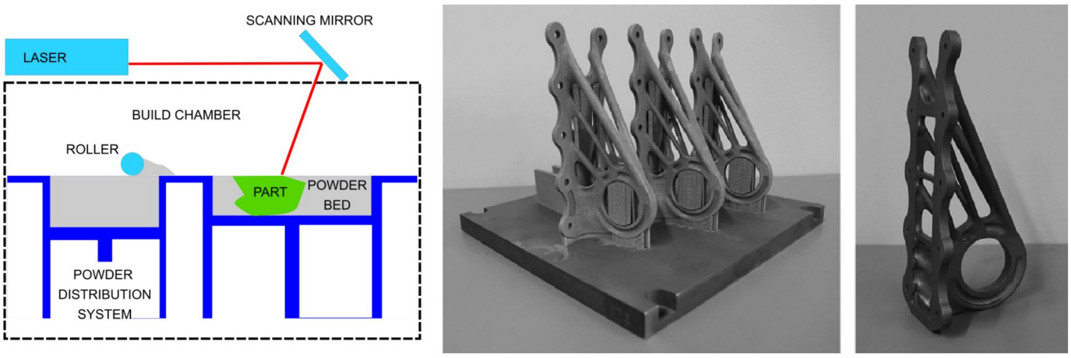

Figure 2.6: (a) Schematic illustration of a PBF system; (b) photograph of topology optimized Ti-6Al-4V brackets for Airbus A350 before build plate and support structure is removed; (c) the finished part after the support structure is removed (Herzog et al., 2016).

2.5 Solid-state processes

2.5.1 Friction Stir AM

Friction Stir Additive Manufacturing (FSAM) is based on the FSW process. In FSAM the rotating tool is submerged into the overlapping surfaces of sheets or plates to be joined while travelling along the joint line. The tool is designed to create the necessary heat and plastic deformation to join the materials in the solid-state (Palanivel et al., 2015). Figure 2.7 shows an illustration of the FSAM process.

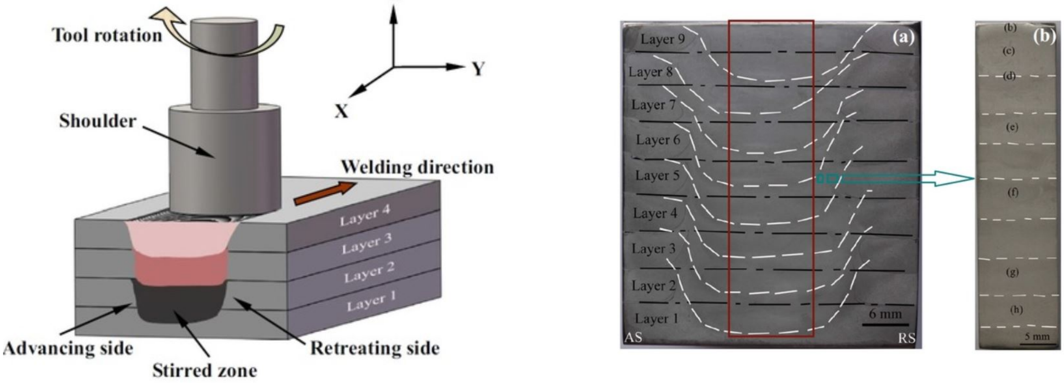
Tool rotation
Shoulder
Y
X
Welding direction
Layer 4
Layer 3
Layer 2
Layer 1
Advancing side
Stirred zone
Retreating side
(a)
Layer 9
Layer 8
Layer 7
Layer 6
Layer 5
Layer 4
Layer 3
Layer 2
Layer 1
6 mm
AS
RS
(b)
(c)
(d)
(e)
(f)
(g)
(h)
5 mm

Figure 2.7: (a) Schematic illustration of the Friction Stir Additive Manufacturing Process. In this case the rotating tool is inserted into the overlapping surfaces of sheets or plates to be joined and traversed along the joint line (Palanivel et al., 2015); (b) cross section of a structure created using the FSAM process (Palanivel et al., 2015).

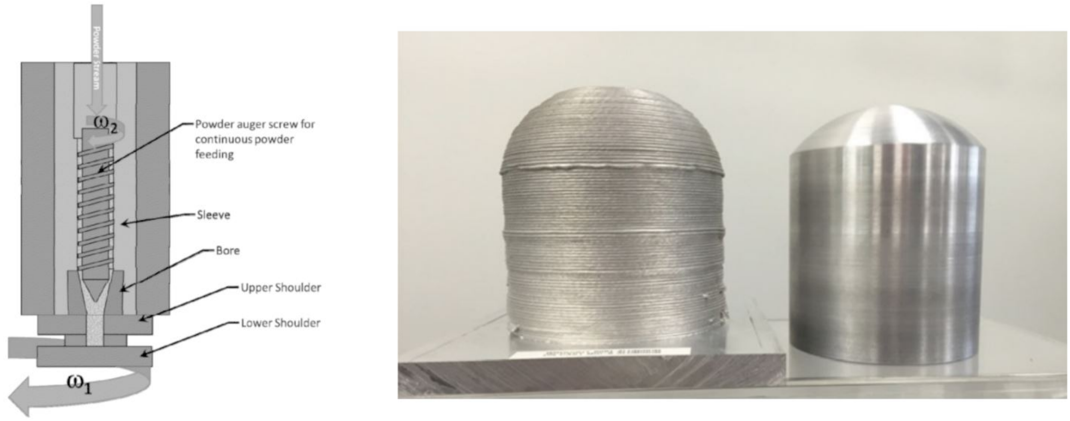
Powder stream
ω_2
Powder auger screw for continuous powder feeding
Sleeve
Bore
Upper Shoulder
Lower Shoulder
ω_1

Figure 2.8: (a) Schematic illustration of the additive friction stir process with continuous powder feeding (Schultz and Creehan, 2014); (b) a part created using the MELD process, before and after post-processing (Aeroprobe).

2.5.2 MELD

MELD is another process based on FSW that can be used for both AM and coating of materials. The process has been developed by Aeroprobe, and is also referred to as Additive Friction Stir (AFS). In the MELD process, the feedstock in the form of solid bars or powders is fed through the rotating tool which acts as a screw extruder (Schultz and Creehan, 2014). Due to the extrusion pressure build-up, the filler metal is forced to flow through the rotating tool and then deposit and bond onto the substrate. The process can be scaled since it is not operating in a vacuum or inert environment. Figure 2.8 shows the operating principle of the rotating tool along with a part being made by the process.

Materials processed using MELD includes magnesium, aluminium silicon carbide, copper, copper metal matrix composites, magnesium, steel, oxide dispersion strengthened steel and ultra high strength steel.

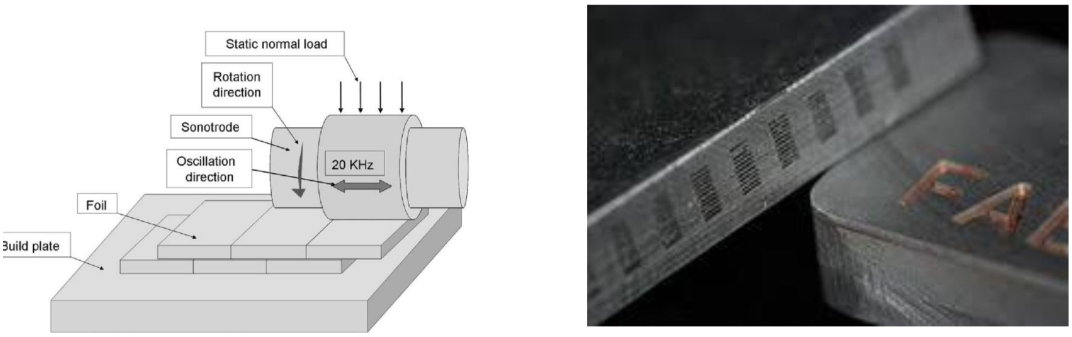

Figure 2.9: (a) Schematic illustration of the Ultrasonic Consolidation process; (b) photograph of a multi-material structure created from this process (Kulakov and Rack, 2009).

2.5.3 Ultrasonic Consolidation AM

AM processes based on friction joining were first patented in 2002 (White, 2002), and have later been commercialized for ultrasonic consolidation of thin sheets or foils (White, 2003). This process is referred to as either Ultrasonic Consolidation (UC) AM or Ultrasonic AM (UAM).

The process is based on stacking and bonding of foils or thin metal sheets. Bonding is achieved by a combination of oxide disruption and pressure. An ultrasonic transducer is used to create pressure and at the same time provide small vibrations that disrupt the oxide layer on the mating surfaces. The metal foil strips are continuously supplied from a roll. Because the metal strips have a fixed, width the resolution of the deposited structure is rough. To achieve the final shape, the process is combined with CNC milling of the contours during processing. UAM operates at low temperatures, and has the ability to bond multiple metal types together (White, 2003). Figure 2.9 presents a schematic illustration of the UAM process along with a multi-material structure created by the process.

2.5.4 Friction Deposition AM

AM utilizing friction deposition has been researched by Dilip et al. (Dilip et al., 2011). This type of deposition basically involves a consumable rod rotating over a substrate at a predefined load. The friction between the surfaces generates heat which softens the material at the abutting end. Deposition occurs when the plastically deformed material gets detached from the consumable rod due to the torsional shear.

3. The Hybrid Metal Extrusion & Bonding process

3.1 General

From the overview in Chapter 2, it is obvious that a large number of different AM processes already exist. Some of these involve melting of the material - others do not. The established AM processes have all their advantages and disadvantages, but none of them has yet reached a level of maturity that makes them outstanding in the sense that they exclude other processes or different approaches. Hence, there is a need for new innovations particularly within the field of AM of aluminium components.

The first part of this chapter provides an introduction to the Hybrid Metal Extrusion & Bonding technology presenting some of the earlier work that is relevant for this thesis. The last part of the chapter is based on extracts from Paper 1, aiming to at demonstrate the potential of using this technology for additive manufacturing.

The HYB technology project was initiated more than 20 years ago at the Department of Materials Science and Engineering at NTNU. In collaboration with SINTEF Materials and Chemistry the project has been continuously developed and has in recent years matured into a promising, new, welding process for aluminium alloys (Sandnes et al., 2018). The basic idea behind the HYB process is to bond aluminium without melting the materials involved; i.e., solid-state bonding. Solid-state bonding or cold bonding, which is another name for the same process, was probably the first technique ever used to bond two pieces of metal. Already in the middle bronze age, 1400-1000 B.C. this technique was used to hammer together small nuggets of gold into larger pieces (Tylecote, 1968).

The first scientific study of cold bonding was inspired by the works of the Swedish scientist Mårten Triewald, and was published by Desaguliers (1724). In his study, he describes how he was able to bond two lead balls by cutting away a segment of each and pressing them together with a little twist. However, it was not before the middle of the 20th century that the research was intensified, leading to a thorough understanding of solid-state bonding processes like cold pressure welding, friction welding, accumulative roll bonding and extrusion of hollow sections.

3.2 Bonding mechanisms

The concept of solid-state bonding can be visualized by thinking of the base material as two pieces of plasticine. If the surfaces of the two pieces are clean, it is sufficient to press them slightly together to unify them into one piece. This is the case for pure gold, which does not form an oxide layer. For metals like aluminium and lead, which react with air to form an oxide layer, the case is somehow different. Imagine now that the two pieces of plasticine are covered with a brittle layer of shellac. To bond the pieces, two different approaches can be undertaken. The first one is to cut away the shellac layer on the mating surfaces (the same way as Desagulier did with the lead balls). The other approach is to press them so hard together that the surface layer cracks due to the expansion of the surfaces, thereby allowing the pure plasticine to flow through the cracks and make contact. It is interesting to note that exactly this setup has been used to physically model the phenomenon by Osias and Tripp back in 1966 (Osias and Tripp, 1966).

The film theory (Bay, 1983), is still the way solid-state bonding is understood today. In general, solid-state bonding is the result of the interplay between three main variables: (1) The surface exposure, (2) the ratio between the contact pressure (p) and the yield strength (p/σ_y) at the mating interface and (3) the type and extent of surface contamination. The mode of deformation also plays a role, and contact on an atomic scale is easier to achieve through shear deformation than by compression (Grong, 2012). A high contact pressure will generally ease the bond formation and reduce the actual surface exposure needed to initiate cold bonding.

In cold pressure welding (CPW), the bonding is based on removal of the oxides rather than breaking up the oxide layer. During compression the oxides are removed through an outward material flow, creating an upset collar. When all oxides are removed a full metallic bonding is achieved (Tylecote, 1968).

Conrad and Rice (1970) performed experiments on the bonding of fractured oxide-free fcc metals like Ag, Al, Cu and Ni in vacuum. They found a close correlation between the bond strength and the force used to compress and bond the specimens. These results have later been supported by other studies of bonding of oxide-free metal surfaces using, e.g., the cut welding process (De Chiffre, 1989; Dorph et al., 1993; Dorph and De Chiffre, 1995). More recently Cooper and Allwood (2014) conducted over 150 experiments to established the basic relationships between deformation parameters and weld strength for cold-bonded aluminium.

Because HYB is based on the principles of continuous rotary extrusion (CRE), also known as Conform extrusion (Green, 1972), this process will be further explained in the following section.

3.3 Extrusion principle

Extrusion is the process by which a metal billet is reduced in cross section by pressing it through the die of an extrusion press. Usually, the extrusion process is carried out at elevated temperatures to reduce the flow stress of the material.

The two most common extrusion processes are direct extrusion and indirect extrusion, as shown schematically in Figure 3.1a and b, respectively. For both processes, the billet is placed in a container and forced through the die by a ram. However, in indirect extrusion, the die is placed in the ram and pressed towards the stationary container and billet. This means that there is no relative motion between the wall of the container and the billet during extrusion, thus leading to reduced frictional forces and power input compared to direct extrusion (Dieter and Bacon, 1986).

Now consider the situation shown in Figure 3.1c, where the bottom plate of the moving container is removed and the billet is kept in place by the frictional forces acting along the side-walls. Under such conditions, indirect extrusion would still be possible as long as the frictional forces are larger than those required to press the material through the extrusion die. A similar situation applies to the continuous rotary extrusion process, where the container is replaced by an extrusion wheel provided with a tapered groove for gripping the feedstock wire. The wheel is surrounded by a stationary housing with abutment and die, as illustrated in Figure 3.1d. Upon rotation of the wheel, the wire will be subjected to a frictional force from the wall of the housing. The force contribution from the friction between the three walls of the groove will provide a net movement in the direction of rotation.

For solid-state bonding of aluminium, a challenge is to remove the oxide layer which immediately forms upon exposure to oxygen. However, one knows from processes like extrusion of hollow sections of aluminium that solid-state bonding occurs under high pressure as the extrudate exits the tool after flowing

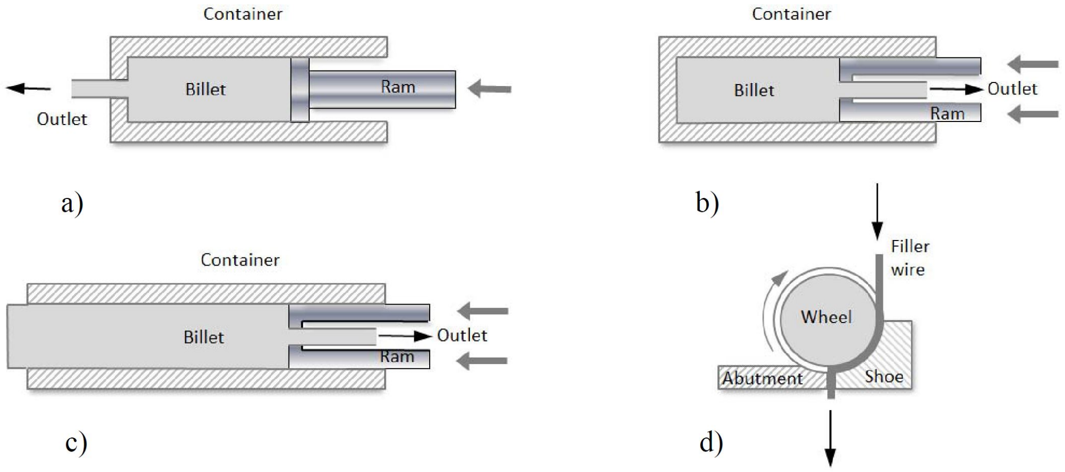

Figure 3.1: Schematic illustrations of different types of extrusion; (a) direct extrusion; (b) indirect extrusion; (c) indirect extrusion where the bottom plate of the container is removed; (d) continuous extrusion (Aakenes, 2013).

between the bridges holding the centre die. At this stage, the oxides initially present on the surface of the billet are dispersed and will not inhibit bonding.

In the HYB process, CRE serves the same two purposes; i.e., to disperse oxides and to provide pressure. When the feedstock is plastically deformed inside the extruder, oxides present on the feedstock surface become dispersed in the extrudate. Finally, the extruder provides the required pressure to obtain bonding between the extrudate and the substrate.

3.4 HYB technology development

The first patent on the HYB technology was filed back in 2002. Since then, a variety of different designs have been explored, and the process has gradually evolved to handle more complex geometries than simple butt joints which it was initially designed for. Looking back at the tracks that have led up to the current process, it is obvious that the directions have changed as new terrain and opportunities have been discovered. Figure 3.2 illustrates the wayfaring journey towards the current extruder design based on the formalism proposed by Steinert and Leifer (2012).

In the following, a brief description of some prototypes and key learning outcomes are presented. This background information provides the foundation for the further journey towards conceptualizing HYB into an AM process. Further details of the individual designs can be found in various technical reports, publications and theses (Sandnes et al., 2018; Aakenes, 2013; Erlien et al., 2002; Erlien and Grong, 2003; Lilleby and Erlien, 2005; Lilleby et al., 2005; Krog et al., 2006; Hermstad et al., 2007a,b).

3.4.1 Wheel extruder

The first generation of extruders was a down-scaled version of the Conform extruder. The development and testing of these extruders are described by Erlien and Grong (2003); Erlien et al. (2002), where they are referred to as Prototype 1-5. The wheel extruder typically has a wheel diameter of Ø40 mm and is equipped with a rectangular slot for wire feeding. The extruder is designed for processing Ø1.6 mm filler wire. The

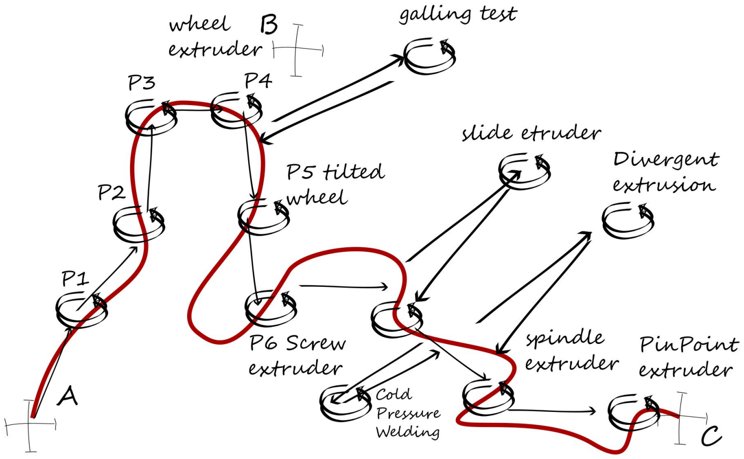
wheel extruder
B
galling test
P3
P4
P2
P5 tilted wheel
slide etruder
Divergent extrusion
P1
P6 Screw extruder
spindle extruder
PinPoint extruder
A
Cold Pressure Welding
C

Figure 3.2: Schematic illustration of the journey leading to the current extruder design used for welding. Note that the design process has not followed a straight path, which is characteristic of many innovation processes (Steinert and Leifer, 2012).

total depth of the slot in the extrusion wheel is 2.4 mm, while the slot width is 1.5 mm. This gives an effective cross-sectional area of the extrusion chamber of 1.4 mm × 1.5 mm. The stationary shoe typically covers less than 50% of the wheel circumference. The chosen wheel and slot dimensions are based on calculations from industrial conform extruders for aluminium alloys to provide sufficient grip length and extrusion pressure (Støren, 1976). The development of the wheel extruder went through a number of iterations, and totally five different extruder designs and sub-variants were tested out in laboratory and used to improve the next design. A photograph of Prototype 4 is shown in Figure 3.4.

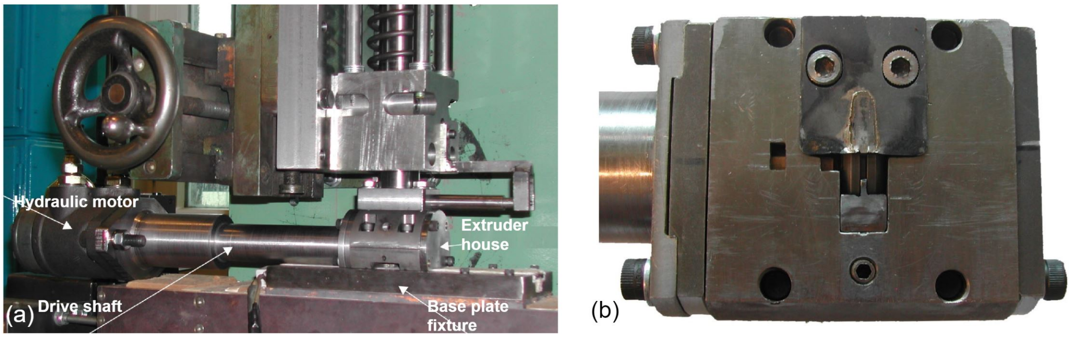
Hydraulic motor
Extruder house
(a)
Drive shaft
Base plate fixture
(b)

Figure 3.4: Photographs of Prototype 4; (a) the extruder mounted in the experimental rig; (b) the wheel extruder from below, showing the drive shaft and the lower ends of the shoe and the extrusion wheel along with the abutment (Erlien and Grong, 2003).

A major challenge with the wheel extruders was to maintain sufficient shoe and abutment stiffness without increasing the die length and thus the pressure drop through the die during extrusion. To deal with the abutment stiffness problem of the previous 4 wheel extruders, the single arm 45° revolving extruder was developed (Prototype 5) by Erlien and Grong (2003). The design is illustrated in Figure 3.5. Here, the extruder head is mounted at the end of the drive shaft, which, in turn, rotates at an angle of 45° with respect to the base plate surface. The design improves the stiffness of the shoe and the abutment because these can be made as one part. In addition, 45° orientation of the drive shaft implies that half of the extrusion force can be transferred to the moving table, assisting the extruder propulsion instead of contributing to a large lift force, which was a major problem with the previous wheel extruders.

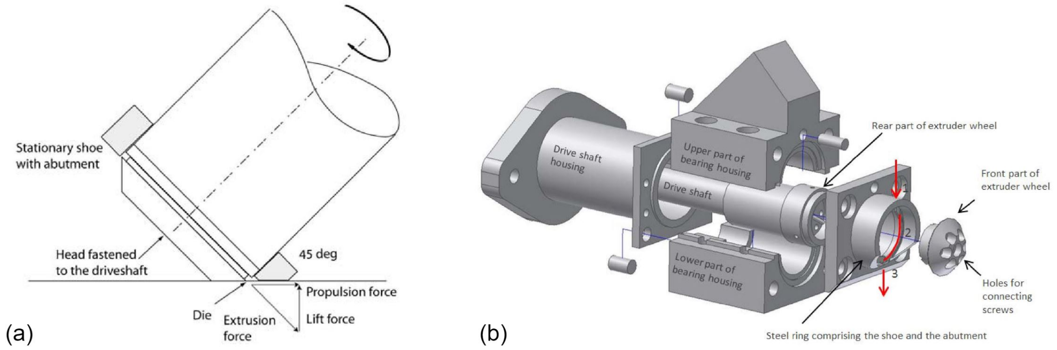
Stationary shoe with abutment
Head fastened to the driveshaft
45 deg
Propulsion force
Die
Extrusion force
Lift force
(a)
Drive shaft housing
Upper part of bearing housing
Drive shaft
Lower part of bearing housing
Rear part of extruder wheel
Front part of extruder wheel
1
2
3
Holes for connecting screws
Steel ring comprising the shoe and the abutment
(b)

Figure 3.5: (a) Schematic illustration of the single arm 45° revolving extruder (Prototype 5); (b) the complete extruder assembly used for experimental testing (Aakenes, 2013).

Among all these versions, the single arm 45° revolving extruder was the most successful in the sense that it did prove useful for butt joining of 4 mm AA6082 plates preheated to 400°C. Still, the wheel extruder concept was abandoned because it did not have the potential of becoming a real industrial process for a number of reasons, including:

1. Lack of robustness (e.g. the risk of wheel and abutment failure during operation is high);
2. Expensive to replace the damaged parts;
3. Disassembling the extruder after use is challenging;
4. Unacceptable large frictional force between the moving parts;
5. Unacceptable large pressure drop through the die due to a constricted die opening;
6. Attachment of oxide scraper in front of the extruder is not possible, making bonding challenging;
7. Local preheating of the aluminium in the groove is very difficult;
8. Lack of flexibility (requires the use of pre-heated base plates at the same time as the extruder is only suitable for butt joining due to geometrical constraints).

3.4.2 Screw extruder

Another design that emerged from the testing of the prototypes of the wheel extruders is the screw extruder. This is referred to as prototype 6 or the single arm 90° revolving extruder (Erlien and Grong, 2003). The extrusion principle for the screw extruder is similar to that of the wheel extruders; however, in this case, the rotational axis of the extruder is tilted such that it is perpendicular to the base plate surfaces.

The screw extruder is designed for processing of Ø1.6 mm aluminium filler wire which is fed into the extrusion chamber with cross-sectional area of 1.4 mm × 1.5 mm. However, the wheel is now replaced by a two-part drive spindle. Its smallest diameter is barely Ø15 mm. To obtain the required extrusion chamber length for providing sufficient pressure, the shoe is now covering almost the entire periphery of the spindle.

The aluminium is allowed to escape through small slots in the extrusion head, acting as moving dies - and not through a stationary die in the shoe, as in the wheel extruders. Also in the case of the screw extruder different variants exist. One of these is illustrated in Figure 3.6.

Although the inner diameter of the extrusion chamber is quite small, the subsequent laboratory testing showed that both the applied system for wire feeding and the concept involving the use of moving dies seemed to work to a certain extent. Still, the screw extruder development project was eventually abandoned, mainly because of the risk of overloading of the inner drive spindle, leading to shear fracture in the spindle head during extrusion. This design flaw could not readily be corrected for by simple countermeasures, thus calling for new solutions (Aakenes, 2013).

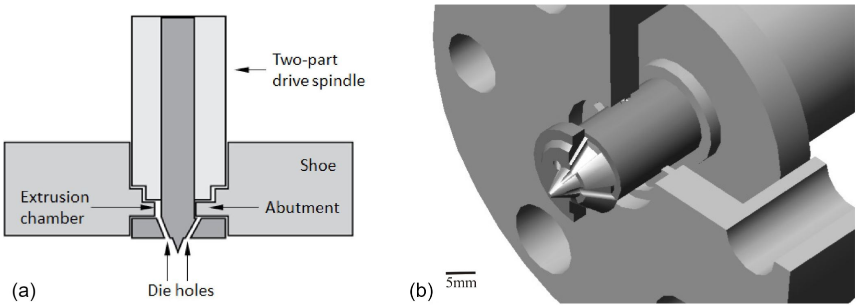

Figure 3.6: Illustrations of Version B1 of the HYB screw extruder; (a) section through the rotating extruder head with its moving dies, the stationary shoe and the abutment; (b) partially sectioned 3D-image of the extrusion head (Aakenes, 2013).

3.4.3 Spindle extruder

The next generation of extruders is the HYB spindle extruder. The conceptual design of the spindle extruder is shown in Figure 3.7. During the PhD thesis work of Ulf Roar Aakenes many different versions of the HYB spindle extruder were built and tested in the laboratory (Aakenes, 2013). The HYB spindle extruder allowed for the first time butt joining of 4 mm AA6082-T6 plates carried out at room temperature without the formation of a heat affected zone (HAZ) due to the characteristic low processing temperature. Nevertheless, the HYB spindle extruder development project was abandoned because of problems with variable bond strength across the base metal - filler metal interface and the fact that the extruder did not provide the extrusion pressure necessary to achieve full penetration welds.

3.4.4 PinPoint extruder

The design principles applied to the PinPoint extruder represent a synthesis of all accumulated knowledge and experience gained from the previous extruder developments. The extruder is built around a Ø10 mm rotating pin, provided with an extrusion head with a set of moving dies through which the aluminium is allowed to flow. This is shown by the drawing in Figure 3.8a. When the pin is rotating, the inner extrusion chamber with three moving walls will drag the filler wire both into and through the extruder due to the imposed friction grip. At the same time, it is kept in place inside the chamber by the stationary housing constituting the fourth wall. The aluminium is then forced to flow against the abutment blocking the extrusion chamber and subsequently, due to the pressure build-up, continuously extruded through the moving dies in the extruder head. They are, in turn, helicoid-shaped, which allow them to act as small "Archimedes

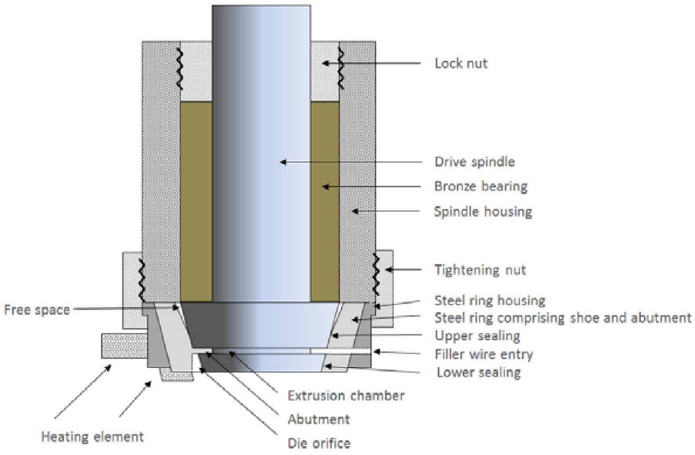
Lock nut
Drive spindle
Bronze bearing
Spindle housing
Tightening nut
Steel ring housing
Steel ring comprising shoe and abutment
Upper sealing
Filler wire entry
Lower sealing
Free space
Extrusion chamber
Abutment
Die orifice
Heating element

Figure 3.7: Conceptual design of the HYB spindle extruder (Aakenes, 2013).

screws" during the pin rotation, thus preventing the pressure from dropping on further extrusion in the axial direction of the pin.

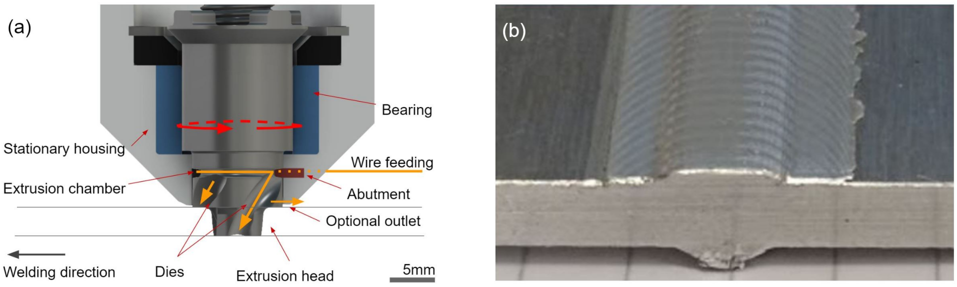
(a)
Bearing
Stationary housing
Wire feeding
Extrusion chamber
Abutment
Optional outlet
Welding direction
Dies
Extrusion head
5mm
(b)

Figure 3.8: (a) The HYB PinPoint extruder is built around a rotating pin provided with an extrusion head with a set of moving dies through which the aluminium is allowed to flow; (b) cross section of a HYB weld with a weld reinforcement on the top (Blindheim et al., 2018).

The PinPoint extruder has the possibility to form a weld reinforcement by extruding material in the radial direction through a separate die at the rear of the housing. By controlling the flow of aluminium in the radial direction, both the width and height of the weld reinforcement can be varied within wide limits, depending on the die geometry, ranging from essentially flat to a fully reinforced weld face. An example of this is shown in Figure 3.8b.

3.5 The feasibility of using the HYB process for additive manufacturing

3.5.1 Benchmarking

In order to determine the potential of HYB-AM, its characteristics must be compared to the alternative or competitive technologies. Chapter 2 presented an overview of different additive processes for metals and alloys. In the following, two established processes within the solid-state and melted-state categories are revisited and used for the subsequent benchmarking of the HYB-AM concept.

Table 3.1: Characteristics of Ultrasonic Additive Manufacturing (UAM) and Wire Arc Additive Manufacturing (WAAM) when used for aluminium alloys (Blindheim et al., 2018).

Parameter	Comments
Deposition rate	The low heat input of UAM makes it suitable for high deposition rates, whereas the deposition rate for WAAM is limited by the cooling rate of the structure to avoid down-melting.
Build volume	Both processes are only limited by the size of the motion system, and do not require a low-pressure environment.
Overhanging structures	Current UAM machines cannot produce overhanging structures as opposed to WAAM which has this flexibility.
Post-processing	Both processes create near-net-shape structures that require machining to obtain the final shape and tolerances.
Material range	UAM allows processing of any aluminium alloy and can even bond dissimilar alloys and materials. In contrast, WAAM is restricted to certain alloys that are not susceptible to hot cracking (e.g. Al-Si and Al-Mg alloys).
Residual stresses	The low processing temperature of UAM means reduced temperature gradients and thus lower thermal-induced stresses during cooling compared to WAAM, which is a melted-state process.
Defects	The WAAM process which involves melting of the feedstock can create problems with porosity and hot tearing, whereas lack of bonding is perhaps a greater problem for UAM.

Wire Arc Additive Manufacturing (WAAM) and Ultrasonic Additive Manufacturing (UAM) are well-known processes within the melted-state and solid-state AM category, respectively, and some characteristics of these processes are presented in Table 3.1. Considering solid-state processes like UAM, some of the advantages are a wide material range to choose from and the possibility to join dissimilar materials. Problems with distortions and residual stresses are also reduced due to lower temperature gradients during processing. WAAM, on the other hand, has advantages when it comes to the possibility to create overhanging structures. Still, distortion and residual stresses can be a challenge.

Regarding deposition rates, both technologies can achieve high deposition rates. WAAM based on the Cold Metal Transfer (CMT) welding process has the ability to achieve high deposition rates, yet with an increase in material waste, since higher deposition rates contribute to a wider melt pool size and thus a thicker wall structure. A typical CMT deposition rate for aluminium, when keeping the buy to fly (BTF) ratio at 1.5, is 1kg/h (Williams et al., 2016).

The first generation machines for UAM did not have sufficient power to achieve high deposition rates. However, commercial machines from Fabrisonic are capable of depositing up to 1.3 kg/h. Contrary to melted-state processes, where the substrate needs to continuously solidify to keep its shape, solid-state processes have no such limitations in deposition rates, as long as the temperature is kept below the melting temperature of the material. This makes solid-state processes favourable for manufacturing of larger structures.

3.5.2 Proof-of-concept

An initial proof-of-concept based on the PinPoint extruder was carried out by Hybond AS prior to this thesis work. Commercial purity aluminium (AA1050) was used both as base and feedstock materials. The dimensions of the two 4 mm thick base plates used in the testing were 240 mm × 50 mm, while the diameter of the feedstock wire was Ø1.2 mm. For the demonstration, a set of used tool parts from an earlier version of the PinPoint extruder was selected. These tool parts were subsequently modified through grinding to allow AM of a layered structure using a combination of stringer bead deposition and butt welding. The recaptured operational conditions are summarized in Table 3.2.

Table 3.2: Parameters used for the initial proof-of-concept experiment (Blindheim et al., 2018).

Parameter	Value
Pin rotation speed	300 RPM
Extruder travel speed	6 mm/s
Wire feed rate	87 mm/s
Gross heat input	0.34 kJ/mm

For the stringer bead deposition two different sets of tools were employed. These include a flat pin equipped with a shaped bottom end for removal of oxides from the underlying surface during welding, and a stationary housing equipped with a rectangular shaped die at the rear (4.5 mm × 3.25 mm). Each base plate was first provided with a longitudinal stringer bead deposited about 1.5 mm from the edge of the plate, see Figure 3.9a. A 3 mm wide groove will then appear between the beads when the edges of the plates are brought together (Figure 3.9b). This, in turn, allowed the plates to be butt welded from the top (Figure 3.9c), using the second tool. Note that in the butt welding case the lower end of the rotating pin is centred in the groove to ensure good surface oxide removal and thus metallic bonding across all interfaces. Finally, on the top of the first layer, the third stringer bead was deposited (Figure 3.9d). This deposition sequence eventually lead to the two-layer structure shown in Figure 3.10.

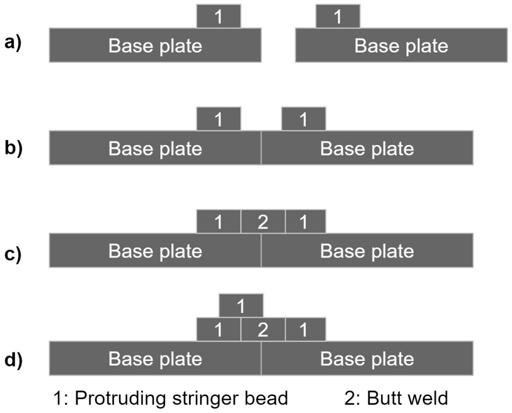

Figure 3.9: Schematic illustration of the deposition sequence used to test the HYB-AM concept (Blindheim et al., 2018).

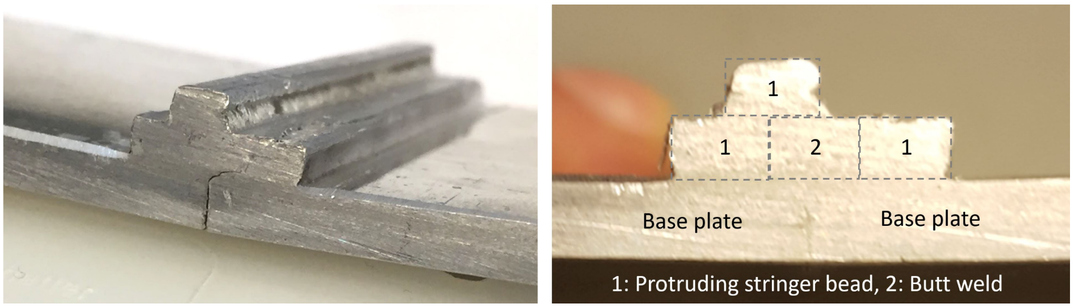

Figure 3.10: Photographs of the layered structure produced using the HYB-AM method (Blindheim et al., 2018).

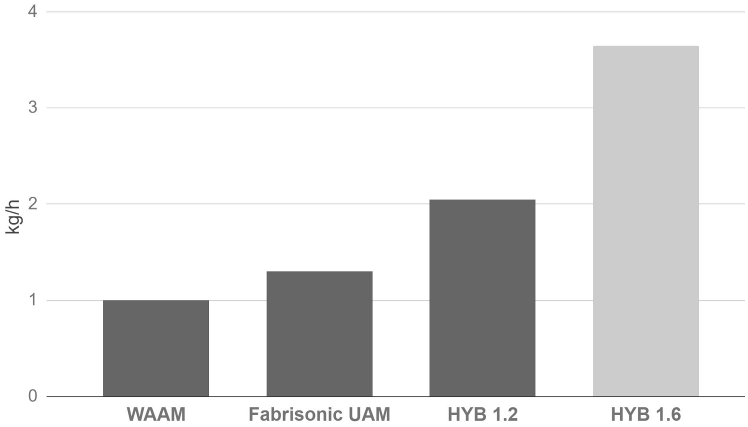

Figure 3.11: Deposition rates for HYB-AM compared to UAM and WAAM for aluminium feed stock (Blindheim et al., 2018).

3.5.3 Potentials

The demonstrated extruder design, using Ø1.2 mm feedstock wire, yields a potential deposition rate of 2 kg/h at 400 RPM and a slip factor of 0.85. The extrusion chamber of the PinPoint extruder can also be adjusted to accommodate up to Ø1.6 mm wire for further increased deposition rates.

Figure 3.11 illustrates how the HYB-AM process performs compared to other technologies with regards to deposition rates; i.e., WAAM and UAM. The deposition rates for HYB-AM are given for both Ø1.2 mm and Ø1.6 mm feedstock wires.

For HYB-AM the deposition rate is only limited by the scaling of the process. However, the deposition rate must be balanced and compatible with the other requirements as well, such as the scanning speed, the die geometry, the process temperature and the contact pressure at the bonding interface. The high potential deposition rates make the HYB-AM technology particularly suitable for manufacturing of larger structures, where this possibility can be fully utilized.

This initial study of the HYB-AM process potential was based on the use of the PinPoint extruder, which is the design currently being used for welding. Still, being a good solution for welding, does not necessarily mean that it is the optimal choice for AM. Prior to further development of the HYB-AM process, it has therefore been of great interest to evaluate other possible designs in order to identify the more optimal solution.

4. Research method and equipment

4.1 General

The previous chapter introduced the HYB-AM process and its potentials based on the initial proof-of-concept experiment. The thesis work has focused on the further development of this process through concept evaluation and full-scale experimental testing, ultimately making it possible to assess the mechanical integrity of a deposited structure and understand the governing mechanisms of the process. In the following, the applied methods and experimental equipment will be introduced.

4.2 Methods

When developing a new product it is desirable to thoroughly explore the solution space in order to increase the chances of arriving at a viable solution. Set-based design can be used to achieve this by developing multiple concepts in parallel and accelerate learning through so-called test-before-design cycles (Kennedy et al., 2014; Sobek et al., 1999). For this particular development project, the concept evaluation will be conducted by a novel approach that combines rapid prototyping and physical modelling (Paper 2 and 3).

The final extruder design will focus on uncovering the special requirements related to AM. It is of interest to design the new extruder in such a manner that it is able to produce samples for further characterization of the process and material capabilities

Laboratory testing will be carried out to determine the microstructure, mechanical properties and the bond strength between the deposited stringers and layers. Specifically, this includes optical microscopy analyses for characterization of the aluminium flow pattern, hardness testing for evaluation of strength distribution across the different layers and tensile testing for determination of the load-bearing capacity of the deposited samples.

Finite element analysis (FEA) is a numerical method for solving complex problems like metal forming operations. When calibrated with observations from real-life experiments, such analysis are capable of producing reliable results. Here, FEA based on Deform 3D software will be used to observe, analyse and interpret some of the governing mechanisms of the process.

4.3 Experimental setup for concept evaluation

The experimental setup used for concept evaluation is shown in Figure 4.1. The setup is based on a modified K8200 Vellemann FDM 3d-printer, allowing the different extruders to be controlled in a similar manner to that of the full-scale process. The machine is a Cartesian type robot which has a lead-screw driven gantry that can move in Z-direction, while the belt-driven bed is allowed to move in the xy-plane. The motion of the machine is provided from the original stepper motors, while the plasticine dispenser and the extruders are

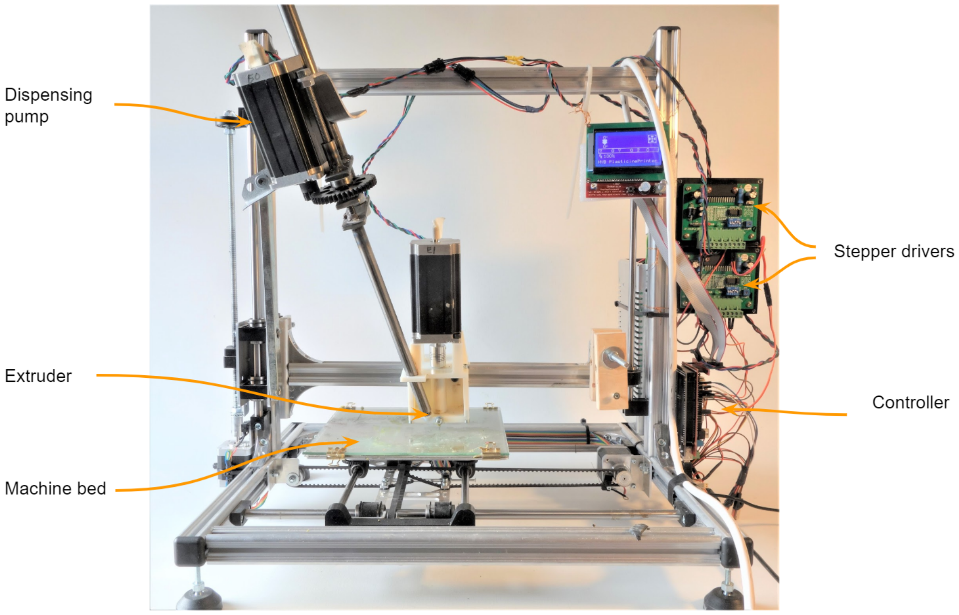

Figure 4.1: Experimental setup for the physical modelling testing.

driven by 3 Nm stepper motors powered by JP6445 36 V stepper drivers. The original controller was replaced by an Arduino Mega running on Marlin 1.4 firmware and equipped with a RAMPS break-out board.

To simplify the material supply process, a dispenser pump was built to directly supply the plasticine at the inlet of the extruders. The dispensing system consists of a steel tube contained with a lead-screw driven piston, having a stroke length similar to the tube length. When the piston is fully retracted, the tube can be filled with plasticine. A gear reduction is used to connect the lead-screw to the stepper motor. The Marlin firmware does not allow for controlling the speed of the dispenser motor independently. However, using the settings for "mixing extruder", made it possible to set the required speed ratio between the extruder motor and the dispenser motor.

4.4 Experimental setup for full-scale testing

Two different machine setups have been used for the full-scale experiments conducted throughout this thesis work. The first full-scale tests relied on a Bridgeport milling machine for motion control. However, the manual operation of the machine made it challenging to control the deposition sequence for longer experimental runs.

A CNC milling machine was thus rebuilt for the purpose of increasing the process control capabilities. The machine is a Sieg SX3 CNC milling machine. The original spindle head was removed, and replaced with a fixture system for the extruder prototypes. The experimental setup is depicted in Figure 4.2

The rotation of the extruder is provided by a 1.8 kW servo motor connected to a gearbox with a gear reduction of 30. The rotation of the extruder is controlled by M08/M09 machine code commands.

A heated bed was designed to allow for heating of the substrate material in order to reduce the flow stress of the material. A PID-controller was used in combination with Nichrome heat-cartridges and a K-type

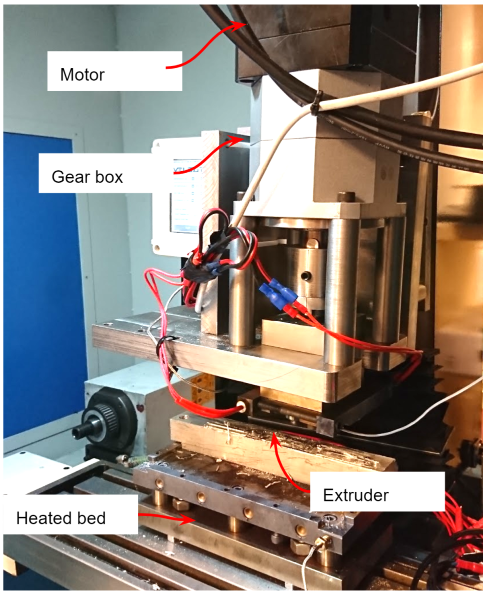

Figure 4.2: Experimental setup for the full-scale testing of the HYB-AM process. A Sieg CNC milling machine was rebuilt for this purpose.

thermocouple to control the temperature of the heated bed. The extruder house was, by the same means, pre-heated to reduce the flow stress of the feedstock material during extrusion.

Torque data was measured by a Smowo LCS-T5 torque cell and a HX711 ADC, wirelessly connected to a computer. Furthermore, the wire speed was measured by a roller connected to a rotary incremental encoder. The aim of measuring the wire speed was to monitor potential wire slip in the extruder.

The individual components of the extruders have been produced from hardened Uddeholm Orvar Supreme tool steel. The steel was machined in its tempered state in order to avoid distortions from quenching. The latest extruder prototype (version 2) is depicted in Figure 4.3.

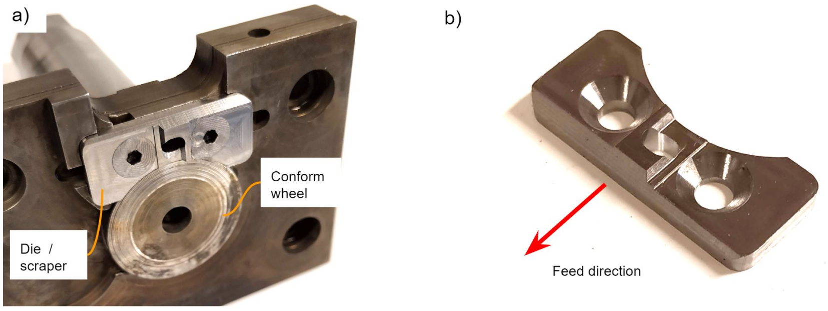

Figure 4.3: Final version of the extruder prototype; (a) as seen from underneath; (b) the die that also is used to scrape the under-laying surfaces.

Table 4.1: Chemical compositions of AA6082 feedstock wire (F) and substrate plate (S).

	Si	Mg	Cu	Fe	Mn	Cr	Zn	Ti	Zr	B	Other	Al
F	1.11	0.61	0.002	0.20	0.51	0.14	-	0.043	0.13	0.006	0.029	Balance
S	0.9	0.8	0.06	0.45	0.42	0.02	0.05	0.02	-	-	0.03	Balance

4.5 Filler wire and substrate material

The feedstock material used for the full-scale testing is AA6082 Ø1.6 mm wire. The wire has been produced for Hybond AS through casting, extrusion, shaving and drawing. Billets for extrusion were produced at Hydro Aluminium and cast using the direct casting (DC) method. The billets were heated at a rate of 200°C/h and homogenized at 540°C for 2h and 15 minutes, and then cooled at a rate of 300°C/h. Billet dimensions were Ø95 mm and length 200 mm. Prior to extrusion the billets were preheated to 500°C at a rate of 100°C/h. Diameter of the extruded wires was Ø2.7 mm. The extruded wire was quenched in water.

The extruded wires were joined into one continuous wire using Cold Pressure Welding (CPW). Prior to drawing, the wire was shaved to remove surface impurities and contaminants. The wire drawing was conducted by MIGWELD who was able to draw the wire down to a diameter of Ø1.6 mm. The final wire diameter was measured at different locations along the wire length axis, yielding an overall mean wire diameter of 1.595 ± 0.015 mm. Vickers hardness measurements have been carried out at a constant load of 0.5 kg. The mean hardness of the as-received wire, which is based on 5 independent measurements, is 123 $HV_{0.5}$.

4 mm rolled plates of AA6082-T6 were used as substrate material. The rolling direction of the plate is parallel to the deposition direction. Table 4.1 gives the chemical composition of the AA6082 feedstock material and the substrate material.

4.6 Microscopy analysis

Samples used for microstructural analyses were prepared according to standard preparation procedures. To reveal the macrostructure, the samples were immersed in a solution of 1% sodium hydroxide and water for 4 minutes. Macrographs were captured using an Olympus BX35M light microscope and an Alicona Confocal Microscope. Finally, fractographs were captured by a Quanta FEG 450 scanning electron microscope (SEM). The fracture surface examination was performed at an acceleration voltage of 20 kV.

5. Present contributions

5.1 General

A total of six papers collectively contribute to the overall aim of this thesis. Figure 5.1 gives an overview of the papers and the topics concerned.

Each individual paper has its own defined objectives that contribute to the overall objective of this thesis. The following sections present the purpose, research approach, results and contributions of the individual papers.

Concept development	Paper 1	**Hybrid Metal Extrusion & Bonding (HYB) - a new technology for solid-state additive manufacturing of aluminium components** Published in Procedia Manufacturing
	Paper 2	**Rapid prototyping and physical modelling in the development of a new additive manufacturing process for aluminium alloys** Published in Procedia Manufacturing
	Paper 3	**Concept evaluation in new product development: A set-based method utilizing rapid prototyping and physical modelling.** Submitted to Journal of Engineering, Design and Technology
Full-scale experiments	Paper 4	**First demonstration of a new additive manufacturing process based on metal extrusion.** Accepted for publication in The International Journal of Advanced Manufacturing Technology.
	Paper 5	**On the mechanical integrity of AA6082 3D structures deposited by hybrid metal extrusion & bonding additive manufacturing** Under review in Journal of Materials Processing Technology
Modelling	Paper 6	**Investigating the Mechanics of Hybrid Metal Extrusion & Bonding Additive Manufacturing by FEA** Published in Metals

Figure 5.1: Chapter structure and overview of the papers included in the thesis

5.2 Paper 1

Title	Hybrid Metal Extrusion & Bonding (HYB) - a new technology for solid-state additive manufacturing of aluminium components.
Authors	Jørgen Blindheim, Øystein Grong, Ulf Roar Aakenes, Torgeir Welo & Martin Steinert
Purpose	The paper presents a feasibility study on the use of the HYB process for additive manufacturing based on the use of the PinPoint extruder for material deposition. The potential of the process is highlighted by comparing it to some existing AM processes for metals - particularly the processes capable of depositing aluminium alloys.
Research objective 1	To investigate the potential of developing an AM process from the HYB technology.
Research objective 2	To present the initial proof-of-concept based on the PinPoint extruder.
Personal contributions	First author; led the writing of article drafts and final version with inputs from co-authors. Adapted the presented deposition sequence to the actual geometry of the PinPoint extruder. Conducted literature review. Prepared figures 1, 2, 5, 6, 9, 10 and 11. The presented proof-of-concept study was conducted by Hybond AS.

Research approach

This paper provides a survey of existing AM processes in order to benchmark the potentials of the HYB-AM process against the established processes. Furthermore, a proof-of-concept experiment using PinPoint extruders is presented. The experiment was conducted by Hybond AS prior to this thesis work.

Results

Some of the results of this paper are already presented in Chapter 3, and are therefore not repeated here. Whereas the deposition sequence used for the proof-of-concept demonstration was done on two separate substrate plates, this paper presents a solution that enables an automated deposition sequence. This is illustrated in Figure 5.2. The first stringers are deposited with a PinPoint extruder equipped with a flat pin and a rectangular die at the rear of the stationary housing, resulting in a stringer bead cross-section of 10 mm × 2.5 mm. The stringer beads are distributed such that a gap of 5 mm is formed between them (Figure 5.2a). The grooves are filled with a second set of tools; i.e., a PinPoint extruder equipped with a pin extending 3 mm below the stationary housing having a diameter larger than the gap width of the groove. The drawback of this setup is that it requires the use of two sets of tools to make a layer in a structure.

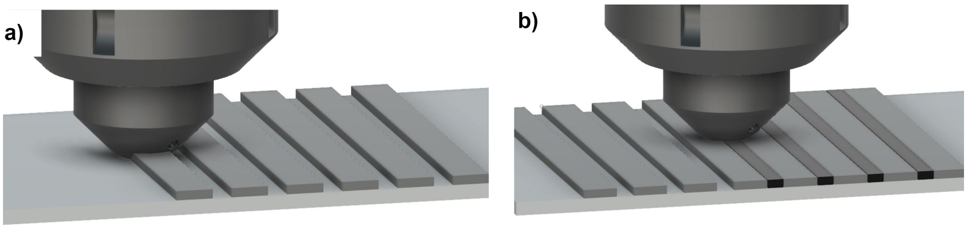

Figure 5.2: Deposition strategy based on the use of two separate PinPoint extruders; (a) first the protruding stringer beads are deposited using the first extruder, keeping the spacing between them fixed; (b) then the gaps are filled using the second extruder (Blindheim et al., 2018)

Implications for the further work

The work presented in this paper justifies the further exploration of the HYB-AM process. Furthermore, a deposition sequence based on the direct implementation of the PinPoint extruder was demonstrated. A drawback of this deposition sequence is that it requires two extruder heads to complete one layer. Before proceeding to further development, a study of alternative extruder designs should be carried out (Paper 2)

5.3 Paper 2

Title	Rapid prototyping and physical modelling in the development of a new additive manufacturing process for aluminium alloys.
Authors	Jørgen Blindheim, Torgeir Welo & Martin Steinert
Purpose	This paper aims at exploring alternative extruder designs for the HYB-AM process. Paper 1 provided a proof-of-concept based on the PinPoint extruder, thus proving the potential of this process. Still, the boundary conditions for an AM process are not the same as that of a welding process; i.e., the optimal design for welding is not necessarily the most suitable design for AM purposes. This study, therefore, takes one step back in order to map the solution space before settling on an extruder design for the further development of the HYB-AM process.
Research objective	To explore and evaluate alternative extruder designs for the HYB-AM process.
Personal contributions	First author; led the writing of article drafts and final version with inputs from co-authors. Developed the research methodology and planned the study. Developed the experimental setup and executed the testing. CAD-design and fabrication of plastic models. Preparations of all illustrations.

Research approach

In this study, a concept evaluation approach based on the combination of rapid prototyping and physical modelling was applied. This approach allowed the different concepts to be tested in operation using plastic prototypes and plasticine feedstock material. Ideally, all concepts should have been tested in full-scale by building steel prototypes. However, such an approach would be time-consuming and costly.

The experimental setup used in this study is described in Section 4.4. Prior to each test, a layer of plasticine was evenly distributed on the machine bed to make up a substrate for the extrudate to be deposited upon. The substrate was levelled to that of the outlet of the extruder. A machine program, reflecting the dimensions and stacking sequence of the stringers to be deposited along with feed and extrusion speeds was written. Due to the directional design of the extruders, the deposition was carried out while scanning in one direction only. A test cycle typically consisted of deposition of two or more stringers side-by-side to make up a layer, and two or more stringers on top of that.

The criteria for evaluating each concept continuously emerged as new insights were gathered from each iteration. The criteria are listed in the following:

- *Tool forces* are resulting from sticking friction between the extruder parts and the substrate. These forces can be reduced by minimising the die outlet and the die wall thickness. Low tool forces can ultimately allow the extruder to be controlled by less rigid robots like Scara-arms.
- *Process control* relates to the tunability of the process and indicates whether parameters like rotational speed, feed-rate and temperatures can be controlled independently.
- *Flash formation* is a result of the pressure level inside the extruder and the clearance between the moving parts, and some flash will always be formed. However, the design should minimize this formation by using the lowest possible extrusion pressure combined with stiff components and tight clearance fit between the moving parts. Furthermore, the design should allow flash to be removed continuously to reduce friction between moving parts.

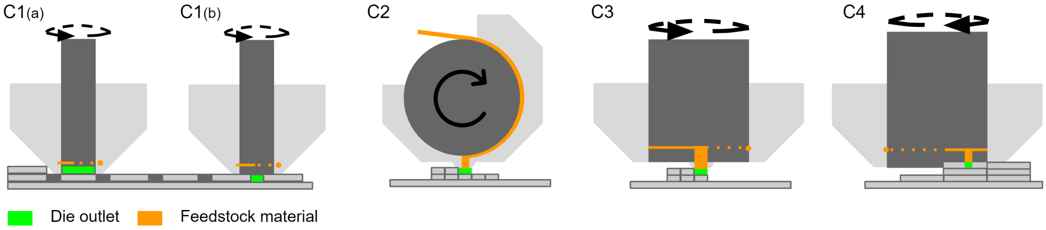

Figure 5.3: Set of alternative extrusion and deposition concepts (C1 - C4) that have been evaluated during the case study; (a1) C1: PinPoint extruder with flat pin; (a2) C1: PinPoint extruder with protruding pin; (b) C2: wheel extruder; (c) C3: Spindle Extruder (d) C4: Rotating die extruder; all of these extruders are based on the wire fed continuous rotary extrusion process.

- *Oxide removal* is crucial for proper bonding between extrudate and substrate. Any oxides present on the mating surfaces will reduce the bond quality.
- *Resolution* is a measure for stringer size and indicates the level of details that can be deposited. A coarse structure is likely to cause more material wastage during post machining and is not preferred.
- *Wire slip* is a measure of the circumferential speed of the spindle compared to the feedstock wire speed. The feedstock wire should be firmly engaged in the conform slot and the length of the slot sufficient to avoid wire slip.
- *Contact friction* between spindle and housing should be reduced to avoid excessive work and heat generation during extrusion.
- *Serviceability and design simplicity*. Ease of assembly and disassembly. When used for aluminium, the parts that are in contact with the feedstock will bond to the aluminium and will need to be cleaned in sodium hydroxide prior to disassembly.
- *Deposition quality* relates to the density of the deposited structure. The structure should be continuous and void-free.

The concepts

A total of four concepts was prototyped and modelled in this study. These are; (1) the PinPoint extruder; (2) the wheel extruder; (3) the spindle extruder, and; (4) the rotating die extruder. Extruders 1-3 are designs that initially were developed for welding purposes, see Chapter 3. The fourth extrusion concept, the rotating die extruder, is a design that has emerged during the exploration of the other concepts. This extruder uses a spindle of the same diameter as that of the spindle extruder, and has the dies cut into the lower section of the spindle. The rotating die extruder aims at reducing the tool forces by minimizing the die outlet area. The material is extruded in radial direction while the spindle is rotating, thus depositing layers transverse of the stringer orientation. The rotation of the spindle is furthermore supposed to interfere with the substrate to continuously break up the oxide layer.

Results

Among the tested concepts, the spindle extruder got the highest rating and was selected for further development of the HYB-AM process. The spindle extruder is built around a spindle that is slightly tilted from the vertical axis in the feed direction. A groove is cut into the lower part of the spindle for providing the required extrusion pressure.

Observations made and their influence on further work

The combination of rapid prototyping and physical modelling allowed for evaluation of the different extruder and deposition concepts for the HYB-AM process. Furthermore, new insights into the process along with requirements for the further development of the process emerged. The applied concept evaluation strategy proved to be efficient in terms of allowing for multiple concepts to be assessed in parallel. Hence, the approach can be valuable for other complex product development projects where the costs of building full-scale prototypes are high. Paper 3 is written as a methodology paper that highlights these potentials.

5.4 Paper 3

Title	Concept evaluation in new product development: A set-based method utilizing rapid prototyping and physical modelling.
Authors	Jørgen Blindheim, Christer Elverum, Torgeir Welo & Martin Steinert
Purpose	Based on the outcome of Paper 2, this paper proposes the combination of rapid prototyping and physical modelling as a concept evaluation method for early stage product development.
Research objective 1	To apply the proposed method on a case study involving concept evaluation using plastic prototypes and physical modelling of the product functionality
Research objective 2	To determine the validity of the approach by comparing the most suitable concept of the first objective to that of a full-scale prototype of the same process.
Personal contributions	First author; led the writing of article drafts and final version with inputs from co-authors. Planning of the study. Conducted the case study, including the full-scale verification experiment. Developed the suggested evaluation method. Prepared all illustrations.

Research approach

The method was demonstrated through the case that was presented in Paper 2. Rather than building parts from tool steel, plastic versions of the extruders were produced by rapid prototyping, and the performance was tested using plasticine as modelling material.

Results

Through multiple test-cycles, new insights along with requirements for the further development of the process emerged. After evaluating all the concepts, one was selected for full-scale prototyping. The full-scale prototype behaves similarly to that of the plastic version of the extruder which suggests that this approach can produce usable results using lower resolution prototypes.

Academic contribution

This set-based approach allows a design team to map the solution space by assessing multiple concepts in parallel. Each concept is explored through incremental iterations until the concept is either abandoned or selected for further development. Rather than converging on a "best guess", the suggested method serves as a way to allow a design team to gather new insights and increase the confidence in the selected concept.

This approach can be applied for other projects where the problem definition and requirement specifications still contain many degrees of freedom and where the expenses of building full-scale prototypes are high.

5.5 Paper 4

Title	First demonstration of a new additive manufacturing process based on metal extrusion.
Authors	Jørgen Blindheim, Torgeir Welo & Martin Steinert
Purpose	This paper presents the first full-scale demonstration of the extrusion and deposition concept identified in Paper 2.
Research objective 1	To conduct a proof-of-concept test of the extruder and deposition sequence
Research objective 2	To assess the technical feasibility and potential of the proposed concept with regards to material properties, deposition rates, energy efficiency and material efficiency.
Personal contributions	First author; led the writing of article drafts and final version with inputs from co-authors. Planned the study. Developed the extruder and deposition sequence. Designed and produced the extruder parts and built the experimental setup. Conducted the experiments. Prepared all illustrations. Sample preparation, microscopy analysis and interpretation of results. Assessment of process potentials including calculations of energy efficiency.

Research approach

A full-scale prototype was produced based on the concept identified from Paper 2. The details of the experimental setup are described in Section 4.4. The process was demonstrated by producing samples from AA6082 feedstock material.

Results - material properties

Optical macrographs of a transverse section of a deposited structure are shown in Figure 5.4. Figure 5.4a shows the substrate material with two layers deposited on top. From the macrograph, it is visible how the stringers have been conformed to the under-laying material, indicating that the interfaces have been subjected to contact pressures above the flow stress of the material. Still, defects in the form of cracks can be observed between the individual stringers, as depicted in Figure 5.4c, meaning that the layers are not fully bonded. A possible reason for this can be oxide formation on the interfaces during deposition. This failure mechanism is similar to that observed in longitudinal seam welds in porthole die extrusion when a gas pocket is present behind the bridge Yu et al. (2016).

Figure 5.4b displays the occurrence of a pore between the two stringers of the first layer. Higher extrusion pressure can to some extent prevent this defect. However, a more suitable solution is to reduce the angle of the sidewall of the adjacent stringer in order to avoid the sharp corner and thus create more favourable material flow conditions.

Results - deposition rates

From an industrial perspective, deposition rates are crucial for increasing the manufacturing efficiency. The deposition rate of the demonstrated process is controlled by the circumferential velocity of the conform wheel and the diameter of the feedstock wire. The extruder was designed for Ø1.6 mm feedstock wire, providing a deposition rate of more than 2 kg/h at its theoretical maximum speed of 100 RPM. This high deposition rate makes this AM technology particularly suitable for manufacturing of larger structures where this capability can be fully utilized. In theory, the deposition rate is only limited by the scaling of the process. However, the deposition rate must be balanced and compatible with other requirements, such as scanning

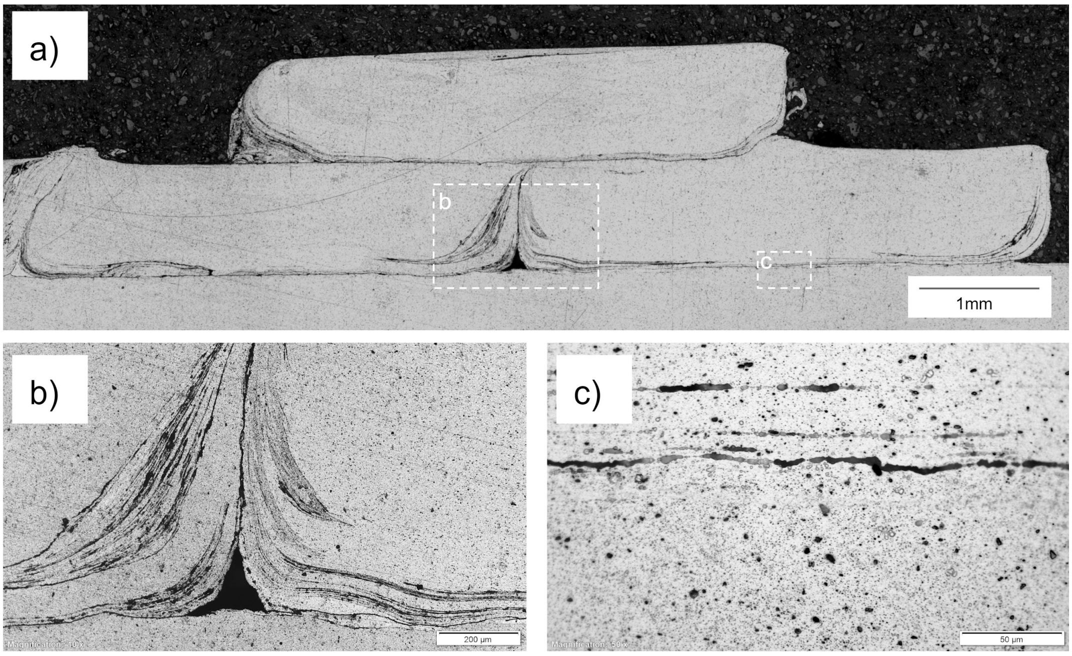

Figure 5.4: Optical macrographs of; (a) a transverse section of a deposited structure; (b) pore formation at the interface between two adjacent stringers; (c) cracks on the interface between the substrate and a stringer.

speed, geometry of the die, as well as the process temperature and the contact pressure at the bonding interface.

Results - energy efficiency

The work done on the deposited material was calculated from the rotational speed and the supplied torque on the extruder along with the feed distance and the applied force in the feed direction from the following formulae; $W_i = 2\pi MN + Fs$.

The extruder is subjected to a torque of M = 175 Nm at a rotational speed of N = 4.3 RPM and a feed speed of 200 mm/min. Assuming sticking friction over the contact area of the die outlet, the force in the feed direction, F, is in the order of 1,500 N at the extrusion temperature used. The supplied power during the experimental run was calculated to 84W.

To calculate the energy efficiency of the process, the applied work was compared to that of the required heat input, Q, to bring the material up to extrusion temperature. This was estimated from the specific heat capacity of the feedstock material, c = 987 J/kgK, the deposition rate and the temperature change, $\Delta T = 430K$ from $Q = cm\Delta T$

Based on this, the overall efficiency of the process was calculated to η = 0.16, thus indicating that the process generates excess heat which needs to be dissipated during processing. Comparable power input for CMT processing is reported to 1,430 W for welding of AA5183 Ø1.2 mm wire at 7m/min (Dutra et al., 2015). Under the assumption of proportionality between the power input and the deposition rate, the energy consumption of the HYB-AM process is 30% less than that of the CMT process.

Results - materials

For the experiments reported in this paper an Al-Mg-Si alloy was used. However, the process also has the potential of depositing other advanced aluminium alloys or extrudable metals, even from the more ad-

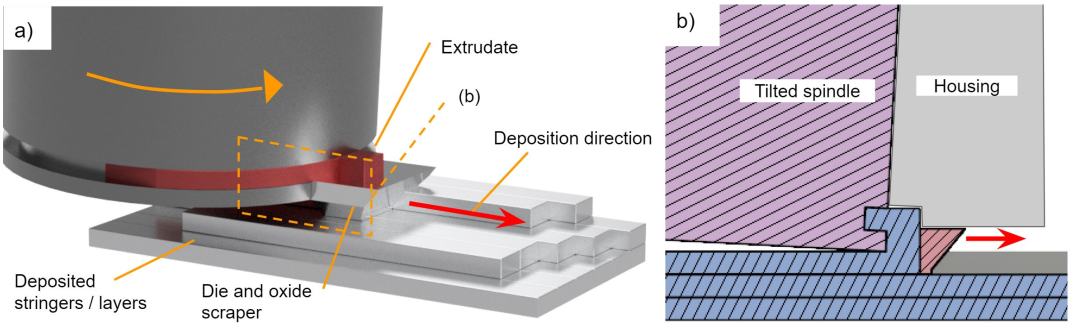

Figure 5.5: Illustration of the first version of the extruder. The spindle constitutes the fourth wall of the die and makes for the shortest possible die length of the designs; (a) a possible deposition sequence where the die is used as an oxide scraper; (b) section through the spindle and die. The spindle is tilted to reduce interference with the substrate.

vanced aerospace AA7000 series, which for most purposes are considered unweldable by the melted-state processes. Furthermore, the nature of additive processing means that the feedstock composition can be altered during processing to create functionally graded components having tailored material properties in specific regions of a part.

For precipitation hardening alloys, like Al-Mg-Si, it is necessary to carry out solution heat treatment followed by quenching and ageing to utilize the full strength potential of the part. By depositing at the solution heat treatment temperature, the part can be soaked for the required time for supersaturation of the whole structure. Finally, after quenching, the desired ageing cycle can be carried out to control the formation of precipitates.

Results - materials efficiency

The relatively coarse near-net-shape structure requires subtractive machining to obtain the final shape and tolerances. This final processing step will cause material waste depending on the requirements of the net-shape; however, obviously with significantly less waste than that of machining from solid blanks. Allen lists BTF ratios ranging from 6 to 20 for some typical titanium aero engine components Allen (2006), while Barnes Barnes et al. (2016) reports a BTF industry average of 11 for machined parts. Martina and Williams (2015) considered different manufacturing options for a 15 kg aluminium wing rib and calculated a cost reduction of 65% for producing it by the WAAM process at a deposition rate of 1 kg/h and a BTF ratio of 2.3, as opposed to 40 for machining from a solid blank. With the new process proposed in this paper, it is reasonable to achieve BTF ratios comparable to that achieved by the WAAM process, depending on the final part geometry.

Industrial contribution

A novel way of depositing a multi-layered structure was presented in this study. Furthermore, some key characteristics related to industrial application were discussed.

Implications for the further work

The die design that was utilized in this version of the spindle extruder is beneficial when it comes to obtaining low extrusion pressure. However, the continuous interference with the deposited stringer leads to material build-up at the end of the spindle. This, ultimately, causes the extruded material to rather stick to the spindle than to the under-laying surface. Hence, a die that is isolated from the wheel is required to further improve the process. This updated die design is implemented in Paper 5.

5.6 Paper 5

Title	On the mechanical integrity of AA6082 3D structures deposited by hybrid metal extrusion & bonding additive manufacturing.
Authors	Jørgen Blindheim, Øystein Grong, Torgeir Welo & Martin Steinert
Purpose	In this paper, the layer bonding of AA6082 samples produced by the latest extruder prototype was investigated by means of tensile testing, hardness measurements and microscopy analysis. Furthermore, a novel tensile testing method was applied.
Research objective 1	To assess the bond strength between layers
Research objective 2	To apply a new method for fabrication of miniature specimens for tensile testing
Personal contributions	First author; led the writing of article drafts and final version with inputs from co-authors. Planned the study. Developed the extruder and deposition sequence. Designed and produced the extruder parts and the experimental setup. Conducted all the experiments. Prepared all illustrations. Sample preparation and microscopy analysis. Post-processing of demo-part. Developed the new method for tensile testing. Produced specimens and conducted tensile testing and hardness measurements.

Research approach
This paper aims at assessing the mechanical integrity of samples produced by the second version of the extruder (Figure 5.6). In order to determine the bond strength between the layers, a new tensile test method was developed. By using a single cutting thread mill, miniature specimens with a length constituting the height of two stringers were machined into the sample. This allowed the bonding interface to be located in the reduced section of the specimen, as depicted in Figure 5.7. The reduced section of the specimens had a length and a diameter of 1.0 mm and Ø0.96 mm, respectively, and a total length of 1.8 mm. A split collar was used to grip the head of the specimens while keeping the sample fixed to the lower section of a test machine. The total displacement and the load were measured on a MTS Criterion Model 42 ball screw universal testing machine, at a cross-head speed of 1 mm/min and a sampling frequency of 10 Hz. Hardness measurements were made using a Mitutoyo Micro (HM200 series) Vickers hardness testing machine at a constant load of 1 kg. Six individual randomly located measurements were carried out for both the substrate and the extrudate for both sample sections.

Results
The macrostructure of a transverse section of a sample is shown in Figure 5.8. The interface between the substrate and the extrudate is clearly visible after etching, showing that the mating interfaces have merged into a fully dense material. Still, the section reveals some defects in the form of cracks, as depicted in Figure 5.8c and d, indicating variable bonding quality. Two possible reason for the crack formation can be: (1) Too low contact pressure during deposition, prohibiting full metallic contact between the merging interfaces; or: (2) Oxide formation on the interfaces during deposition due to exposure to oxygen. The latter being similar to that observed in longitudinal seam welds in porthole die extrusion when a gas pocket is present behind the bridge, as reported by Yu and Zhao (2018).

The mean tensile properties of all specimens indicate that there are no significant difference in the ultimate tensile strength (UTS) of the layered material as opposed to the substrate material. Still, when considering

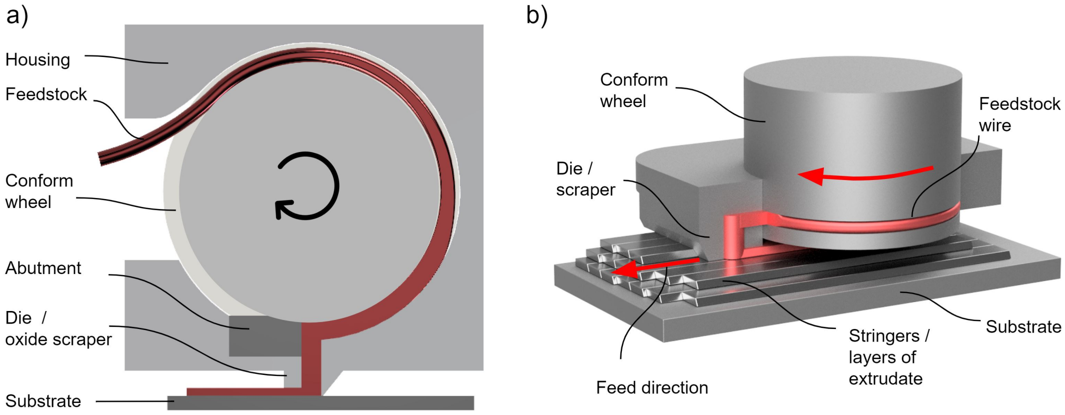
a)
Housing
Feedstock
Conform wheel
Abutment
Die / oxide scraper
Substrate
b)
Conform wheel
Feedstock wire
Die / scraper
Substrate
Stringers / layers of extrudate
Feed direction

Figure 5.6: Principal illustrations of the second version of the extruder; (a) the extruder consists of a wheel with a groove surrounded by a stationary housing. The feedstock wire is pressed into the groove, and upon rotation the extrusion pressure is built up as the material is blocked by an abutment close to the die. The die also act as a scraper in order to remove oxides from the substrate prior to bonding with the extrudate; (b) rendering of the extruder and a deposited structure.

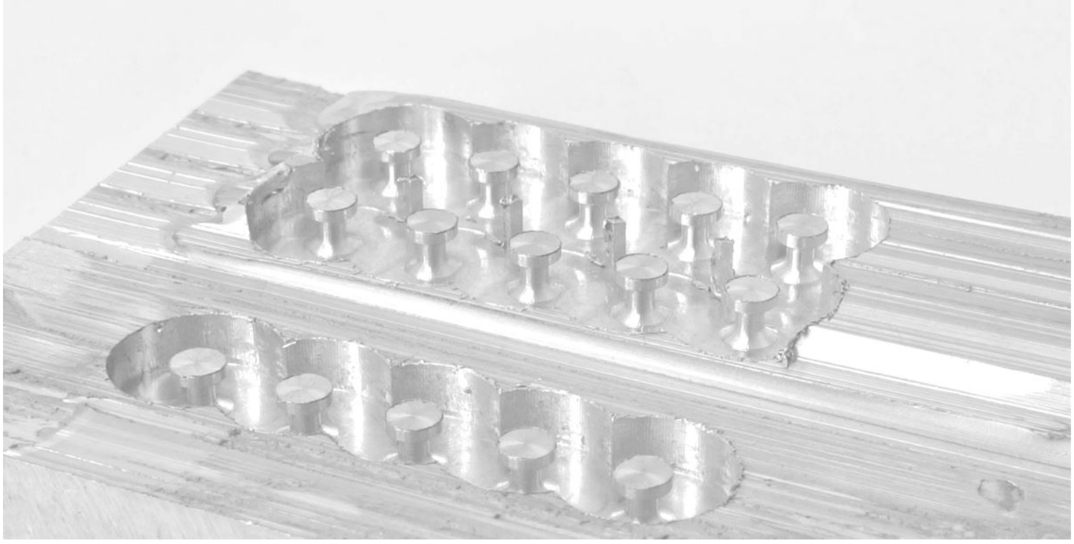

Figure 5.7: Tensile specimens used for testing of the substrate material and the layered structure.

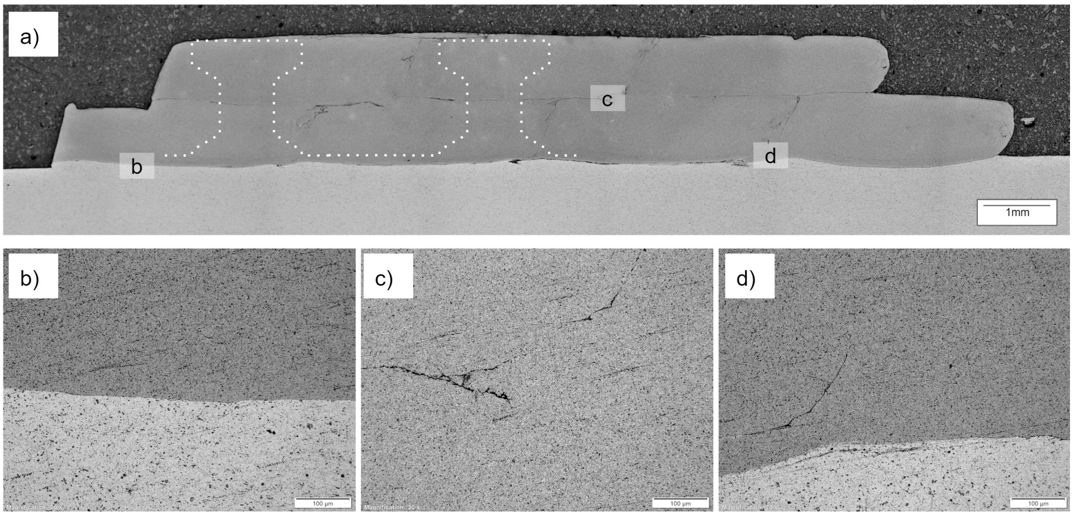

Figure 5.8: Optical micrographs of; (a) section of a deposited structure along with the superimposed contours of the tensile specimens; (b) the bonding interface between the substrate and the first layer; (c) and (d) voids observed at the interface between two stringers.

the stress vs. displacement curve for one of the samples (Figure 5.10), it is obvious that the elongation, and thus, the ductility is lower for the specimens covering the layer interface.

Fractographs of representative specimens (Figure 5.9) furthermore confirms this behaviour. Figure 5.9a clearly shows regions with lack of bonding. Figure 5.9b represents the specimen with the highest elongation prior to fracture, and also here, regions of kissing-bond formation are visible. Still, extensive dimple formation is observed, indicating that metallic bonding is obtained (Figure 5.9d and e).

Figure 5.9c shows the comparable fractograph from a specimen made from the substrate material. The dimple formation (f) is similar to that observed for the layer interface. The difference in cross-section is also noticeable, reflecting a more ductile response of the substrate specimens, as shown by the tensile test data in Figure 5.10.

The hardness values are ~12% lower for the substrate material compared to the extruded material. The higher hardness of the extruded material is believed to be the result of the high silisium content of the extruded material, which contributes to significant solid solution hardening, as pointed out by Callister et al. (2013). In addition, the extrudate contains the dispersoid-forming elements Mn, Cr and Zr. These elements prevent recrystallization during deposition and therefore facilitate the formation of a substructure in the bonded layers with a high dislocation density and thus higher hardness than that of the substrate material (Hatch, 1984).

Industrial contribution

Through the fabrication of samples and the subsequent assessment of the layer bonding, the technical feasibility of the HYB-AM process was conclusively demonstrated in producing mechanically sound 3D structures.

Academic contribution

A novel method for fabrication of tensile specimens for assessing the bond strength across the layers was developed. The miniature specimens were milled from the samples using a thread cutting mill. In this way, the specimens could be located such that the interface between separate layers crosses the reduced section of the specimens. This allowed the bond strength between the layers to be tested in pure tension.

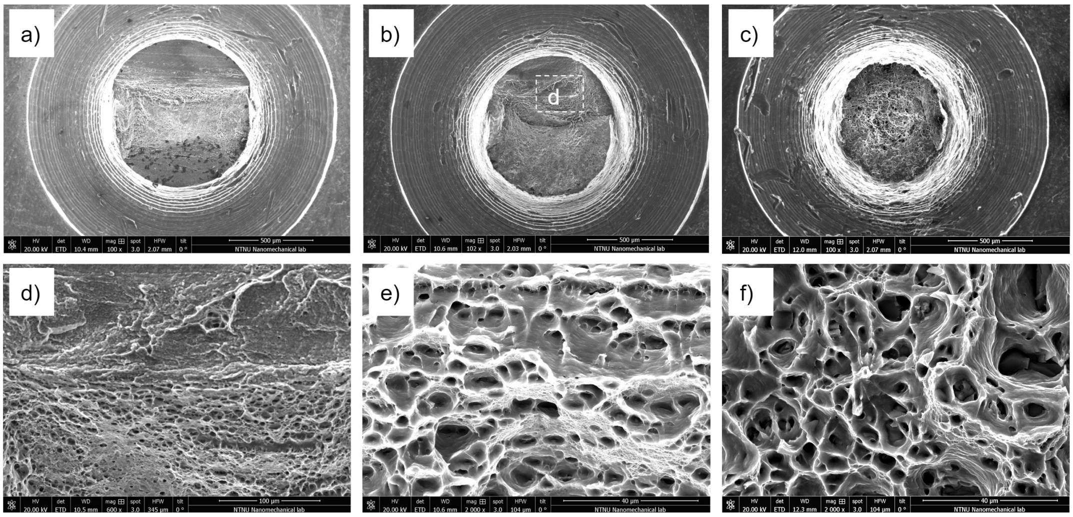

Figure 5.9: SEM fractographs of fracture surfaces from three broken specimens. The corresponding tensile test results are plotted in Figure 5.10; (a) fracture surface of specimen B3; (b) fracture surface of specimen B4; (c) fracture surface of substrate specimen S1; (d) mixed region with kissing-bond and dimple formation in specimen B4; (e) dimpled fracture surface observed in specimen B3, and; (f) dimpled fracture surface observed in specimen S3.

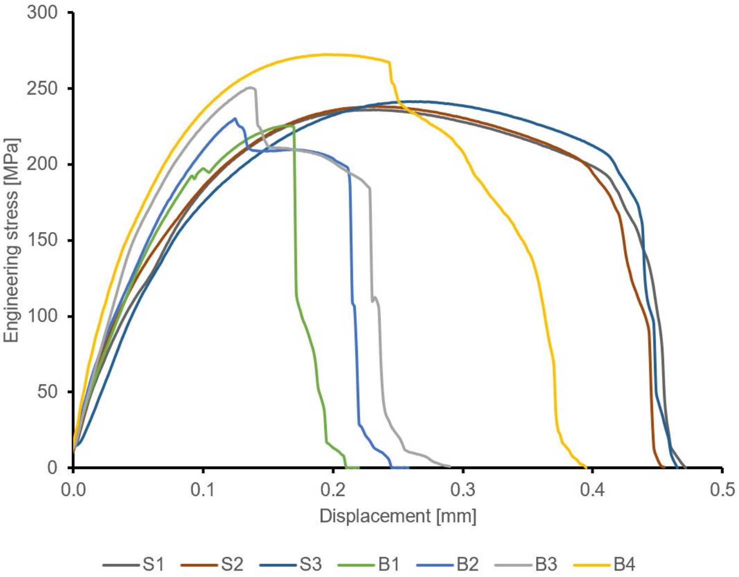

Figure 5.10: Engineering stress vs. displacement curves for different tensile specimens. Four specimens, B1-B4, crossing two bonded layers, and three specimens representing the substrate material, S1-S3.

Implications for the further work

The results from the mechanical testing display an ultimate tensile strength of the bonded layers approaching that of the substrate material, yet at lower elongation prior to fracture. Moreover, inspections of the fracture surfaces show evidence of extensive dimple formation. This indicates that metallic bonding is achieved between the layers. However, regions of kissing-bonds and lack of bonding are also present, thus calling for further process optimization. In order to better understand the material flow, FEM-analyses will be employed in the following study.

5.7 Paper 6

Title	Investigating the Mechanics of Hybrid Metal Extrusion & Bonding Additive Manufacturing by FEA.
Authors	Jørgen Blindheim, Torgeir Welo & Martin Steinert
Purpose	In this study FEA was applied, using Deform 3D software, to observe, analyse and interpret the material flow in the extruder and at the bonding interface between the substrate and the extrudate. The purpose of this study has been to increase the understanding of the governing mechanisms in order to identify optimal processing parameters.
Research objective 1	To study the material flow in the extruder with regard to extrusion grip length, contact pressure, peak temperatures and strain-rates at steady-state for two different deposition rates.
Research objective 2	To investigate the thermo-mechanical conditions for the bonding interface between the extrudate and the substrate with regard to the obtained contact pressure at different ratios between extrusion flow rate and feed speed.
Personal contributions	First author; led the writing of article drafts and final version with inputs from co-authors. Planned the study. Prepared CAD models. Made FEM-models and conducted all simulations. Prepared all illustrations.

Research approach

The FEM analyses were conducted in commercially available Lagrangian Deform 3D software. The overall design of the parts for the FEM-model was similar to that used for the final full-scale experiment. However, the geometry was modified such that interference was added between all moving parts to prevent loss of nodes during simulations. Flow stress data for AA6082, as a function of strain and temperature for various strain rates, were obtained from the material library in the software. Two separate models were prepared to address the two objectives; Pressure generating mechanism (model 1), and stringer deposition sequence (model 2)

Model 1: The numerical model of the extruder consisted of; the housing, the conform wheel and the feedstock material. The abutment and the die geometry were merged with the housing to simplify the meshing of the FEM-model. Referring to the first objective (1), the investigations were focused on observing the material flow at steady-state conditions. Simulations were, therefore, started with a filled chamber and die, however, the extrusion grip length was shorter than what was expected to see at steady-state. The feedstock wire was partially formed to the shape of the groove in the wheel, yet having the same cross-section as that of the Ø1.6 mm feedstock wire. A rigid geometry, representing the substrate was placed at the die outlet to obtain extrusion pressures at the same level as that achieved during normal operation. Two different simulations were carried out for model 1, where the angular velocity of the wheel was the only parameter subjected to change. The Tresca friction model was used for modelling contact friction; $\tau = m \cdot k$, (Valberg, 2006), where τ is the frictional stress, m is the friction factor and k is the shear yield stress. The friction factor between the feedstock material and the tooling was kept constant with an arbitrary high friction factor, $m = 2$, to ensure sticking friction condition with no sliding. The feedstock was modelled as a rigid-plastic material and the tooling was modelled as a rigid surface.

Model 2: A separate model was made to study the material flow and normal pressure at the interface between the die outlet and the substrate. In this model, both the substrate and the feedstock were modelled

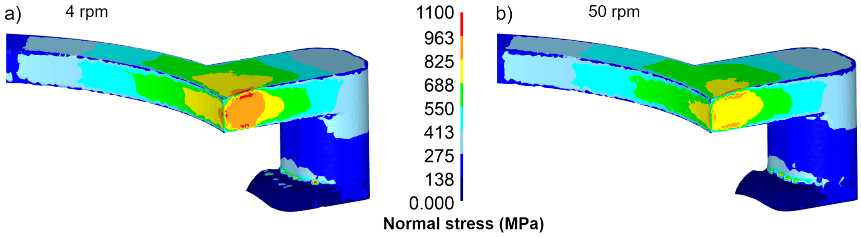

Figure 5.11: Normal pressure in the extrusion grip zone; (a) rotational speed 4 RPM; (b) Rotational speed 50 RPM.

as rigid-plastic. The material supply in this model was simplified using the direct extrusion principle. The substrate model resembled the shape of multiple preceding layers and some stringers of the current layer. The substrate was fixed on a rigid bed, which could move along the feed axis. For the two simulations carried out for model 2, the feed speed was kept constant, while the material flow rate was altered.

Results

Model 1: Simulations were carried out at two different deposition rates, 4 RPM and 50 RPM, the former being the speed used for the final full-scale experiments. At 50 RPM, the flow stress was expected to increase due to the increased strain-rates; however, the temperature also increased. At 4 RPM the temperature peaked at 330°C, while at 50 RPM the temperature reached 550°C.

Figure 5.11 illustrates the contact pressure between the feedstock material and the walls of the groove and the housing. For both rotational speeds, the contact pressure was of the same magnitude, despite the difference in flow rate.

Model 2: The only parameter subjected to change in model 2 was the ratio between the ram speed and the feed speed. At a balanced ratio, the volumetric flows at both the inlet and the outlet (the rear opening between the substrate and the die) were equal, whereas at high speed the inlet flow was increased by 20 % through increased ram speed. In the simulations, the ram was moved for 1 second to have the extrudate fill the die cavity prior to moving the bed.

Figure 5.12 illustrates the effective stress for the balanced and high ratios of ram vs. feed speed, respectively. For the balanced ratio, it can be seen that after 1.2 s the section of the die cavity is completely filled (5.12a). However, as deposition proceeds, a pocket is formed in the front part of the die (5.12b). For the high ratio (5.12c and d), the plastic region of the substrate is higher than for the balanced ratio after 1.2 s, and the stress levels have further increased after 5 s.

Figure 5.13 illustrates the normal stress in a section through the die, perpendicular to the deposition direction. For the balanced speed ratio, the normal stresses exceed 55 MPa only in the centre part of the die, whereas for the high ratio, the full width of the stringer is subjected to contact stresses above the estimated bonding threshold.

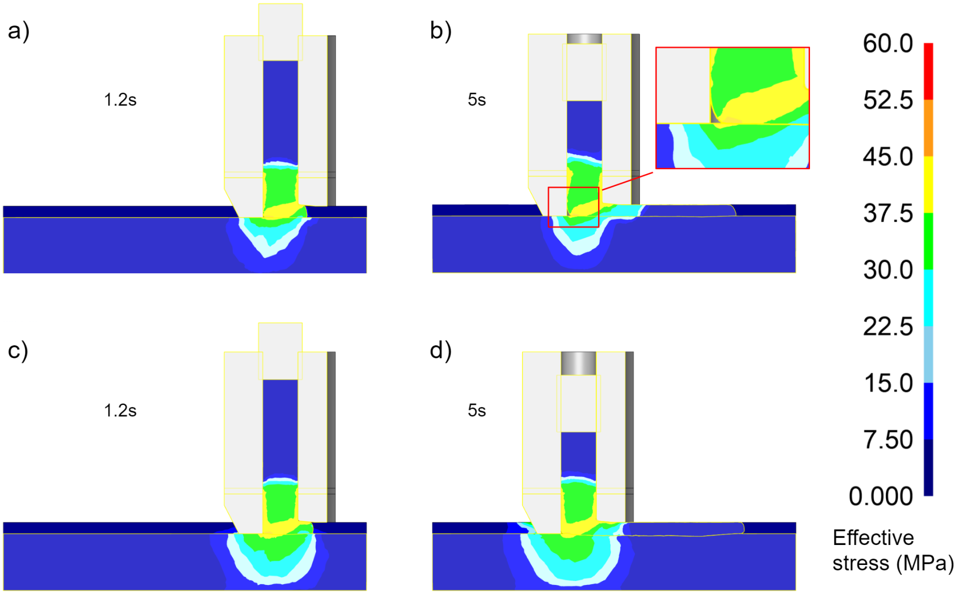

Figure 5.12: Effective stress during deposition at 500°C; (a) balanced ratio - after 1.2s the die cavity is filled and the feeding has started; (b) balanced ratio - after 5s a pocket is formed in the front section of the die; (c) high ratio - after 1.2s the die cavity is filled. (d) high ratio - after 5s the die cavity is still full and the effective stress has increased.

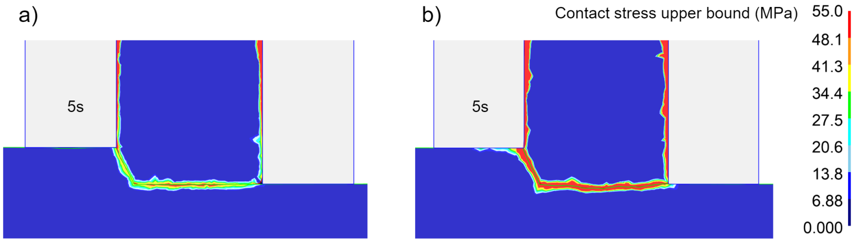

Figure 5.13: Normal pressure in a section through the die transverse to the feed direction; (a) balanced speed ratio; (b) high speed ratio, 20% over-extrusion.

New insights

At high rotational speeds, the strain rates in the plastic zone obviously increase. However, the temperatures also increase as a result of (adiabatic) heating due to deformation work. This temperature increase, in turn, reduces the flow stress of the material, and despite the higher strain-rate, the length of the extrusion grip zone remains virtually unchanged.

Prior full-scale experiments have been carried out at low deposition rates to avoid putting excessive stress on the prototype extruder. However, from the FEA results it is clear that there is no significant increase in contact pressures at higher deposition rates. Hence, future experiments can utilize higher flow rates without damaging the extruder.

Considering the bonding interface between the extrudate and the substrate, the FEA results clearly show the importance of using a correct deposition rate vs. feed speed. If the extruder fails to deliver the correct volume flow, the contact pressure at the interface will drop below the bonding threshold, resulting in substandard samples. Moreover, the simulations show that a gas-pocket is formed inside the die. When the scraped surface of the substrate is exposed to this pocket, a new oxide layer can be formed, causing potential conditions for further reduced layer bonding.

When using feedstock material with a smaller cross-sectional area than that of the groove, the length of the extrusion grip zone will vary depending on the extrusion pressure. A change in the conditions at the die outlet will call for a change in pressure, and thus, the extrusion grip length will have to adapt similarly. Since the feedstock material is supplied at a constant speed, the flow rate out of the die will be subject to reduced flow while the extrusion grip length is increased. Thus, the process is in such vulnerable to fluctuations in the provided flow rate and pressures. However, by filling the entire cross-section in the grip zone by means of a coining wheel, the process will respond better to changes in pressures. This can also be beneficial in terms of reduced heat generation, as the slip in the extrusion grip zone will be reduced correspondingly.

6. Conclusions and suggestions for future work

6.1 Conclusion on the main objective

The overall contribution of this thesis work is the demonstration of a new method for solid-state deposition of 3D metal structures. The main objective of the thesis has been:

> To develop the HYB-AM process through concept evaluation and full-scale experimental testing, making it possible to assess the mechanical integrity of a deposited structure and understand the governing mechanisms of the process.

In this work, the HYB-AM process has been taken from concept level to a working prototype, capable of depositing aluminium feedstock material. A new method based on rapid prototyping and physical modelling has been used to evaluate different deposition concepts, and the full-scale process has been demonstrated by deposition of samples of AA6082. Microscopy analyses and mechanical testing have been used to assess the mechanical integrity of samples. Furthermore, FEA has been used to simulate the material flow during processing, thus providing new insights into the governing mechanisms of the process.

6.2 Task-based conclusions

A novel set-based approach for concept evaluation has been developed and applied in this work. The combination of rapid prototyping and physical modelling made it possible to test and evaluate multiple extruder and deposition concepts without having to build full-scale steel prototypes. Plastic models of the different extruder concepts were produced by rapid prototyping and attached to a small CNC-machine. To test the function of each design, plasticine was processed through the extruders and deposited on the machine bed. Through the evaluation of all the modelled concepts the extruder design for full-scale testing was identified.

The process has been demonstrated in full scale by successfully depositing samples of AA6082. The layer-to-layer bonding has been investigated by means of tensile testing, hardness measurements and microscopy analysis. A novel method for the fabrication of miniature specimens for tensile testing was developed and applied. The test results demonstrate an ultimate tensile strength approaching that of the substrate material of the same alloy, yet with somewhat lower tensile ductility. Microscopy analyses show that the bonding interfaces are fully dense; however, the fracture surfaces reveal regions of kissing-bonds and lack of bonding. Still, the technical feasibility of the HYB-AM process has been conclusively demonstrated in producing mechanically sound 3D structures.

Numerical simulations have been used to identify and characterize the optimal processing parameters, and further understand the governing mechanism of the process. More specifically FEA was used to study material flow in the extruder, as well as the conditions at the interfaces of the deposited extrudate and the substrate. Analysis of the material flow shows that the extrusion pressure is virtually independent of the deposition rate. Furthermore, from the simulations of the material deposition sequence, it is visible how the contact pressure at the interface will drop below the bonding threshold if the feed speed becomes too high relative to the material flow through the die.

6.3 Industrial and academic implications

The industrial implications of this thesis work are mainly related to the developed process itself.

- A new AM process based on wire feedstock material which is processed through a continuous extruder. The material is deposited in a stringer-by-stringer manner to form layers and eventually near-net-shapes. The material is deposited and bonded in the solid-state, thus enabling the use of advanced aluminium alloys.

Furthermore, throughout this work several results of academic interest have been discovered.

- A new AM process. Future research should target processing of other metals as well as process improvements.
- A new method for concept evaluation, based on physical modelling and rapid prototyping. The method can be useful for early-stage projects where the costs of building full-scale prototypes are high.
- A new method for tensile testing has been developed and used for investigation of layer-layer bond quality. This method can be applicable for material testing of other materials of small sample size.

6.4 Recommendations for further work

Referring to the main objective, this work has mainly focused on the conceptualization and the preliminary testing of the process. Hence, there are still many issues that need to be resolved prior to further industrialization of the process.

Process stability	Orientation of spindle should be adjusted to avoid interference with the deposited material. Furthermore, the die should be redesigned to allow for stronger bolt connections.
Durability	The extruder needs to be tested on longer time spans to assess its durability. Wear of the internal parts in contact with the feedstock needs to be observed and controlled.
Other materials	Despite having been demonstrated only for aluminium alloys, the HYB-AM process has the potential of processing other extrudable metals like Mg and Cu. Even Ti alloys have been extruded by the conform process and are such of interest for AM-processing.
Improved bonding	In its current state the process is vulnerable to lack of bonding due to oxide formation on the bonding interface. Future developments should aim at increased deformations of the bonding interface to disperse surface oxides of the substrate.
Energy efficiency	Lower processing temperatures (reduced heat radiation and convection), reduced contact surfaces (optimize spindle diameter) as well as reduced extrusion pressures (shorter die length, coatings) can contribute to increased energy efficiency of the process.

Microstructure	For the further development, microstructural characterization of the resulting AM deposit needs be carried out.
Coining of feedstock	Slip can be reduced in the extrusion zone by coining the feedstock material to the same cross-section as that of the groove in the wheel. At high deposition rates, preheating of the feedstock material using induction heating should be considered.

Bibliography

Aakenes, U. (2013). *Industrialising of the Hybrid Metal Extrusion & Bonding (HYB) Methodfrom Prototype towards Commercial Process.* PhD thesis, Norwegian University of Science and Technology.

Aeroprobe. MELD Overview.

Allen, J. (2006). An Investigation into the Comparative Costs of Additive Manufacture vs. Machine from Solid for Aero Engine Parts. In *RTO-MP-AVT-139*, page 10.

ASTM (2015). *Standard Terminology for Additive Manufacturing – General Principles – Terminology.* ISO/ASTM 52900:2015(E).

Atwood, C., Ensz, M., Greene, D., Griffith, M., Harwell, L., Reckaway, D., Romero, T., Schlienger, E., and Smugeresky, J. (1998). Laser engineered net shaping (LENS (TM)): A tool for direct fabrication of metal parts. Technical report, Sandia National Laboratories, Albuquerque, NM, and Livermore, CA.

Barnes, J., Kingsbury, A., and Bono, E. (2016). Does " Low Cost " Titanium Powder Yield Low Cost Titanium Parts?

Bay, N. (1983). Mechanisms producing metallic bonds in cold welding. *WELDING J.*, 62(5):137.

Blindheim, J., Grong, Ø., Aakenes, U. R., Welo, T., and Steinert, M. (2018). Hybrid Metal Extrusion & Bonding (HYB) - a new technology for solid-state additive manufacturing of aluminium components. *Procedia Manufacturing*, 26:782–789.

Callister, W. D., Rethwisch, D. G., and others (2013). *Materials science and engineering: an introduction*, volume 9.

Conrad, H. and Rice, L. (1970). The cohesion of previously fractured Fcc metals in ultrahigh vacuum. *Metallurgical Transactions*, 1(11):3019–3029.

Cooper, D. R. and Allwood, J. M. (2014). The influence of deformation conditions in solid-state aluminium welding processes on the resulting weld strength. *Journal of Materials Processing Technology*, 214(11):2576–2592.

Crump, S. S. (1992). Apparatus and method for creating three-dimensional objects.

De Chiffre, L. (1989). Cut welding. *CIRP Annals-Manufacturing Technology*, 38(1):125–128.

Deckard, C. R. Method and apparatus for producing parts by selective sintering.

Desaguliers, J. T. (1724). Some experiments concerning the cohesion of lead. *Philosophical Transactions of the Royal Society of London*, 33(389):345–347.

Deshpande, A. and Hsu, K. (2018). Acoustoplastic metal direct-write: Towards solid aluminum 3d printing in ambient conditions. *Additive Manufacturing*, 19:73–80.

Dieter, G. E. and Bacon, D. J. (1986). *Mechanical metallurgy*, volume 3. McGraw-hill New York.

Dilip, J. J. S., Rafi, H. K., and Ram, G. J. (2011). A new additive manufacturing process based on friction deposition. *Transactions of the Indian Institute of Metals*, 64(1-2):27.

Ding, D., Pan, Z., Cuiuri, D., and Li, H. (2015). Wire-feed additive manufacturing of metal components: technologies, developments and future interests. *The International Journal of Advanced Manufacturing Technology*, 81(1-4):465–481.

Dorph, P. and De Chiffre, L. (1995). Physical modelling of cut welding. *Journal of materials processing technology*, 51(1-4):131–149.

Dorph, P., De Chiffre, L., and Bay, N. (1993). Experimental analysis of cut welding in aluminium. *CIRP Annals-Manufacturing Technology*, 42(1):357–360.

Dutra, J. C., Gonçalves e Silva, R. H., and Marques, C. (2015). Melting and welding power characteristics of MIG–CMT versus conventional MIG for aluminium 5183. *Welding International*, 29(3):181–186.

Erlien, T. and Grong, Ø. (2003). HYMEN Bonding – The Search for the Optimal Design. Technical report, SINTEF.

Erlien, T., Grong, Ø., and Nilsen, N.-I. (2002). HYMEN Bonding – Experiments, Testing and Running-in of Equipment. Technical Report STF24 F02346, SINTEF.

Frazier, W. E. (2014). Metal Additive Manufacturing: A Review. *Journal of Materials Engineering and Performance*, 23(6):1917–1928.

Fulcher, B. A., Leigh, D. K., and Watt, T. J. (2014). Comparison of AlSi10mg and Al 6061 processed through DMLS. In *Proceedings of the Solid Freeform Fabrication (SFF) Symposium, Austin, TX, USA*, volume 46.

Green, D. (1972). Continuous extrusion-forming of wire sections. *J INST MET*, 100:295–300.

Grong, Ø. (2006). Method and device for joining of metal components, particularly light metal components. *Patent*.

Grong, Ø. (2012). Recent advances in solid-state joining of aluminum. *Welding journal*, 91(1):26–33.

Hatch, J. (1984). *Aluminum: properties and physical metallurgy*. Materials Park (OH): American Society for Metals.

Hermstad, O. A., Grong, Ø., Lilleby, A., and Erlien, T. (2007a). HYMEN Bonding metoden – Forslag til nytt design av sledeekstruder basert på resultater oppnådd i test av prototype. Technical Report STF80MK F07022.

Hermstad, O. A., Lilleby, A., Grong, Ø., and Erlien, T. (2007b). Design og utprøving av ny sledeekstruder.

Herzog, D., Seyda, V., Wycisk, E., and Emmelmann, C. (2016). Additive manufacturing of metals. *Acta Materialia*, 117:371–392.

Hull, C. W. (1986). Apparatus for production of three-dimensional objects by stereolithography.

Jiang, W. and Molian, P. (2002). Laser based flexible fabrication of functionally graded mould inserts. *The International Journal of Advanced Manufacturing Technology*, 19(9):646–654.

Kennedy, B. M., Sobek, D. K., and Kennedy, M. N. (2014). Reducing Rework by Applying Set-Based Practices Early in the Systems Engineering Process. *Systems Engineering*, 17(3):278–296.

Kodama, H. (1981). Automatic method for fabricating a three-dimensional plastic model with photo-hardening polymer. *Review of Scientific Instruments*, 52(11):1770–1773.

Krog, K., Erlien, T., Lilleby, A., and Grong, Ø. (2006). Studier av bindingsmekanismer i aluminium sammenføyd ved bruk av kaldsveisemaskin og HYMEN Bonding metoden. Technical report, SINTEF.

Kulakov, M. and Rack, H. J. (2009). Control of 3003-H18 Aluminum Ultrasonic Consolidation. *Journal of Engineering Materials and Technology*, 131(2):021006.

Lewis, G. K., Nemec, R., Milewski, J., Thoma, D. J., Cremers, D., and Barbe, M. (1994). Directed light fabrication. Technical report, Los Alamos National Lab., NM (United States).

Lilleby, A. and Erlien, T. (2005). HYMEN Bonding – Eksperimentelle og teoretiske studier av materialflyt og temperaturforhold ved Conform-ekstrudering av aluminium. Technical report, SINTEF.

Lilleby, A., Erlien, T., and Grong, Ø. (2005). Materialflyt og deformasjoner ved ekstrudering og sammenføyning av aluminium basert på ”HYMEN Bonding” metoden. Technical report, SINTEF.

Louvis, E., Fox, P., and Sutcliffe, C. J. (2011). Selective laser melting of aluminium components. *Journal of Materials Processing Technology*, 211(2):275–284.

M. B. Taminger, K. and Hafley, R. (2003). *Electron beam freeform fabrication: A rapid metal deposition process.*

Martina, F. and Williams, S. (2015). Wire+arc additive manufacturing vs. traditional machining from solid: a cost comparison. Technical report.

Mazumder, J., Choi, J., Nagarathnam, K., Koch, J., and Hetzner, D. (1997). The direct metal deposition of H13 tool steel for 3-D components. *JOM*, 49(5):55–60.

McGregor, G., Islam, M.-U., Xue, L., and Campbell, G. (2003). Laser consolidation methodology and apparatus for manufacturing precise structures.

Meiners, W., Wissenbach, K., and Gasser, A. (1998). Shaped body especially prototype or replacement part production.

Milewski, J. O., Lewis, G. K., Thoma, D. J., Keel, G. I., Nemec, R. B., and Reinert, R. A. (1998). Directed light fabrication of a solid metal hemisphere using 5-axis powder deposition. *Journal of Materials Processing Technology*, 75(1-3):165–172.

Murr, L. E., Gaytan, S. M., Ramirez, D. A., Martinez, E., Hernandez, J., Amato, K. N., Shindo, P. W., Medina, F. R., and Wicker, R. B. (2012). Metal fabrication by additive manufacturing using laser and electron beam melting technologies. *Journal of Materials Science & Technology*, 28(1):1–14.

Osias, J. R. and Tripp, J. H. (1966). Mechanical disruption of surface films on metals. *Wear*, 9(5):388–397.

Palanivel, S., Nelaturu, P., Glass, B., and Mishra, R. (2015). Friction stir additive manufacturing for high structural performance through microstructural control in an Mg based WE43 alloy. *Materials & Design (1980-2015)*, 65:934–952.

Sandnes, L., Grong, Ø., Torgersen, J., Welo, T., and Berto, F. (2018). Exploring the hybrid metal extrusion and bonding process for butt welding of Al–Mg–Si alloys. *The International Journal of Advanced Manufacturing Technology*, 98(5-8):1059–1065.

Schultz, J. and Creehan, K. (2014). System for continuous feeding of filler material for friction stir welding, processing and fabrication.

Sobek, D. K., Liker, J. K., and Ward, A. C. (1999). Another Look at How Toyota Integrates Product Development. *Harvard business review*, page 12.

Steinert, M. and Leifer, L. J. (2012). ’Finding One’s Way’: Re-Discovering a Hunter-Gatherer Model based on Wayfaring. *International Journal of Engineering Education*, 28(2):251.

Støren, S. (1976). Continuous Extrusion. SINTEF arbeidsnotat, SINTEF.

Tylecote, R. (1968). *The solid phase welding of metals.* The Solid Phase Welding of Metals. Edward Arnold.

Valberg, H. S. (2006). *Applied Metal Forming.* Cambridge University Press - M.U.A.

White, D. (2002). Object consolidation employing friction joining. *US6457629.*

White, D. R. (2003). Ultrasonic consolidation of aluminum tooling. *Advanced Materials & Processes*, 161(1):64–65.

Williams, S. W., Martina, F., Addison, A. C., Ding, J., Pardal, G., and Colegrove, P. (2016). Wire + Arc Additive Manufacturing. *Materials Science and Technology*, 32(7):641–647.

Yu, J. and Zhao, G. (2018). Interfacial structure and bonding mechanism of weld seams during porthole die extrusion of aluminum alloy profiles. *Materials Characterization*, 138:56–66.

Yu, J., Zhao, G., and Chen, L. (2016). Analysis of longitudinal weld seam defects and investigation of solid-state bonding criteria in porthole die extrusion process of aluminum alloy profiles. *Journal of Materials Processing Technology*, 237:31–47.

Appendix

Paper 1

Available online at www.sciencedirect.com

ScienceDirect

Procedia Manufacturing 26 (2018) 782–789

Procedia MANUFACTURING

www.elsevier.com/locate/procedia

46th SME North American Manufacturing Research Conference, NAMRC 46, Texas, USA

Hybrid Metal Extrusion & Bonding (HYB) - a new technology for solid-state additive manufacturing of aluminium components

Jørgen Blindheim[a], Øystein Grong[a,b], Ulf Roar Aakenes[b], Torgeir Welo[a], Martin Steinert[a]

[a] *Norwegian University of Science and Technology, Department of Mechanical and Industrial Engineering, NTNU, 7491 Trondheim, Norway*
[b] *Hybond AS, Alfred Getz vei 2, 7491 Trondheim, Norway*

Abstract

This paper demonstrates a concept for a new additive manufacturing process for aluminium alloys, based on the Hybrid Metal Extrusion & Bonding (HYB) technology, along with the potential for further development of the process. The process is capable of producing near net shape structures at high deposition rates, utilizing metallic bonding to consolidate the feedstock to the substrate in the solid-state. The aluminium feedstock wire is processed through a specially designed extruder, which serves the purpose of dispersing inherent oxides of both the feedstock and the substrate. At the same time it provides sufficient pressure for metallic bonding to occur. The process has been tested on a concept level by successfully depositing a two-layered structure of commercial purity aluminium.

© 2018 The Authors. Published by Elsevier B.V.
Peer-review under responsibility of the scientific committee of the 46th SME North American Manufacturing Research Conference.

Keywords: Additive manufacturing ; HYB-AM ; Continuous extrusion ; Aluminium alloys ; Solid-state bonding

1. Introduction

In order to determine whether the Hybrid Metal Extrusion & Bonding (HYB) process has the prospect of becoming a new solid-state additive manufacturing (AM) technology for aluminium components in the future, its characteristics must be compared with those of the alternative or competitive technologies.

1.1. Overview of additive manufacturing processes for aluminium

During the last years we have seen an increase in the use of AM technology in the industry, opening for mass customization of net shape or near net shape parts that can lead to less labour time, less energy consumption and less material waste compared to the traditional subtractive processes. It can also provide increased design freedom by allowing for weight savings that are not achievable by the traditional subtractive processes. In some cases it is even possible to replace complex assemblies with one single AM part.

AM of metals is by ASTM divided into three main categories when it comes to process; Powder Bed Fusion (PBF), Directed Energy Deposition (DED) and sheet lamination [1], see Fig. 1. In PBF the part is supported by the unconsolidated powder, thus giving a great design freedom and the possibility to create detailed and complex shapes that are otherwise impossible to manufacture. However, the deposition rate is low, and the part size is limited by the powder bed size. DED and sheet lamination, on the other hand, cannot produce such complex shapes, but permit manufacturing of larger near net shape parts at higher deposition rates.

---

* Corresponding author. Tel.: +47-90-50-22-16
E-mail address: jorgen.blindheim@ntnu.no

2351-9789 © 2018 The Authors. Published by Elsevier B.V.
Peer-review under responsibility of the scientific committee of the 46th SME North American Manufacturing Research Conference.
10.1016/j.promfg.2018.07.092

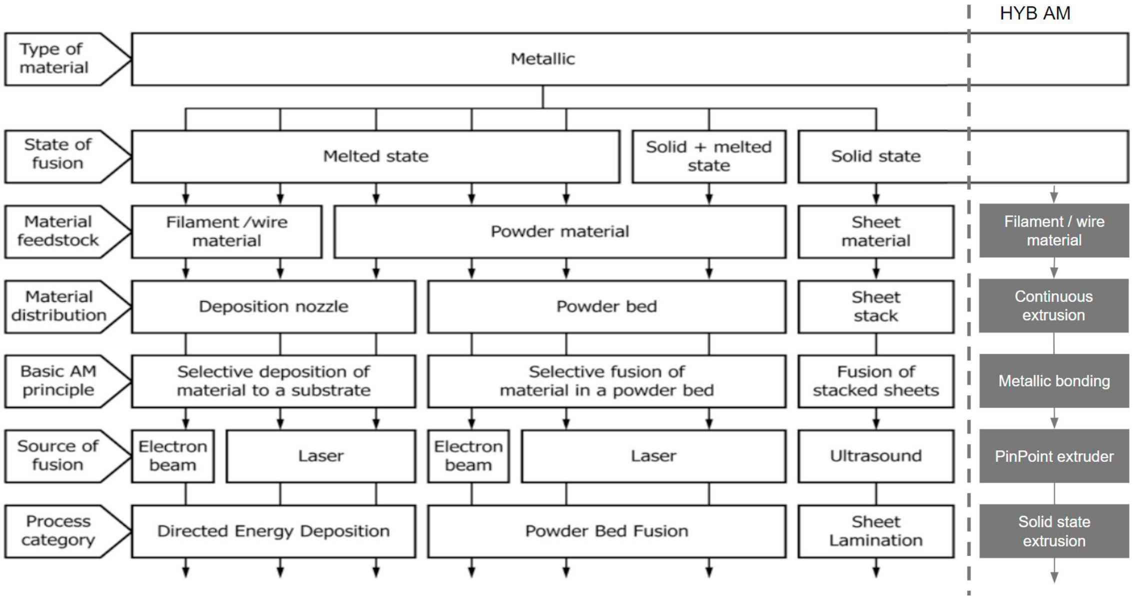
HYB AM
Type of material
Metallic
State of fusion
Melted state
Solid + melted state
Solid state
Material feedstock
Filament /wire material
Powder material
Sheet material
Filament / wire material
Material distribution
Deposition nozzle
Powder bed
Sheet stack
Continuous extrusion
Basic AM principle
Selective deposition of material to a substrate
Selective fusion of material in a powder bed
Fusion of stacked sheets
Metallic bonding
Source of fusion
Electron beam
Laser
Electron beam
Laser
Ultrasound
PinPoint extruder
Process category
Directed Energy Deposition
Powder Bed Fusion
Sheet Lamination
Solid state extrusion

Fig. 1. Overview of additive manufacturing processes for metals. The new HYB-AM process can be considered as a new branch of the solid-state process tree suggested by ISO/ASTM 52900:2015(E) [1].

For most processes the part size is not restricted by the need for a low pressure environment.

1.2. Melted-state AM processes for aluminium

Most of the current AM technologies for building larger components are based on directed energy deposition, where the energy is supplied either from a laser beam, an electron beam or an electric arc. Both the feedstock and the substrate are heated above its melting temperature so that bonding is achieved upon solidification.

For melted-state AM the use of aluminium has been limited to only a few alloys due to the resulting ”as-cast” microstructure inherited from the fusion process. Only recently it has been demonstrated that this problem can be overcome by the addition of nanoparticles acting as nucleation sites for new grains during powder bed processing of AA7075 and AA6061, resulting in material strengths comparable to those of wrought material [2].

Still the melted-state processes suffer from restrictions in the deposition rate due to limitations in the melt pool size. In addition, the contractions occurring during solidification and subsequent cooling lead to build-up of residual stresses in the structure along with global deformations and distortions. Various mitigating or precautionary actions have been undertaken to avoid distortions arising from residual stresses, like symmetric building, back-to-back building and the use of high pressure inter-pass rolling [3].

1.3. Solid-state AM processes for aluminium

AM processes based on friction joining were first patented in 2002 [4], and have later been commercialized for ultrasonic consolidation of thin sheets or foils [5]. In recent years a solid-state process, based on friction welding, has been developed, where the material is deposited onto the substrate using a rotating consumable rod [6]. Also, a process based on friction stir welding (FSW) has been demonstrated for bonding of stacked metal plates [7]. In recent years, Aeroprobe has developed a modified FSW process, MELD, where the feedstock is added through the tool [8].

Wire Arc Additive Manufacturing (WAAM) and Ultrasonic Additive Manufacturing (UAM) are well-known processes within the melted-state and solid-state AM category, respectively, and some characteristics of these processes are presented in Table 1. Considering solid-state processes like UAM, some of the advantages are a wide material range to choose from and the possi-

Table 1. Characteristics of Ultrasonic Additive Manufacturing (UAM) and Wire Arc Additive Manufacturing (WAAM) when used for aluminium alloys.

Parameter	Comments
Deposition rate	The low heat input of UAM makes it suitable for high deposition rates, whereas the deposition rate for WAAM is limited by the cooling rate of the structure to avoid down-melting.
Build volume	Both processes are only limited by the size of the motion system, and do not require a low pressure environment.
Overhanging structures	Current UAM machines cannot produce overhanging structures as opposed to WAAM which has this flexibility.
Post processing	Both processes create near net shape structures that require machining to obtain the final shape and tolerances.
Material range	UAM allows processing of any aluminium alloy and can even bond dissimilar alloys and materials. In contrast, WAAM is restricted to certain alloys that are not susceptible to hot cracking (e.g. Al-Si and Al-Mg alloys).
Residual stresses	The low processing temperature of UAM means reduced temperature gradients and thus lower thermal-induced stresses during cooling compared to WAAM, which is a melted-state process.
Defects	The WAAM process which involves melting of the feedstock can create problems with porosity and hot tearing, whereas lack of bonding is perhaps a greater problem for UAM.

bility to join dissimilar materials. Problems with distortions and residual stresses are also reduced due to lower temperature gradients during processing. WAAM, on the other hand, has advantages when it comes to the possibility to create overhanging structures. Still, distortion and residual stresses can be a challenge.

When it comes to deposition rates both technologies can achieve high deposition rates. WAAM based on the Cold Metal Transfer (CMT) welding process has the ability to achieve high deposition rates, yet with an increase in material waste, since higher deposition rates contribute to a wider melt pool size and thus a thicker wall structure. A typical CMT deposition rate for aluminium when keeping the buy to fly (BTF) ratio at 1.5 is 1kg/h [3].

The first generation machines for UAM did not have sufficient power to achieve high deposition rates. However, commercial machines from Fabrisonic are capable of depositing up to 1.3 kg/h. Contrary to melted-state processes, where the substrate needs to continuously solidify to keep its shape, solid-state processes have no such limitations in the deposition rate, as long as the temperature is kept below the melting temperature of the material. This makes solid-state processes favourable for manufacturing of larger structures.

In the following a new AM concept based on the Hybrid Metal Extrusion & Bonding (HYB) process will be presented. Originally, the HYB process was developed for solid-state joining of aluminium plates and profiles [9,10]. However, because HYB involves the use of filler metal additions it has also the potential of becoming a new solid-state AM process.

2. Hybrid Metal Extrusion & Bonding (HYB)

2.1. The HYB PinPoint extruder

The HYB method is based on the principle of continuous extrusion - also known as Conform extrusion

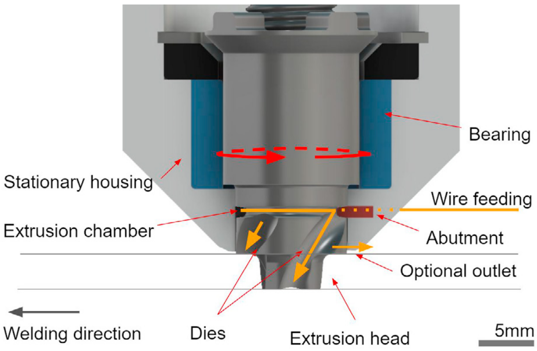

Fig. 2. The HYB PinPoint extruder is built around a rotating pin provided with an extrusion head with a set of moving dies through which the aluminium is allowed to flow.

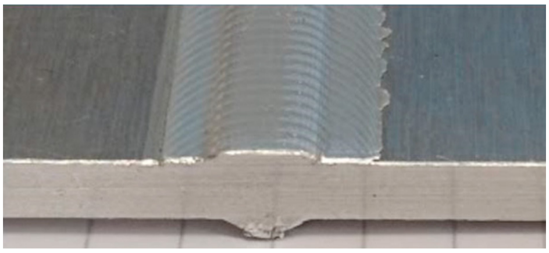

Fig. 3. Example of a HYB butt weld. The separate die at the rear of the stationary housing makes it possible to control the shape of the weld face.

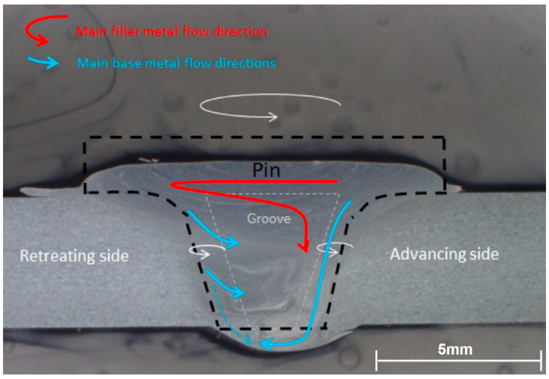
Main filler metal flow direction
Main base metal flow directions
Pin
Groove
Retreating side
Advancing side
5mm

Fig. 4. A cross section of a HYB butt joint. Metallic bonding is mainly achieved by oxide dispersion and shear deformation along the side walls, whereas in the root region where the metal flows meet, surface expansion and pressure contribute most to bonding.

[11,12]. The current version of the HYB PinPoint extruder is built around a 10mm diameter rotating pin, provided with an extrusion head with a set of moving dies through which the aluminium is allowed to flow. This is shown by the drawing in Fig. 2. When the pin is rotating, the inner extrusion chamber with three moving walls will drag the filler wire both into and through the extruder due to the imposed friction grip. At the same time it is kept in place inside the chamber by the stationary housing constituting the fourth wall. The aluminium is then forced to flow against the abutment blocking the extrusion chamber and subsequently (owing to the pressure build-up) continuously extruded through the moving dies in the extruder head. They are, in turn, helicoid-shaped, which allow them to act as small ”Archimedes screws” during the pin rotation, thus preventing the pressure from dropping on further extrusion in the axial direction of the pin. Furthermore, if the stationary housing is provided with a separate die at the rear, a weld face can be formed by controlling the flow of aluminium in the radial direction as illustrated in Fig. 3. In this case both the width and height of the weld reinforcement can be varied within wide limits, depending on the die geometry, ranging from essentially flat to a fully reinforced weld face. As a matter of fact, it is this feature that makes plate surfacing and eventually AM possible.

2.2. *HYB bonding mechanisms*

In the HYB case, metallic bonding is achieved through a combination of oxide dispersion, shear deformation, surface expansion and pressure. An illustration of the material flow pattern in butt welding of aluminium plates is shown in Fig. 4. In a real welding situation the temperature in the groove between the two base plates to be joined is typically 350 - 400°C. This creates favourable conditions for metallic bonding between the filler metal and the base material when the new oxide-free interfaces (being formed following the re-shaping of the groove by the rotating pin) immediately become sealed-off by the filler metal under high pressure.

3. Testing of the HYB-AM concept

The preliminary testing of the HYB PinPoint extruder in a real AM situation was carried out using commercial purity aluminium (AA1050) both as base and feedstock materials. The dimensions of the two 4mm thick base plates used in the testing were 240mm × 50mm, while the diameter of the feedstock wire was 1.2 mm.

3.1. Experimental setup and results

For the laboratory testing of the HYB-AM concept a set of used tool parts from an earlier version of the PinPoint extruder was selected. These tool parts were subsequently modified through grinding to allow AM of a layered structure using a combination of stringer bead deposition and butt welding. The recaptured operational conditions are summarized in Table 2.

For the stringer bead deposition the tool parts shown to the left in Fig. 5 were employed. These include a flat pin equipped with a shaped bottom end for removal of oxides from the underlying surface during welding, and a stationary housing equipped with a rectangular shaped die at the rear (4.5mm × 3.25mm). Each base plate was first provided with a longitudinal stringer bead deposited about 1.5mm from the edge of the plate, see Fig. 6a. A 3mm wide groove will then appear between the beads when the plates edges are brought together (Fig. 6b). This, in turn, allowed the plates to be butt welded from the top (Fig. 6c), using the tool parts shown to the right in Fig. 5. Note that in the butt welding case the lower end of the rotating pin is centered in the groove to ensure good surface oxide removal and thus metallic bonding along all interfaces. Finally, on the top of the first layer the third stringer bead was deposited (Fig. 6d). This deposition sequence eventually lead to the two-layer structure shown in Fig. 7.

Fig. 8 shows a front view of the same two-layer structure. As expected, the outer contour is a reflection of the shape of the individual stringer beads from which it is made. Their dimensions are, in turn, determined by the geometry of the die at the rear of the stationary housing. This indicates that the HYB PinPoint extruder has the potential to be used in AM of near net shaped aluminium components in the future. Hence, the HYB-AM concept has passed the first qualifying test, which justifies a closer exploration of its potentials.

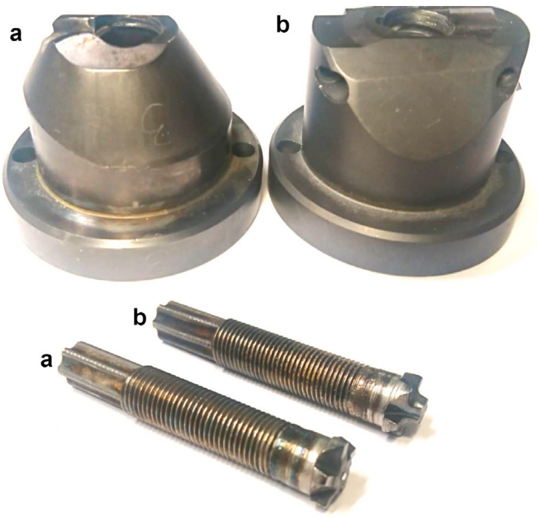

Fig. 5. Photograph of the tool parts used to build the layered structure; (a) pin and stationary housing used for stringer bead deposition; (b) pin and stationary housing used to fill the groove between the stringer beads.

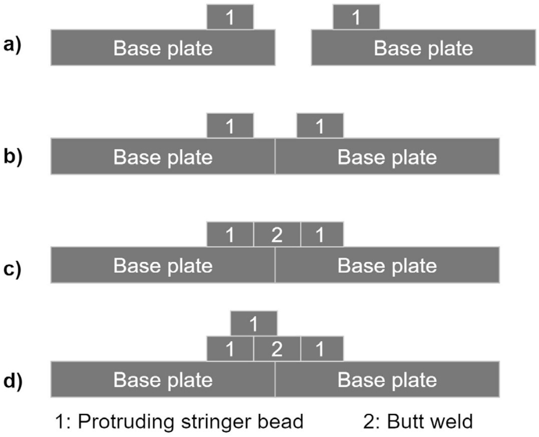

Fig. 6. Schematic illustration of the deposition sequence used to test the HYB-AM concept.

4. Exploration of the HYB-AM potentials

The stringer bead deposition sequence is largely determined by the geometry and shape of the stationary housing of the extruder. In the latest version of the HYB PinPoint extruder, the new conical design makes it possible to deposit the individual stringer beads at a distance similar to that of the groove width used for the butt welds.

Table 2. Parameters used in the experimental setup.

Parameter	Value
Pin rotation speed	300 RPM
Extruder travel speed	6 mm/s
Wire feed rate	87 mm/s
Gross heat input	0.34 kJ/mm

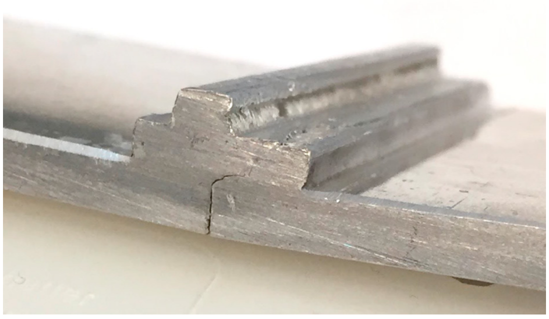

Fig. 7. Photograph of the layered structure produced using the HYB-AM method.

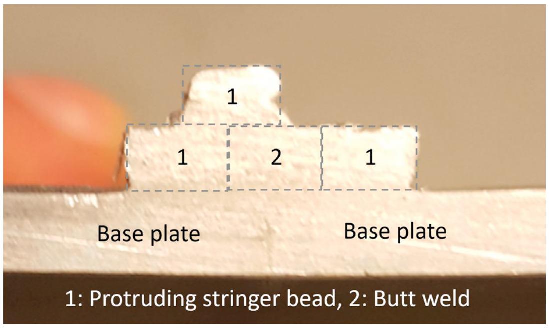

Fig. 8. Front view of the same layered structure shown in Fig. 7.

4.1. Deposition strategy

Fig. 9 illustrates a possible deposition strategy for making a layered structure. The first stringers are deposited with a PinPoint extruder equipped with a flat pin and a rectangular die at the rear of the stationary housing, resulting in a stringer bead cross section of 10mm × 2.5mm. The stringer beads are distributed such that a gap of 5mm is formed between them (Fig. 9a). The grooves are filled with a second set of tools; i.e., a PinPoint extruder equipped with a pin extending 3mm below the stationary housing having a diameter larger than the gap width of the groove. The drawback of this setup is that it requires the use of two sets of tools to make a layer in a structure. Still, a full 3D-structure can be built by employing this technique, as shown in Fig. 10.

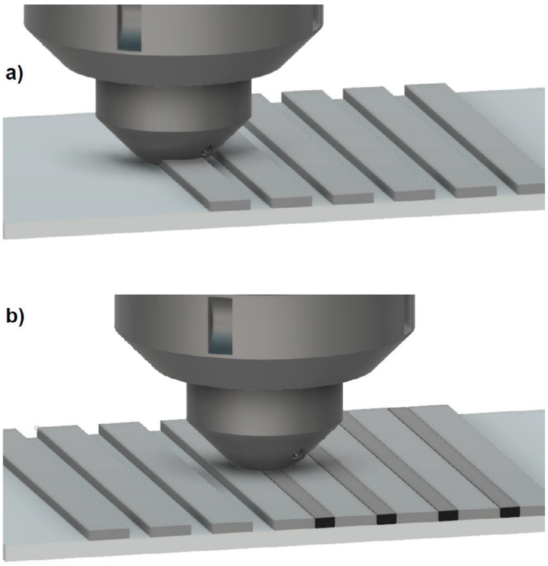

Fig. 9. Deposition strategy based on the use of two separate PinPoint extruders; (a) first the protruding stringer beads are deposited using the first extruder, keeping the spacing between them fixed; (b) then the gaps are filled using the second extruder.

4.2. Deposition rates

In the HYB-AM case, the deposition rate is controlled by the circumferential velocity of the extrusion chamber, the diameter of the feedstock and the slip between the walls inside the extrusion chamber and the feedstock. The current extruder design, which uses Ø1.2mm feedstock wire, yields a deposition rate of 2 kg/h at 400 RPM and a slip factor of 0.85. However, the

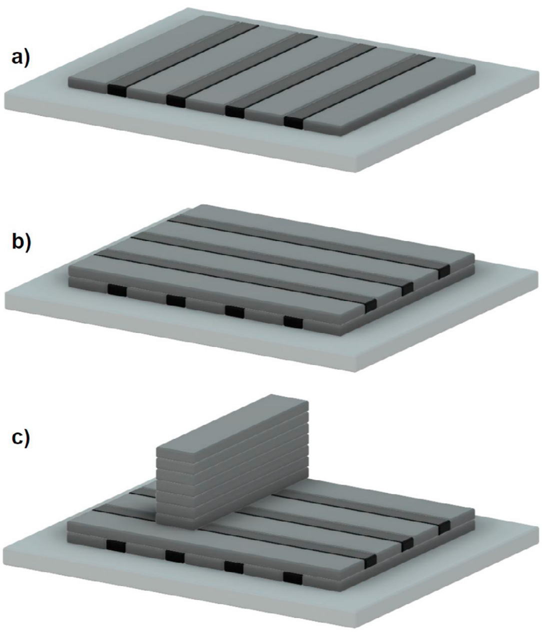

Fig. 10. Possible deposition sequence for building a 3D layered structure; (a) deposition of the first layer on top of the base plate; (b) deposition of the second layer normal to that of the first layer; (c) finally a wall structure can be built on the top by depositing layers of protruding stringer beads.

extrusion chamber of the PinPoint extruder can also be adjusted to accommodate up to 1.6mm diameter wire if increased deposition volumes are aimed at.

Fig. 11 illustrates how the HYB-AM process performs compared to other technologies with regards to deposition rates, i.e. WAAM and UAM. The deposition rates for HYB-AM are given for both Ø1.2mm and Ø1.6mm feedstock wires.

For HYB-AM the deposition rate is only limited by the scaling of the process. However, the deposition rate must be balanced and compatible with the other requirements as well, such as the scanning speed, the die geometry, the process temperature and the contact pressure at the bonding interface. The high potential deposition rates make the HYB-AM technology particularly suitable for manufacturing of larger structures where this possibility can be fully utilized.

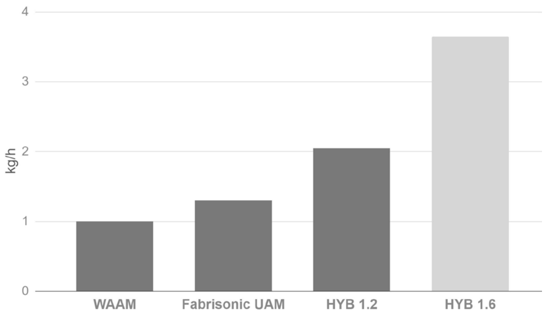

Fig. 11. Deposition rates for HYB-AM compared to UAM and WAAM for aluminium feed stock

4.3. *Choice of feedstock material*

For melted-state processes, the variants of aluminium alloys that can be used for AM are limited since the wrought properties of the material cannot be reverted after melting. In the case of HYB-AM no melting is involved, which means that there will be a wider range of alloys to choose from.

HYB-AM has also the potential of being used for other ductile metals, although the process in its present form is developed for aluminium alloys. By using different alloys within the same part it can be possible to create components with tailored mechanical properties throughout the structure.

4.4. *Post processing*

For precipitation hardened alloys the reheating occurring during extrusion can affect the microstructure and thus the properties of the final structure. Therefore, it may be necessary to age the part after manufacturing to increase the strength of the component. In cases where the part is in an over-aged condition after processing, a full solution heat treatment followed by quenching and aging can be carried out.

The near net shape structures produced using the HYB-AM process requires for most practical purposes milling to achieve their final shape. In cases where heat treatment is needed, this should be carried out before milling to eliminate distortions.

5. Conclusions and further work

In this paper the background for the HYB-AM process has been presented along with the potential for further development of the process for manufacturing of near net shape aluminum structures.

The main advantages of the HYB-AM process are the high deposition rates and the wide material range of aluminium alloys to choose from. By altering between different alloys within a single part the process has the potential to produce tailored mechanical properties throughout the structure. The process is operating below the melting point of the material, meaning that the problems related to hot cracking and residual stresses are reduced compared to those normally associated with the conventional melted-state processes.

For the current extruder design, deposition rates 2-3 times higher than those reporter for melted-state processes are achievable. Future work will focus on further process development, along with laboratory testing to determine the microstructure, mechanical properties and the bond strength between the deposited stringer beads and the layers.

Acknowledgements

The authors acknowledge the financial support from Hybond AS, NTNU and NAPIC (NTNU Aluminium Product Innovation Center). They are also indebted to Tor Austigard, who is the third member of the Hybond technology team, for valuable assistance in producing the HYB-AM layered structure and for providing the CAD models of the HYB PinPoint extruder.

References

[1] Standard Terminology for Additive Manufacturing General Principles Terminology, ASTM, 2015.
[2] J. H. Martin, B. D. Yahata, J. M. Hundley, J. A. Mayer, T. A. Schaedler, T. M. Pollock, Nature 549 (2017) 365--369.
[3] S. W. Williams, F. Martina, A. C. Addison, J. Ding, G. Pardal, P. Colegrove, Materials Science and Technology 32 (2016) 641--647.
[4] D. White, Object consolidation employing friction joining, 2002.
[5] D. R. White, Ultrasonic consolidation of aluminum tooling, volume 161, ASM International, 2003.
[6] J. J. S. Dilip, H. K. Rafi, G. J. Ram, Transactions of the Indian Institute of Metals 64 (2011) 27.
[7] S. Palanivel, P. Nelaturu, B. Glass, R. Mishra, Materials & Design (1980-2015) 65 (2015) 934--952.
[8] J. Schultz, K. Creehan, System for continuous feeding of filler material for friction stir welding, processing and fabrication, 2014.
[9] Ø. Grong, Method and device for joining of metal components, particularly light metal components, 2006.
[10] Ø. Grong, Welding Journal 91 (2012) 26--33.
[11] D. Green, J INST MET 100 (1972) 295--300.
[12] C. Etherington, Journal of Engineering for Industry 96 (1974) 893--900.

Paper 2

Available online at www.sciencedirect.com

ScienceDirect

Procedia Manufacturing 00 (2019) 000–000

Procedia MANUFACTURING

www.elsevier.com/locate/procedia

47th SME North American Manufacturing Research Conference, NAMRC 47, Pennsylvania, USA

Rapid prototyping and physical modelling in the development of a new additive manufacturing process for aluminium alloys

Jørgen Blindheim[a], Torgeir Welo[a], Martin Steinert[a]

[a]*Norwegian University of Science and Technology, Department of Mechanical and Industrial Engineering, NTNU, 7491 Trondheim, Norway*

Abstract

In this work, rapid prototyping and physical modelling are used to evaluate four different extruder and deposition concepts for the Hybrid Metal Extrusion & Bonding (HYB) additive manufacturing (AM) process for aluminium alloys. The HYB-AM process is a branch of the HYB joining technology and is currently utilizing an extruder design that was initially developed for welding purposes. However, due to the different operating conditions of an AM process compared to a welding process, it is of interest to compare the current extruder to that of other alternatives to identify the optimal design. Plastic models of the different extruders have been produced by rapid prototyping and attached to a CNC-machine. To test the performance of each design, plasticine has been processed through the extruders and deposited on the machine bed. Key learnings from each cycle of designing, building and testing have been used as inputs for the next iteration, to finally end up with a design and the associated requirements upon which the further development process will be based.

© 2019 The Authors. Published by Elsevier B.V.
This is an open access article under the CC BY-NC-ND license (http://creativecommons.org/licenses/by-nc-nd/3.0/)
Peer-review under responsibility of the Scientific Committee of NAMRI/SME.

Keywords: Additive manufacturing ; Physical modelling ; Continuous extrusion ; Aluminium alloys ; Solid-state bonding

1. Introduction

In this study, we combine prototyping and physical modelling with the aim of identifying the more suitable extruder and deposition concept for the further development of the Hybrid Metal Extrusion & Bonding (HYB) additive manufacturing (AM) process. The HYB-AM process normally requires pressures that generate stresses well beyond the flow stress of the aluminium feedstock material to deform and bond the extrudate to the substrate in the solid-state. However, using plasticine to physically model the feedstock material, drastically reduces the extrusion pressures and opens for producing parts from simpler materials than tool steel. This, in turn, both reduces the costs and the time consumption of testing a solution.

Developing a new process or product is, unlike in incremental product development, an exploration of yet unknown requirements. However, this early product development phase is important, as later changes to the design can generate high costs [1].

1.1. *Prototyping towards new insights*

While many people will consider a prototype as the final step before a product is ready for serial production, here we interpret a prototype as a tool to learn [2]. This is especially important in the early product development phase where the final requirements are still unknown. Some inherent problems of the product are not yet discovered and are hence lacking a valid solution (unknown unknowns) [3].

A wayfaring approach [2] has been applied to explore the opportunity landscape of the problem to be solved. A wayfaring journey usually consists of many probes, where each probe is a cycle of designing, building and testing an idea or prototype [4]. In this way, the next prototyping iteration can build onto the newly discovered knowledge from the previous probing cycle until a satisfying solution is found [5].

Elverum and Welo [6] state that for complex physical products where the costs of a prototype are high, it is even more important to understand how to prototype in an efficient manner in order to save money and still achieve highly valuable learning outcomes. By applying a wayfaring approach, and physically modelling the performance of each prototype, we aim at dis-

---

* Corresponding author. Tel.: +47-90-50-22-16
E-mail address: jorgen.blindheim@ntnu.no (Jørgen Blindheim).

2351-9789 © 2019 The Authors. Published by Elsevier B.V.
This is an open access article under the CC BY-NC-ND license (http://creativecommons.org/licenses/by-nc-nd/3.0/)
Peer-review under responsibility of the Scientific Committee of NAMRI/SME.

covering some of the 'unknown unknowns' and finally end up with a design and valid requirements upon which the further development will be based.

1.2. Physical modelling

Plasticine and ductile metals share some of the same flow properties, and already in the 1950s Green [7] explored some of these for modelling of metal flow and stablishing a foundation for physical modelling. Physical modelling is an alternative to the analytical and numerical methods for modelling the plastic flow of metals [8], where the main advantage is its relative simplicity and ease of implementation. Since the load required to deform a modelling material is much lower than those necessary to deform the actual material, inexpensive equipment may be used to perform the analysis [9]. In recent years physical modelling using plasticine has been applied for processes like Friction Stir Welding [10] and Equal Channel Angular Pressing [11], to further establish the relationships between metal flow and plasticine flow behaviour.

Oil-based modelling clays are referred to by a number of generic trademarks like Plasticine, Plastilin, and Plastilina; here we have chosen to use the term plasticine, in accordance with the literature in the field.

2. The HYB-AM technology

The HYB-AM process is a branch of the HYB joining technology, which was initially developed for welding of aluminium plates and profiles [12, 13, 14]. The potential advantages of this process are the high deposition rates achievable and the wide material range of aluminium alloys to choose from. The process operates below the melting point of the material, meaning that problems related to hot cracking and residual stresses in theory are reduced compared to those normally associated with the conventional melted-state processes [15].

2.1. HYB working principles

The HYB technology is based on the principle of continuous extrusion, also known as Conform extrusion [16, 17]. The extrusion step serves two purposes in this process; to disperse oxides present on the feedstock material and to provide bonding pressure. The current version of the extruder, the PinPoint extruder, is built around a 10 mm diameter rotating pin, provided with an extrusion head with a set of moving dies through which the aluminium is allowed to flow. This principle is illustrated in Fig. 1. When the pin is rotating, the three walls of the inner extrusion chamber will drag the filler wire both into and through the extruder due to the imposed friction grip. At the same time, it is kept in place inside the chamber by the stationary housing constituting the fourth wall. The aluminium is then forced to flow against the abutment blocking the extrusion chamber and subsequently (owing to the pressure build-up) being continuously extruded through the dies in the extruder head. The dies are helicoid-shaped, which allow them to act as screws during the pin rotation, thus preventing the pressure from dropping on further extrusion in the axial direction of the pin. For the PinPoint extruder, metallic bonding is achieved through a combination of oxide dispersion, shear deformation, surface expansion and pressure [15].

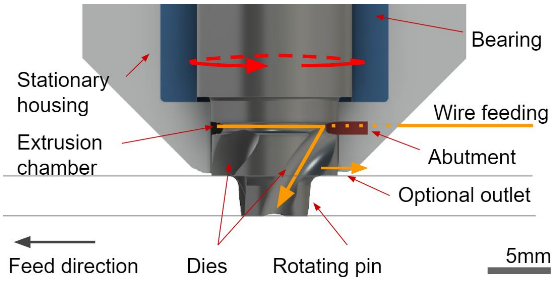

Fig. 1. The PinPoint extruder is built around a rotating pin provided with an extrusion head with a set of helical dies through which the aluminium is allowed to flow [15].

Fig. 2 illustrates a possible deposition sequence for making a layered structure using the PinPoint extruder. The first stringers are deposited using a flat pin and a rectangular die at the rear of the stationary housing, resulting in a stringer bead cross-section of 10 mm × 2.5 mm. The stringer beads are distributed such that a gap of 5 mm is formed between them (Fig. 2a). The grooves are filled with an extruder equipped with a pin extending 3 mm below the stationary housing having a diameter larger than the gap width of the groove (Fig. 2b). This process has been successfully demonstrated on a concept level by depositing a two-layered structure of commercial purity aluminium (AA1050) [15].

2.2. Further development of the HYB-AM process

Over the last two decades, the HYB welding technology has gradually been improved and refined through testing of the different extruder designs. Now, when branching this welding technology into AM, it is important to consider that the boundary conditions of a welding process are not the same as those of an additive process.

Fig. 3 illustrates how the Pinpoint extruder is geometrically constrained to allow for fillet welding. For an AM structure, which is deposited layer by layer, this constraint is not applicable, thus providing increased design freedom. Furthermore, in a welding situation, the extrusion pressure needs to compensate for the pressure drop through the plate thickness, as opposed to in AM, where the thickness of the deposited layer, and thus the pressure drop, can be reduced correspondingly, see Fig. 4.

As a consequence, concepts that previously have been discarded for welding purposes might now be viable solutions when applied for AM. With this in mind, we have set out to re-explore the landscape of solid-state bonding. In the following sections, we will compare the current extruder design with

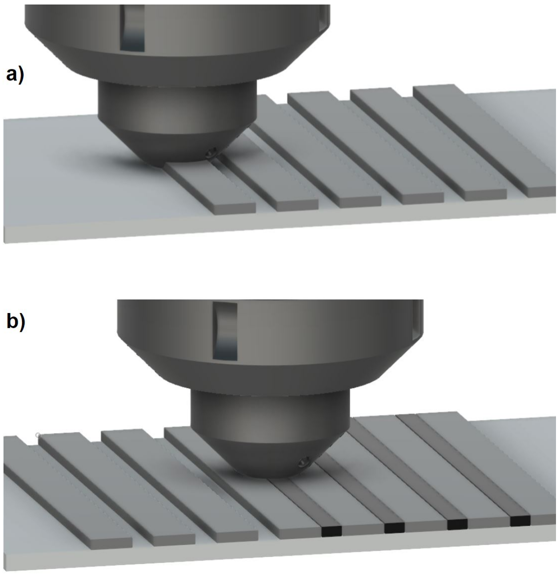

Fig. 2. Deposition strategy based on the use of two separate PinPoint extruders; (a) first the protruding stringer beads are deposited using the first extruder, keeping the spacing between them fixed; (b) then the gaps are filled using the second extruder [15].

three other possible concepts in order to identify the most suitable concept for the further development of this new process.

3. Experimental setup

3.1. Extruder prototypes

The parts for the different extruders were modelled in CAD software and produced on an Objet Alaris30 3D-printer using VeroWhite material. The actual designs of the extruders were optimized for rapid prototyping and made to reflect the critical functionality to be tested.

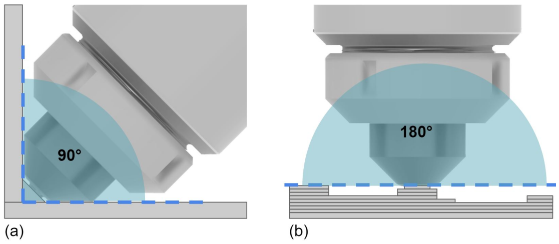

(a) (b)

Fig. 3. Design freedom; (a) the PinPoint extruder is geometrically constrained for fillet welding purposes; (b) the layer-by-layer deposition sequence of an AM structure implies more design freedom for the extruder.

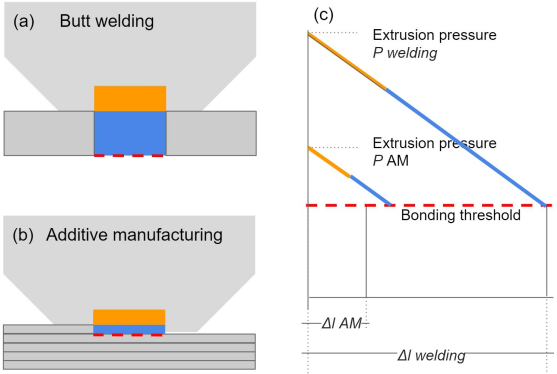

Fig. 4. The required extrusion pressure needs to overcome the pressure drop through the die and the thickness of the base material; (a) in a butt joining situation the plate thickness deems for higher extrusion pressures; (b) for AM purposes the layer thickness can be reduced, thus allowing for reduced extrusion pressure; (c) schematically illustration of the pressure levels of butt joining as compared to AM.

3.2. Motion control system

In order to control the deposition speed and the position of the extruders, a K8200 Vellemann FDM 3d-printer was modified to allow for attaching the equipment to be tested. The setup is shown in Fig. 5. The machine has a lead-screw driven gantry that can move in Z-direction, while the belt driven bed is allowed to move in the horizontal plane. The motion of the machine is provided from stepper motors. The plasticine dispenser and the extruder spindle is driven by 3Nm NEMA 23 stepper motor powered from JP6445 36V stepper drivers. The original controller was replaced by an Arduino Mega running on Marlin 1.4 firmware and equipped with a RAMPS break-out board.

For the full-scale AM process, the aluminium feedstock is supplied in the form of a solid wire. On the first modelling iterations, the plasticine was extruded to the required thickness and put on a reel. However, handling and feeding the thin plasticine wire was challenging, so a dispenser pump was designed to directly supply the plasticine at the inlet of the extruders. The dispensing system consists of a steel tube contained with a lead-screw driven piston, having a stroke length similar to the tube length. When the piston is fully retracted, the tube can be filled with plasticine. A gear reduction is used to connect the lead-screw to the stepper motor.

The Marlin firmware does not allow for controlling the speed of the dispenser motor independently. However, using the mixing extruder settings, allowed the required speed ratio between the extruder motor and the dispenser motor to be set.

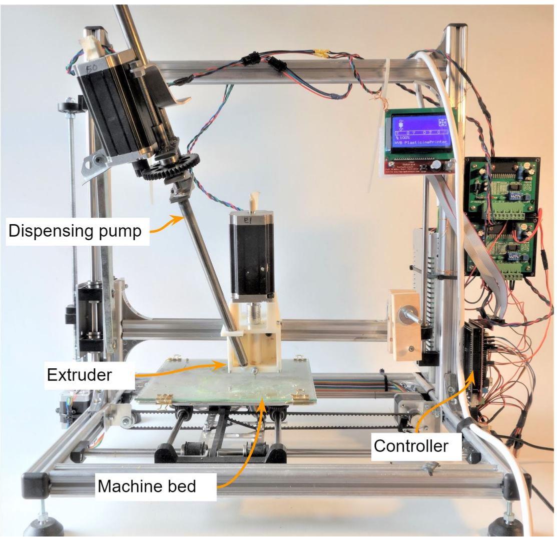

Fig. 5. The experimental setup; a 3d-printer has been rebuilt to allow controlling motion of the different extruders to be tested.

3.3. Test procedure

Before each test, a slab of plasticine was smeared on the machine bed to make up a substrate for the extrudate to be deposited upon. The slab was levelled to that of the outlet of the extruder.

A machine program was written to reflect the dimensions and stacking sequence of the stringers to be deposited along with feed and extrusion speeds. Due to the directional design of the extruders, the deposition was carried out while scanning in one direction only. A test typically consisted of deposition of two or more stringers side-by-side to make up a layer, and two or more stringers on top of that.

Deposition rates for the extruders are controlled by the rotational speed of the extruder axle. This, in turn, also has to be balanced with the scanning speed to fill the desired cross-section of the stringer. A cross-section of the deposited structure from the wheel extruder is shown in Fig. 7c and resembles a typical deposition sequence.

Criteria for evaluating each concept have continuously emerged as new insights have been gathered from each probing cycle. The criteria are listed in the following:

- *Tool forces* are resulting from sticking friction between the extruder parts and the substrate. These forces can be reduced by minimising the die outlet and the die wall thickness. Low tool forces can ultimately allow the extruder to be controlled by less rigid robots like Scara-arms.
- *Process control* relates to the tunability of the process and indicates whether parameters like rotational speed, feedrate and temperatures can be controlled independently.
- *Flash formation* is a result of the pressure level inside the extruder and the clearance between the moving parts, and some flash will always be formed. However, the design should minimize this formation by using the lowest possible extrusion pressure combined with stiff components and tight clearance fit between the moving parts. Furthermore, the design should allow flash to be removed continuously to reduce friction between moving parts.
- *Oxide removal* is crucial for proper bonding between extrudate and substrate. Any oxides present on the mating surfaces will reduce the bond quality.
- *Resolution* is a measure for stringer size and indicates the level of details that can be deposited. A coarse structure is likely to cause more material wastage during post machining and is not preferred.
- *Wire slip* is a measure of the circumferential speed of the spindle compared to the feedstock wire speed. The feedstock wire should be firmly engaged in the conform slot and the length of the slot sufficient to avoid wire slip.
- *Contact friction* between spindle and housing should be reduced to avoid excessive work and heat generation during extrusion.
- *Serviceability and design simplicity*. Ease of assembly and disassembly. When used for aluminium, the parts that are in contact with the feedstock will bond to the aluminium and will need to be cleaned in sodium hydroxide prior to disassembly.
- *Deposition quality* relates to the density of the deposited structure. The structure should be continuous and void-free.

3.4. Limitations

Sofuoglo and Rasty [9] states that there can be a significant variation in deformation behaviour from one color of plasticine to another due to the different agents used in the coloring process of the plasticine. When using physical modelling for calculations, the properties of the actual plasticine have to be matched with the behaviour of the real material. In this study, the plasticine has not been quantified as the aim has not been to use the model for other analysis than verifying overall material flow through the extruders.

Furthermore, during deposition of aluminium, it is necessary to remove or disperse oxides from the mating interfaces of the substrate and the extrudate for proper bonding to occur. However, plasticine does not allow for modelling this mechanism of the process.

4. Results and discussion

In the following, we will present the four different extruder concepts, and discuss their performance based on the outcome

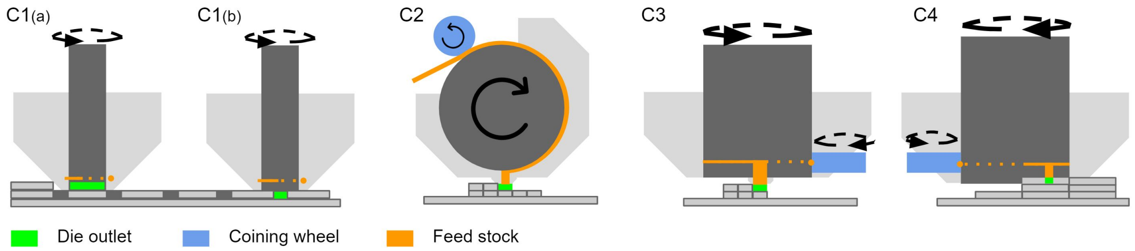

Fig. 6. The alternative extruder concepts that have been evaluated; C1(a): PinPoint extruder with flat pin; C1(b): PinPoint extruder with protruding pin; C2: Wheel extruder; C3: Spindle extruder; C4: Rotating die extruder.

of the probing cycles. An overview of the different concept is included in Fig. 6. A summary of the conducted experiments is listed in Table 1. The overall evaluations of the designs that passed the physical testing are listed in Table 2.

4.1. Concept 1: Pinpoint extruder

The working principle of the PinPoint extruder is described in Section 2. A probing cycle was carried out for the PinPoint extruder with a flat pin and a rear outlet width equal to the diameter of the pin.

In the tested configuration the location of the abutment causes the pressure to be higher on the right side of the stringer bead. A drawback of the PinPoint extruder when used for AM purposes is the relatively large footprint that leads to a course structure and increased tool forces. An attempt was made to limit the die outlet area; however, such a deposition technique will not work when stacking two or more singular stringer beads on top of each other because of flash formation due to lack of sealing of the area of the pin that is unsupported by the substrate. Another drawback of the PinPoint extruder when employed for AM, is that it requires the use of two sets of tools to complete a layer in a structure, see Fig. 2.

4.2. Concept 2: Wheel extruder

The wheel extruder was the first extruder design to be explored for the HYB joining process and is a down-scaled version of a Conform extruder. However, the solution was later abandoned due to trouble with achieving the required stiffness of die and abutment area. When applied for AM, however, the lower operating pressure can be reduced significantly compared to welding, thus making it possible to resolve the stiffness problems of the initial design.

With the wheel extruder, the oxide layer on the substrate is cut away by the sharp die edge just at the outlet of the die such that the newly cut surface is continuously covered and bonded with the extruded feedstock material. The wheel extruder used for one of the probing cycles is shown in Fig. 7a and 7b along with a section of a deposited structure in Fig. 7c. The die is designed to scrape the side-wall of the adjacent stringer and the top of the under-laying stringer to remove oxides. In Fig. 7a the flash build-up on the faces adjacent to the conform slot is clearly visible. By cutting away this flash just after the abutment, the contact area of sticking friction and thus the torque to rotate the wheel can be reduced significantly.

4.3. Concept 3: Spindle extruder

The spindle extruder is a later iteration of the HYB welding extruders [18], and is built around a vertical-oriented axle or ”spindle” that is slightly tilted towards the feed direction. A conform slot is cut into the lower part of the axle and the material is extruded in the axial direction through the die.

The spindle extruder was tested in three different configurations. The most promising result with regards to deposition quality was obtained when using a die that was separated from the spindle (C3.1), similarly to that of the wheel extruder. How-

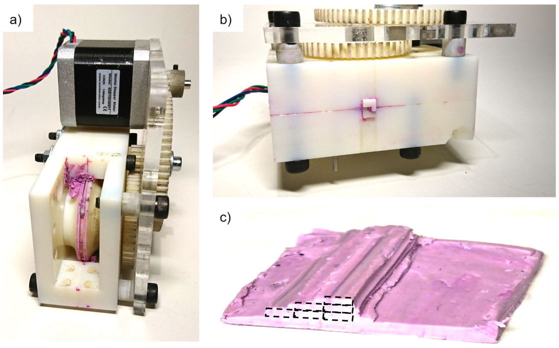

Fig. 7. The wheel extruder prototype; (a) the flash formation causes material to build up at the inlet of the extruder; (b) the extruder seen from underneath, the die shape is similar to the design shown in Fig. 8; (c) a cross-section of a deposited structure.

Table 1. Summary of key learnings from the probing cycles

Nr.	Type	Description	Key Learning's
C1.1	PinPoint extruder	Full-width stringer bead deposition	Pressure is higher on right side of the bead. Abutment location needs to be re-positioned
C2.1	Wheel Extruder	Die dimension 2x3 mm	The shape of the housing makes it hard to clean the edges of the die. Flash build up on the wheel.
C3.1	Spindle extruder	Isolated die	Oxide scraper is easy accessible
C3.2		Vertical spindle	Material transfer from previous layer
C3.3		Tilted spindle	Some transverse material transfer from top of substrate.
C4.1	Rotating die extruder	Flat spindle	Uncomplete stringers. Forward flash
C4.2		Flat spindle	Substrate sticks to bottom of spindle
C4.3		Semi hollow pin	Substrate sticks to bottom of spindle
C4.4		Concave spindle tip	Substrate sticks to bottom of spindle

ever, a drawback of this particular design is the internal length of the die that calling for a higher extrusion pressure.

C3.3 has a die design that is similar to that used for welding [18] where the die length is minimized by letting the spindle constitute one of the die walls, see Fig. 8. When used in this configuration, the lower part of the spindle will stick to the top of the deposited stringer, causing some transverse shearing of the top of the stringer as depicted in Fig. 9. Still, this design is favourable due to the significantly shorter die length.

The spindle extruder allows for the addition of a coining wheel to firmly engage the feedstock wire into the conform slot to prevent wire slip and reduce excess heat generation during extrusion.

4.4. Concept 4: Rotating die extruder

The fourth extrusion concept is the rotating die extruder which is a design that emerged during the exploration of the other designs. The concept is a hybrid of the Spindle extruder and the PinPoint extruder.

The rotating die extruder aims at reducing the tool forces by reducing the die outlet area while still being able to deposit wide stringers. The dies are cut into the conform slot and the bottom of the pin is supposed to interfere with the substrate to continuously break up the oxide layer, while the spindle is rotating.

Table 2. Evaluation of the four extruder concepts C1-C4. Each criterion is weighted (W) and given a score from 1 to 3.

Criteria	W	C1	C2	C3	C4
Tool forces	2	1	3	3	1
Process control	2	1	2	3	1
Flash formation	2	1	2	3	2
Oxide removal	2	3	1	1	2
Resolution	1	1	2	2	1
Wire slip	1	1	3	3	3
Contact friction	1	2	3	3	3
Serviceability	1	1	2	2	1
Deposition quality	3	2	2	2	1
Sum		23	32	36	23

From testing, it became visible how the substrate would stick to the bottom of the spindle and cause the top of the substrate to distort. Despite the attempts to address these issues, the extruder failed when it came to stacking two stringer beads on top of each other.

4.5. Other emerging requirements and insights

4.5.1. Extrusion pressure and processing temperature

The required extrusion pressure is the sum of the pressure loss through the die in addition to the pressure that is required for bonding with the substrate. Assuming sticking friction between walls and feedstock, the force required to push the extrudate through the die is roughly given by the surface area of the die walls multiplied by the shear strength of the feedstock material. Heating the feedstock will reduce the flow stress; however, for precipitation hardening alloys the structure will end up in an over-aged condition requiring solution heat treatment and subsequent ageing to regain the strength.

The diameter of the conform extruder is deciding the length of the extrusion chamber and the maximum pressure obtainable. If the chamber length becomes too short compared to what is required to counteract the pressure drop through the die, this will cause wire slip thus generating excessive heat. On the other hand, increasing the diameter will also increase the torque required to rotate the spindle.

4.5.2. Contact friction and flash formation

During extrusion, the feedstock will start to flow through the gap between the spindle and the housing in the extrusion grip zone of the extruder. This material leakage is considered flash, and is a loss of material and should thus be reduced to a minimum. Reducing the extrusion pressure as well as tighter tolerances between spindle and housing can reduce these leaks. This flash formation will also add a lot of friction between the spindle and the housing, and if this flash is not removed, the whole circumference of the spindle will get covered in aluminium,

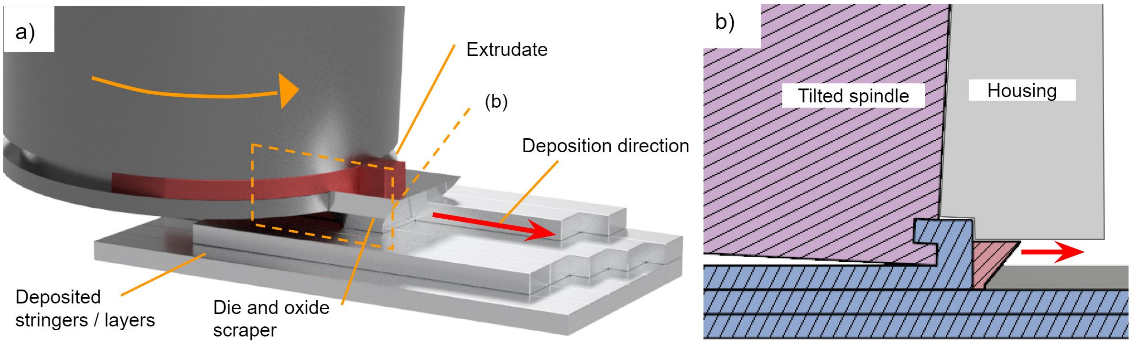

Fig. 8. Illustration of the Spindle extruder. The spindle constitutes the fourth wall of the die and makes for the shortest possible die length of the designs; (a) a possible deposition sequence where the die is used as an oxide scraper; (b) Section through the spindle and die. The spindle is tilted to reduce interference with the substrate.

causing the spindle to stick to the housing. However, by cutting away the newly formed flash after the abutment, the spindle can rotate without contact in the sector between the flash cutter and the extrusion grip zone. Fig. 10 illustrates how the removal of flash can reduce the friction between the spindle and the housing. Similarly, the flash needs to be removed to avoid entering the bearings of the spindle.

4.6. Post processing

The near net shape structures produced using the HYB-AM process requires for most practical purposes milling to achieve their final shape. In cases where post heat treatment is needed, this should be carried out before milling to eliminate distortions.

5. Conclusions

Prototyping combined with physical modelling has allowed us to evaluate a total of four different extruder and deposition concepts for the HYB-AM process. New insights in the process along with requirements for the further development of the process have emerged through the probing cycles of designing, building and testing the prototypes.

Based on the experiments conducted herein, we conclude that the further development of the HYB-AM process should focus on the Spindle extruder. The Spindle Extruder is built around a spindle that is slightly tilted from the vertical axis in the feed direction. A conform slot is cut into the lower part of the spindle for providing the required extrusion pressure. The die length can be minimized by having the spindle itself constitute one of the die walls. The diameter of the spindle can be optimized to reflect the required extrusion length to prevent wire slippage.

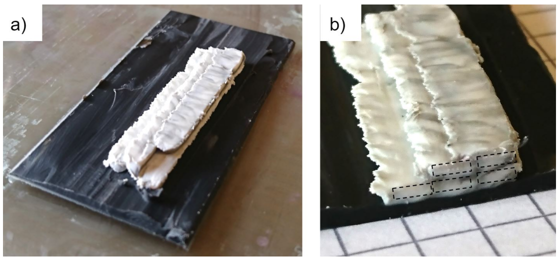

Fig. 9. Structure deposited by the Spindle extruder; (a) the coarse structure will need post processing in terms om milling to obtain the final shape; (b) section through the structure.

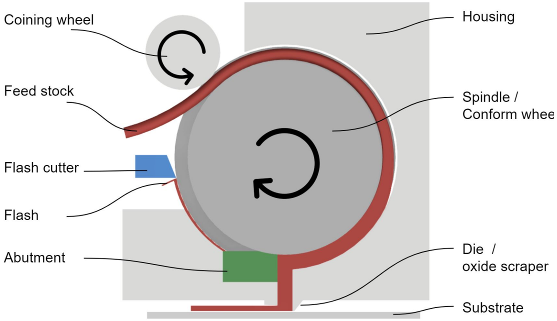

Fig. 10. Principal illustration of the Spindle extruder when used for additive manufacturing

Acknowledgements

The authors acknowledge the financial support from NAPIC (NTNU Aluminium Product Innovation Center) and the KPN project Value sponsored by Research Council of Norway, Hydro and Alcoa. They are also indebted to Hybond AS and Øystein Grong for valuable input in the design process.

References

[1] B. M. Kennedy, D. K. Sobek, M. N. Kennedy, Reducing Rework by Applying Set-Based Practices Early in the Systems Engineering Process, Systems Engineering 17 (3) (2014) 278–296. `doi:10.1002/sys.21269`.
URL `http://doi.wiley.com/10.1002/sys.21269`

[2] M. Steinert, L. J. Leifer, 'Finding One's Way': Re-Discovering a Hunter-Gatherer Model based on Wayfaring, International Journal of Engineering Education 28 (2) (2012) 251.

[3] A. Sutcliffe, P. Sawyer, Requirements elicitation: Towards the unknown unknowns, in: Requirements Engineering Conference (RE), 2013 21st IEEE International, IEEE, 2013, pp. 92–104.

[4] A. Gerstenberg, H. Sjöman, T. Reime, P. Abrahamsson, M. Steinert, A Simultaneous, Multidisciplinary Development and Design Journey – Reflections on Prototyping, in: K. Chorianopoulos, M. Divitini, J. B. Hauge, L. Jaccheri, R. Malaka (Eds.), Entertainment Computing - ICEC 2015, no. 9353 in Lecture Notes in Computer Science, Springer International Publishing, 2015, pp. 409–416.
URL `http://link.springer.com/chapter/10.1007/978-3-319-24589-8_33`

[5] C. Kriesi, J. Blindheim, Ø. Bjelland, M. Steinert, Creating Dynamic Requirements through Iteratively Prototyping Critical Functionalities, Procedia CIRP 50 (2016) 790–795. `doi:10.1016/j.procir.2016.04.122`.
URL `http://linkinghub.elsevier.com/retrieve/pii/S2212827116303109`

[6] C. W. Elverum, T. Welo, On the use of directional and incremental prototyping in the development of high novelty products: Two case studies in the automotive industry, Journal of Engineering and Technology Management 38 (2015) 71–88. `doi:10.1016/j.jengtecman.2015.09.003`.
URL `http://linkinghub.elsevier.com/retrieve/pii/S0923474815000405`

[7] A. Green, The use of plasticine models to simulate the plastic flow of metals., The London, Edinburgh, and Dublin Philosophical Magazine and Journal of Science 42 (327) (1951) 365–373.

[8] T. Wanheim, M. P. Schreiber, J. GrØnbaek, J. Danckert, Physical modelling of metal forming processes, Journal of Applied Metalworking 1 (3) (1980) 5–14. `doi:10.1007/BF02833900`.
URL `https://doi.org/10.1007/BF02833900`

[9] H. Sofuoglu, J. Rasty, Flow behavior of Plasticine used in physical modeling of metal forming processes, Tribology International 33 (8) (2000) 523–529. `doi:10.1016/S0301-679X(00)00092-X`.
URL `http://linkinghub.elsevier.com/retrieve/pii/S0301679X0000092X`

[10] B. Liechty, B. Webb, The use of plasticine as an analog to explore material flow in friction stir welding, Journal of Materials Processing Technology 184 (1-3) (2007) 240–250. `doi:10.1016/j.jmatprotec.2006.10.049`.
URL `http://linkinghub.elsevier.com/retrieve/pii/S092401360600940X`

[11] R. Manna, P. Agrawal, S. Joshi, B. K. Mudda, N. Mukhopadhyay, G. Sastry, Physical modeling of equal channel angular pressing using plasticine, Scripta Materialia 53 (12) (2005) 1357–1361. `doi:10.1016/j.scriptamat.2005.08.031`.
URL `http://linkinghub.elsevier.com/retrieve/pii/S1359646205005154`

[12] Ø. Grong, Method and device for joining of metal components, particularly light metal components, Patent.

[13] Ø. Grong, Recent advances in solid-state joining of aluminum, Welding journal 91 (1) (2012) 26–33.

[14] L. Sandnes, Ø. Grong, J. Torgersen, T. Welo, F. Berto, Exploring the Hybrid Metal Extrusion & Bonding Process for Butt Welding of Al-Mg-Si Alloys, The internasjonal journal og advanced manufacturing technology`doi:10.1007/s00170-018-2234-0`.

[15] J. Blindheim, Ø. Grong, U. R. Aakenes, T. Welo, M. Steinert, Hybrid Metal Extrusion & Bonding (HYB) - a new technology for solid-state additive manufacturing of aluminium components, Procedia Manufacturing 26 (2018) 782–789. `doi:10.1016/j.promfg.2018.07.092`.
URL `https://linkinghub.elsevier.com/retrieve/pii/S2351978918307637`

[16] D. Green, Continuous extrusion-forming of wire sections, J INST MET 100 (1972) 295–300.

[17] C. Etherington, CONFORM—a new concept for the continuous extrusion forming of metals, Journal of Engineering for Industry 96 (3) (1974) 893–900.

[18] U. Aakenes, Industrialising of the Hybrid Metal Extrusion & Bonding (HYB) Methodfrom Prototype towards Commercial Process, Ph.D. thesis, Norwegian University of Science and Technology (2013).

Paper 3

This Paper is awaiting publication and is not included in NTNU Open

Paper 4

Noname manuscript No.
(will be inserted by the editor)

First demonstration of a new additive manufacturing process based on metal extrusion and solid-state bonding

Jørgen Blindheim · Torgeir Welo · Martin Steinert

Received: date / Accepted: date

Abstract In this paper, a new additive manufacturing (AM) process based on extrusion and solid-state bonding is presented. The process uses metal feedstock wire which is processed in a continuous rotary extruder in order to disperse the surface oxides of the feedstock and to provide the required bonding pressure. Simultaneously, the die outlet is scraping the contact surface to provide an oxide-free interface between the extrudate and the substrate. Optical analyses of samples from a layered structure produced from AA6082 reveal that the stringers are fully merged; however, some voids and cracks are observed between the individual stringers. Still, this initial demonstration indicates that the process, upon further development, has high potential of producing near-net-shape parts at high deposition rates.

Keywords Additive manufacturing · Solid-state bonding · Continuous rotary extrusion

Acknowledgements The authors acknowledge the financial support from NTNU, NAPIC (NTNU Aluminium Product Innovation Center) and the KPN project Value sponsored by Research Council of Norway, Hydro and Alcoa. Thanks to Vidar Berg for providing a solution to transferring torque data from a rotating shaft. They are also indebted to Hybond AS and Øystein Grong for valuable assistance.

Norwegian University of Science and Technology, NTNU
Department of Mechanical and Industrial Engineering, 7491 Trondheim, Norway
Tel.: +47 90 50 22 16
E-mail: jorgen.blindheim@ntnu.no

1 Introduction

During the last years, we have seen an increase in the industrial use of additive manufacturing (AM) technologies, opening for mass customization of net-shape or near-net-shape parts that can potentially lead to less labour time, as well as reduced energy consumption and material waste compared to traditional subtractive processes. Additive processes can also provide increased design freedom as well as weight savings not achievable by traditional manufacturing processes.

AM of metals can be divided into three main categories regarding processing; Powder Bed Fusion (PBF), Directed Energy Deposition (DED) and Sheet Lamination (SL) [1]. In PBF, the part being produced is supported by the unconsolidated powder, thus providing great design freedom and the possibility to create detailed and complex shapes that are otherwise impossible to manufacture. However, the deposition rates for these processes are low, and the part size is limited by the powder bed size. For both the DED and SL categories, one finds processes covering the whole range from small or complex net-shape parts to the larger near-net-shape components at higher deposition rates. In the lower end of this range, one find processes like droplet-based 3D printing [2, 3] and Acoustoplastic metal write [4], whereas Wire Arc Additive Manufacturing (WAAM)[5] and Ultrasonic AM [6] are examples of high deposition rate processes for the DED and SL categories respectively.

1.1 Melted-state AM processes for aluminium

For melted-state AM, the use of aluminium has been limited to a few alloys due to the resulting ”as-cast” microstructure inherited from the melting. Only recently it has been demonstrated that this problem can be overcome by the addition of nanoparticles acting as nucleation sites for new grains during PBF processing of AA7075 and AA6061, resulting in material strengths comparable to wrought material [7].

Still, most melted-state processes suffer from restrictions in the deposition rate due to limitations in the melt pool size. In addition, the contractions occurring during solidification and subsequent cooling usually lead to build-up of residual stresses in the structure, causing undesirable local and global deformations. Various mitigating actions have been undertaken to avoid such thermally-induced distortions, like symmetric building, back-to-back building and the use of high-pressure interpass rolling [5]. WAAM based on the Cold Metal Transfer (CMT) welding process has the capability to achieve high deposition rates, yet with increased material waste, since higher deposition rates contribute to a wider melt pool size and thus a thicker wall structure. A typical CMT deposition rate for aluminium, when keeping the Buy to Fly (BTF) ratio at 1.5, is 1kg/h [5].

1.2 Solid-state AM processes for aluminium

AM processes based on friction joining were first patented in 2002 [8], and have later been commercialized for ultrasonic consolidation of thin sheets or foils [6]. Commercial ultrasonic machines from Fabrisonic are capable of depositing up to 1.3 kg/h. In recent years, a solid-state process based on friction welding has been developed, where the material is deposited onto the substrate using a rotating consumable rod [9]. Also, a process based on friction stir welding (FSW) has been demonstrated for bonding of stacked metal plates [10]. More recently, Aeroprobe has developed a modified FSW process, called MELD, where the feedstock is added through a rotating stirring tool [11].

Unlike melted-state processes, where the substrate is required to continuously solidify to keep its shape, solid-state processes have no such limitations in the deposition rate, as long as the deposition temperature is kept below the melting temperature of the material. This makes solid-state processes attractive for manufacturing of larger structures.

The overall aim of this research is to add knowledge to the field of solid-state AM, as a basis for development of new technology that enables deposition of the aluminium alloys commonly used in the automotive and aerospace industry today. The scope of this research covers a proof-of-concept demonstration of a new AM process based on continuous rotary extrusion and solid-state bonding.

In order for new manufacturing technology to be attractive to the industry, it needs to provide increased value as compared to commercially available manufacturing methods. For near-net-shape AM processes, when compared to the subtractive methods, added value can be attributed to e.g, the ability to replace complex assemblies by a single part, reduced material waste, or the possibility of producing functionally graded components. Therefore, in order to investigate the capabilities of this new process relative to more established AM processes, we use the following main performance parameters: (1) material properties; (2) deposition rates; (3) energy efficiency and; (4) material efficiency.

Overall, the goals in this study are; (1) to conduct a proof-of-concept test of an extruder and a deposition sequence and; (2) to assess the technical feasibility and potentials of the proposed concept within the abovementioned boundary conditions.

In the following section (2) the operating principles of the proposed AM process are presented. Section 3 describes the experimental setup, while Section 4 presents the results and discusses the outcome based on the goals of this study. Finally, conclusions are given in Section 5.

2 Process description

The new process presented in this paper has emerged from the Hybrid Metal Extrusion & Bonding (HYB) technology, which originally was developed for joining of aluminium plates and profiles [12, 13]. The use of filler material addition during HYB welding may have some obvious advantages if adapted for AM purposes, which have sparked our interest in exploring the potential of such a process. The initial exploration and conceptualization prior to this work are presented in previous studies [14, 15].

2.1 Bonding mechanisms

Historically, solid-state bonding was one of the first techniques used to bond two pieces of metal. Already in the middle bronze age this technique was used for hammering smaller nuggets of gold to form larger pieces [16]. The first scientific study of cold welding was inspired by the Swedish scientist Mårten Triewald and published in 1724 by Desaguliers [17]. He describes how to bond two lead balls by cutting away a segment of each, and pressing them together with a little twist. However, it was not until the middle of the 20th century that the research was intensified, ultimately leading to a deeper understanding of processes like cold pressure welding,

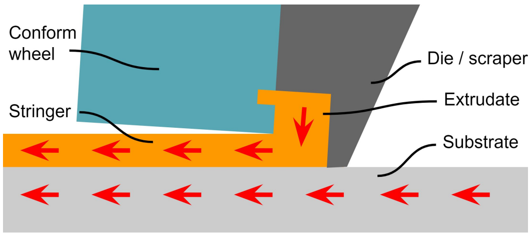

Fig. 1 Bonding is achieved as the metal streams of the oxide dispersed extrudate and the scraped substrate merges under high pressure.

friction welding, accumulative roll bonding and extrusion of hollow sections.

The film theory was described by Bay in 1983 [18] and is still the way the bonding mechanisms are understood today. To achieve solid-state bonding, the virgin metal surfaces must be brought so closely together that metallic bonding occurs. For reactive materials like aluminium, however, the oxide layer either has to be removed prior to mating the bonding surfaces. Alternatively, the surfaces have to be expanded or deformed such that the oxide layer is cracked to allow the virgin materials to contact during deformation. An example of the former category is cold pressure welding, where oxides are removed through an outward material flow during compression [16]. Bonding through surface expansion, on the other hand, is utilized in processes like cold roll bonding and accumulative cold roll bonding [19].

Similar bonding mechanisms can also be observed in longitudinal seam welds of porthole-die extrusions, where welds are formed under high pressure as the different material streams merge after flowing around the die bridges or webs [20, 21, 22, 23]. The bonding mechanisms of these welds can be understood in both the above-mentioned ways, depending on whether a gas-pocket is formed behind the bridge during extrusion causing oxides to form on the bonding interfaces, as pointed out by Yu et al. [23].

The metal flow in the new process proposed in this work resembles the one occurring during porthole die extrusion. However, in this case, the merging metal streams should be considered as mating streams of extrudate and substrate, as illustrated in Fig. 1.

2.2 Extrusion principle

Continuous rotary extrusion - also known as Conform extrusion [24, 25] - serves two purposes in this process: First, when the feedstock is deformed in the extruder, oxides present on the feedstock surface are dispersed into the extrudate. Secondly, the extruder provides the required pressure to obtain bonding at the interface between the extrudate and the substrate. Following the illustration in Fig. 2a, the feedstock wire is firmly pressed into the groove of a rotation wheel. The wheel is sealed by a housing provided with an abutment with a die at the end. The surface area of the grove is larger than the exposed surface of the housing, thus creating a net driving force in the direction of rotation. When the feedstock is blocked by the abutment, axial compression is induced, causing the material to fill the entire cross section. This, in turn, increases the contact area and friction further, and leads to a pressure build-up. When the required extrusion pressure is obtained, the material is extruded through the die outlet close to the abutment.

2.3 Deposition sequence

Fig. 2b illustrates the deposition sequence applied in this study. A blank of aluminium is fixed in the machine, acting as a substrate upon which the first layer is bonded .The extruder adds material as it moves in the deposition direction, placing stringers side-by-side to form a layer, allowing new layers to be added . The die-outlet is scraping both the underlying layer and the side wall of the adjacent stringer to remove the oxides and create favourable conditions for bonding with the extrudate. To ensure that the scraper touches the mating surfaces, 0.1 mm of the adjacent stringer and underlaying surface is cut away by the scraper within each pass.

3 Experimental

3.1 Setup

A Sieg SX3 CNC milling machine was used to control the speed and position of the extruder during deposition. The extruder wheel, house and the die of the extruder (Fig. 3) were produced from hardened Uddeholm Orvar Supreme tool steel. The extruder is driven by a 1.8kW servo motor connected through a gearbox with a gear reduction of 30. Torque data was measured through a Smowo LCS-T5 torque cell and a HX711 ADC, wirelessly connected to a computer. Nichrome heat-cartridges and a K-type thermocouple were inserted into the print bed and used to control the substrate temperature during deposition from a PID-controller. The extruder house was, by the same means, pre-heated to soften and increase the formability of the feedstock

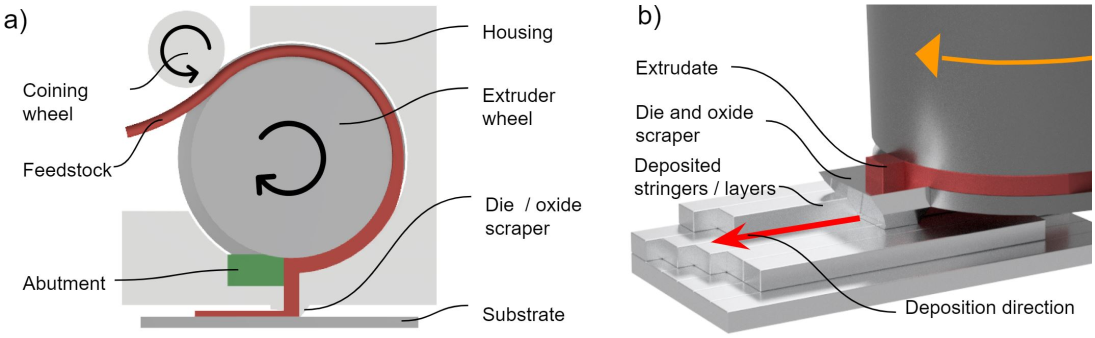
a)
Housing
Coining wheel
Extruder wheel
Feedstock
Die / oxide scraper
Abutment
Substrate
b)
Extrudate
Die and oxide scraper
Deposited stringers / layers
Deposition direction

Fig. 2 Principal illustrations of the extruder (a) The extruder consists of a slotted wheel running over a stationary housing. A coining wheel is used to firmly press the wire into the slot, causing the rotating wheel to grip the wire. The extrusion pressure is built up as the material is blocked by the abutment. The die also act as a scraper in order to remove oxides from the substrate prior to bonding with the extrudate; (b) the wheel and the die along with a deposited structure

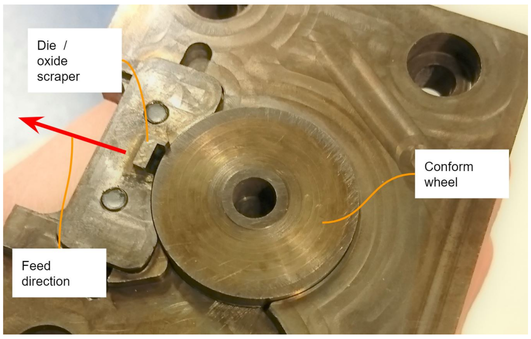
Die / oxide scraper
Conform wheel
Feed direction

Fig. 3 The extruder head as seen from underneath.

Table 1 Specifications for the extruder.

Parameter	Value
Wire diameter	1.6 mm
Max speed	100 RPM
Max deposition rate	2150 g/h
Outlet dimensions (w x h)	4 mm x 1 mm
Extruder wheel outer diameter	28 mm

material prior to extrusion. The experimental setup is depicted in Fig. 4 and some key data for the extruder is listed in Table 1.

3.2 Process parameters

Fig. 5 shows a two-layered structure deposited by this process. The operational conditions are summarized in Table 2. The feedstock material was 1.6mm AA6082 wire in T4 temper, deposited to a cross-section of 0.9mm

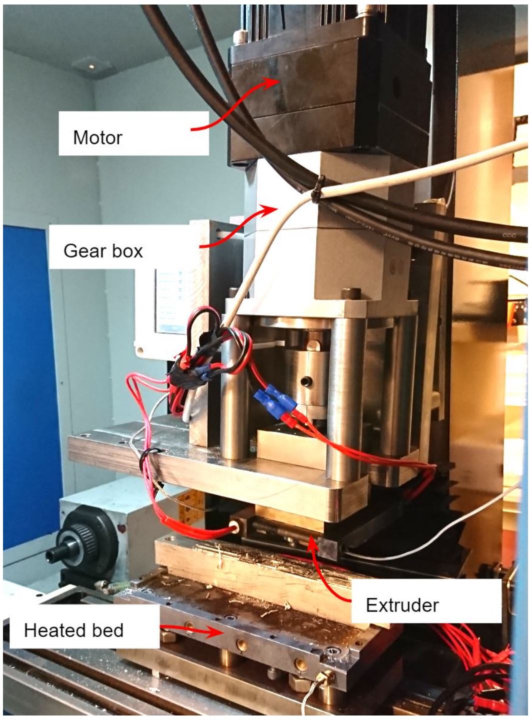
Motor
Gear box
Extruder
Heated bed

Fig. 4 The extruder attached to a CNC milling machine. A heated bed is used to control the temperature of the deposited structure.

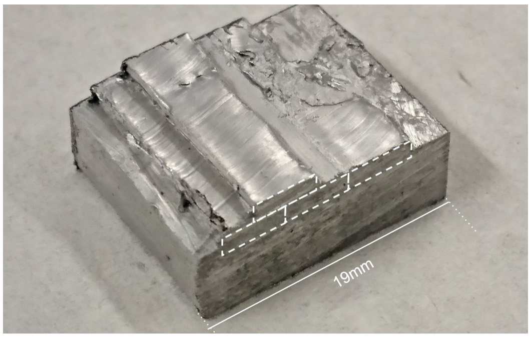

Fig. 5 Photograph of a deposited sample of AA6082.

Table 2 Parameters used in the experimental setup.

Parameter	Value
Pin rotation speed	4.3 RPM
Feed rate	200 mm/min
Deposition rate	116 g/h
Applied torque	175 Nm
Deposition temperature	450 °C

x 4mm onto a substrate of the same alloy. Table 3 gives the chemical composition of the AA6082 feedstock material.

3.3 Sample preparation

Samples used for macrostructural analyses were prepared according to standard preparation procedures. To reveal the macrotructure of the bonding interfaces, the specimens were immersed in a 1% sodium hydroxide solution for 10 minutes. The macrographs of the samples were captured using an Olympus BX35M light microscope and an Alicona Confocal Microscope.

4 Results and Discussion

4.1 Interpretation of governing mechanisms

The sample depicted in Fig. 5 has been sectioned for observation of the bonding interfaces between the individual stringers. Optical macrographs are shown in Fig. 6.

Fig. 6a shows the substrate material with two layers deposited on top. From the macrograph, it is visible how the stringers have been conformed to the underlying material, indicating that the interfaces have been subjected to contact pressures above the flow stress of the material. Still, defects in the form of cracks can be observed between the individual stringers, as depicted in Fig. 6c, meaning that the layers are not fully bonded. A possible reason for this can be oxide formation on the interfaces during deposition. This failure mode is similar to that observed in longitudinal seam welds in porthole die extrusion, when a gas pocket is present behind the bridge [23]. In the case of the demonstrated process, the pressure at the bonding interface is controlled by the rotational speed and the scanning speed of the extruder. If the extruder moves too fast, it will not provide sufficient material flow to allow for pressure build-up in the die cavity, thus, forming a gas pocket.

Fig. 6b displays a pore between the two stringers of the first layer. Higher extrusion pressure can to some extent prevent this defect. However, a more suitable solution is to reduce the angle of the sidewall of the adjacent stringer in order to avoid the sharp corner and thus create more favourable material flow conditions. Still, this proof-of-concept study has demonstrated that the extruder is capable of processing and depositing advanced aluminium alloys. More extensive laboratory testing is required to further investigate the governing mechanisms of this process and to determine the mechanical properties of the deposited material. Future work will focus on these aspects.

4.2 Deposition rates

From an industrial perspective, deposition rates are crucial for increasing the manufacturing efficiency. The deposition rate of the suggested process is controlled by the circumferential velocity of the conform wheel and the diameter of the feedstock wire. The current extruder design, which uses Ø1.6 mm feedstock wire, yields a deposition rate of more than 2 kg/h at its maximum speed of 100 RPM. This high deposition rate makes this AM technology particularly suitable for manufacturing of larger structures where this capability can be fully utilized. In theory, the deposition rate is only limited by the scaling of the process. However, the deposition rate must be balanced and compatible with other requirements, such as the scanning speed, the die geometry, the process temperature and the contact pressure at the bonding interface. Future experiments will be carried out at higher deposition rates to investigate the optimal parameters for achieving proper bonding between the extrudate and the substrate.

4.3 Energy efficiency

The work done on the deposited material can be calculated from the rotational speed and the supplied torque

Table 3 Chemical compositions of AA6082 feedstock material.

Fe	Si	Zn	Mn	Mg	Cu	Ti	Al (balance)
<0.50	0.7-1.3	<0.2	0.4-1.0	0.6-1.2	<0.1	<0.1	95.2-98.3

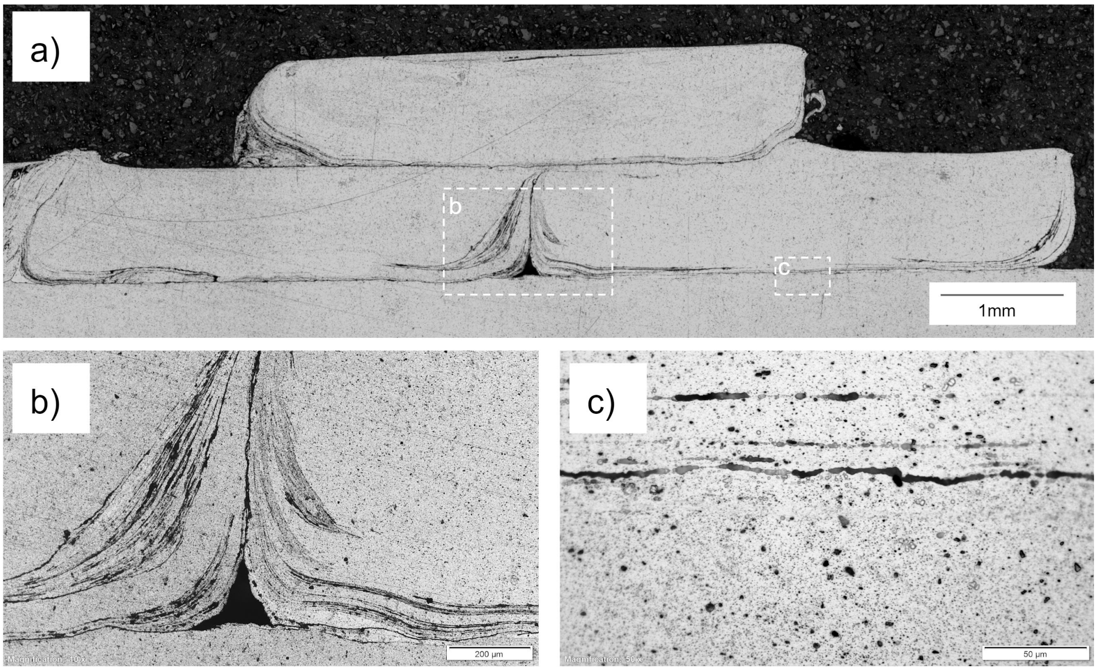

Fig. 6 Optical macrographs of (a) a transverse section of a deposited structure; (b) pore formation at the interface between two adjacent stringers; (c) cracks on the interface between the substrate and a stringer.

on the extruder along with the feed distance and the applied force in the feed direction from the following formulae:

$$W_i = 2\pi MN + Fs$$

Referring to Table 2, the extruder is subjected to a torque of M=175 Nm at a rotational speed of N=4.3 RPM and a feed speed of 200 mm/min. Assuming sticking friction over the contact area of the die outlet, the force in the feed direction, F, will be in the order of 1,500 N at the extrusion temperature. The supplied power during the experimental run is calculated to be 84 W.

Furthermore, to calculate the energy efficiency of the process, the applied work should be compared to that of the required heat input to bring the material up to extrusion temperature. The latter can be estimated from the specific heat capacity of the feedstock material, c=987 J/kgK, the deposition rate and the temperature change, $\Delta T = 430K$ from:

$$Q_r = cm\Delta T$$

The overall efficiency of the process then becomes $\eta = 0.16$, conclusively demonstrating that the process generates excess heat which needs to be dissipated during processing. Still, when comparing against the CMT process, Dutra et al. reported a power consumption of 1,430 W for welding of AA5183 Ø1.2 mm wire at 7 m/min [26]. Under the assumption of linearity between the power input and the deposition speed, the energy consumption of this new process is 30% less than that of the CMT process.

4.4 Materials

In this proof-of-concept study, the technology has been demonstrated for an Al-Mg-Si alloy commonly used for various structural applications. However, the process also has the potential of depositing other advanced aluminium alloys or extrudable metals. Joining the material in the solid-state eliminates the defects associated with melting of the material and maintains the wrought properties of the material through processing. This opens for creating AM parts from a wider range of aluminium alloys, even from the more advanced aerospace 7000-series, which for most purposes are considered unweldable by the melted-state processes. Furthermore, the nature of additive processing means that the feedstock composition can be altered during processing to create functionally graded components having tailored material properties in specific regions of a part.

For precipitation hardening alloys, like Al-Mg-Si, it is necessary to carry out solution heat treatment followed by quenching and ageing to utilize the full strength potential of the part. By depositing at the solution heat treatment temperature, the part can be soaked for the required time for supersaturation of the whole structure. Finally, after quenching, the desired ageing cycle can be carried out to control the formation of precipitates.

4.5 Material utilization

The relatively coarse near-net-shape structure requires subtractive machining to obtain the final shape and tolerances. This final processing step will cause material waste depending on the requirements of the net-shape; however, obviously with significantly less waste than that of machining from solid blanks. Allen lists BTF ratios ranging from 6 to 20 for some typical titanium aero engine components [27], while Barnes [28] reports a BTF industry average of 11 for machined parts. Martina & Williams [29] considered different manufacturing options for a 15 kg aluminium wing rib and calculated a cost reduction of 65% for producing it by the WAAM process at a deposition rate of 1 kg/h and a BTF ratio of 2.3, as opposed to 40 for machining from a solid blank. With the new process proposed in this paper, it is reasonable to achieve BTF ratios comparable to that achieved by the WAAM process, depending on the final part geometry.

4.6 Further developments

The further development of this AM process towards real-world industrial application will focus on optimizations with regards to extruder design and process control. From the proof-of-concept testing conducted herein, it was observed material accumulation on the bottom of the extruder wheel, causing some process instability. An isolated die design, inhibiting the extruder wheel to interfere with the deposited material has the potential to prevent this issue, but at the cost of increased extrusion pressure due to increased die length. Furthermore, the diameter of the extruder wheel should be adapted to the required extrusion chamber length for the required extrusion pressure in order to reduce friction, and thus the required torque to rotate the extruder.

5 Conclusions

This paper has presented a new solid-state AM process based on continuous extrusion and bonding of metal feedstock wire. The main objectives of the investigation were to conduct a proof-of-concept demonstration of the process and assess its potentials. Through this preliminary investigations, the technical feasibility has been conclusively demonstrated by successfully depositing a near-net-shape structure of AA6082. The process operates below the melting temperature and has thus the potential of achieving high deposition rates. The fact that no material melting is involved, means that potential problems related to hot cracking and residual stresses are reduced compared to those associated with conventional melted-state processes. The energy efficiency of the process is higher or comparable to that of established AM processes.

Future work will focus on process optimization, along with laboratory testing to determine mechanical properties and the bonding strength between the deposited stringer beads and the layers.

References

1. ASTM (2015) Standard Terminology for Additive Manufacturing General Principles Terminology. ISO/ASTM 52900:2015(E)
2. Yi H, Qi L, Luo J, Zhang D, Li N (2019) Direct fabrication of metal tubes with high-quality inner surfaces via droplet deposition over soluble cores. Journal of Materials Processing Technology 264:145–154, DOI 10.1016/j.jmatprotec.2018.09.004, URL `https://linkinghub.elsevier.com/retrieve/pii/S0924013618303959`
3. Yi H, Qi L, Luo J, Zhang D, Li H, Hou X (2018) Effect of the surface morphology of solidified droplet on remelting between neighboring aluminum droplets. International Journal of Machine Tools and Manufacture 130-131:1–11, DOI 10.1016/j.ijmachtools.2018.03.006, URL `https://linkinghub.elsevier.com/retrieve/pii/S089069551830066X`
4. Deshpande A, Hsu K (2018) Acoustoplastic metal direct-write: Towards solid aluminum 3d print-

ing in ambient conditions. Additive Manufacturing 19:73–80, DOI 10.1016/j.addma.2017.11.006, URL https://linkinghub.elsevier.com/retrieve/pii/S2214860417300234

5. Williams SW, Martina F, Addison AC, Ding J, Pardal G, Colegrove P (2016) Wire + Arc Additive Manufacturing. Materials Science and Technology 32(7):641–647, DOI 10.1179/1743284715Y.0000000073
6. White DR (2003) Ultrasonic consolidation of aluminum tooling. Advanced Materials & Processes 161(1):64–65
7. Martin JH, Yahata BD, Hundley JM, Mayer JA, Schaedler TA, Pollock TM (2017) 3d printing of high-strength aluminium alloys. Nature 549(7672):365–369, DOI 10.1038/nature23894
8. White D (2002) Object consolidation employing friction joining. US6457629
9. Dilip JJS, Rafi HK, Ram GJ (2011) A new additive manufacturing process based on friction deposition. Transactions of the Indian Institute of Metals 64(1-2):27
10. Palanivel S, Nelaturu P, Glass B, Mishra R (2015) Friction stir additive manufacturing for high structural performance through microstructural control in an Mg based WE43 alloy. Materials & Design (1980-2015) 65:934–952, DOI 10.1016/j.matdes.2014.09.082
11. Schultz J, Creehan K (2014) System for continuous feeding of filler material for friction stir welding, processing and fabrication
12. Grong (2012) Recent advances in solid-state joining of aluminum. Welding journal 91(1):26–33
13. Sandnes L (2017) Preliminary Benchmarking of the HYB (Hybrid Metal Extrusion & Bonding) Process for Butt Welding of AA6082-T6 Plates Against FSW and GMAW. Master's thesis, Norwegian University of Science and Technology
14. Blindheim J, Grong , Aakenes UR, Welo T, Steinert M (2018) Hybrid Metal Extrusion & Bonding (HYB) - a new technology for solid-state additive manufacturing of aluminium components. Procedia Manufacturing 26:782–789, DOI 10.1016/j.promfg.2018.07.092, URL https://linkinghub.elsevier.com/retrieve/pii/S2351978918307637
15. Blindheim J, Welo T, Steinert M (2019) Rapid prototyping and physical modelling in the development of a new additive manufacturing process for aluminium alloys. Procedia Manufacturing DOI https://doi.org/10.1016/j.promfg.2019.06.212
16. Tylecote R (1968) The solid phase welding of metals. The Solid Phase Welding of Metals, Edward Arnold
17. Desaguliers JT (1724) Some experiments concerning the cohesion of lead. Philosophical Transactions of the Royal Society of London 33(389):345–347, DOI https://doi.org/10.1098/rstl.1724.0065
18. Bay N (1983) Mechanisms producing metallic bonds in cold welding. WELDING J 62(5):137
19. Saito Y, Utsunomiya H, Tsuji N, Sakai T (1999) Novel ultra-high straining process for bulk materialsdevelopment of the accumulative roll-bonding (ARB) process. Acta materialia 47(2):579–583
20. Akeret R (1992) Extrusion welds-quality aspects are now center stage. In: Proceedings of the 5th International Aluminium Extrusion Technology Seminar, 1992
21. Valberg H (2002) Extrusion welding in aluminium extrusion. International Journal of Materials and Product Technology 17(7):497–556
22. Yu J, Zhao G (2018) Interfacial structure and bonding mechanism of weld seams during porthole die extrusion of aluminum alloy profiles. Materials Characterization 138:56–66, DOI 10.1016/j.matchar.2018.01.052
23. Yu J, Zhao G, Chen L (2016) Analysis of longitudinal weld seam defects and investigation of solid-state bonding criteria in porthole die extrusion process of aluminum alloy profiles. Journal of Materials Processing Technology 237:31–47, DOI 10.1016/j.jmatprotec.2016.05.024
24. Etherington C (1974) Conform - a new concept for the continuous extrusion forming of metals. Journal of Engineering for Industry 96(3):893–900
25. Green D (1972) Continuous extrusion-forming of wire sections. J INST MET 100:295–300
26. Dutra JC, Gonalves e Silva RH, Marques C (2015) Melting and welding power characteristics of MIGCMT versus conventional MIG for aluminium 5183. Welding International 29(3):181–186, DOI 10.1080/09507116.2014.932974, URL http://www.tandfonline.com/doi/abs/10.1080/09507116.2014.932974
27. Allen J (2006) An Investigation into the Comparative Costs of Additive Manufacture vs. Machine from Solid for Aero Engine Parts. In: RTO-MP-AVT-139, p 10
28. Barnes J, Kingsbury A, Bono E (2016) Does " Low Cost " Titanium Powder Yield Low Cost Titanium Parts?
29. Martina F, Williams S (2015) Wire+arc additive manufacturing vs. traditional machining from solid: a cost comparison. Tech. rep.

Paper 5

On the mechanical integrity of AA6082 3D structures deposited by hybrid metal extrusion & bonding additive manufacturing

Jørgen Blindheim[a,*], Øystein Grong[a,b], Torgeir Welo[a], Martin Steinert[a]

[a] *Norwegian University of Science and Technology. 7045 Trondheim, Norway*
[b] *HyBond AS, NAPIC, 7045 Trondheim, Norway*

Abstract

Hybrid Metal Extrusion and Bonding Additive Manufacturing (HYB-AM) is a new solid-state process for the production of 3D metal structures. In HYB-AM, the wire feedstock is processed through a continuous extruder and deposited in a stringer-by-stringer manner to form layers and eventually a near net-shape component. In this work, the layer bonding of AA6082 samples produced by this process has been investigated by means of tensile testing, hardness measurements and microscopy analysis. Furthermore, a novel method for the fabrication of miniature specimens for tensile testing is presented. The test results demonstrate an ultimate tensile strength approaching that of the substrate material of the same alloy, yet with somewhat lower tensile ductility. Microscopy analyses show that the bonding interfaces are fully dense; however, the fracture surfaces reveal regions of kissing-bonds and lack of bonding. Still, these preliminary investigations indicate that the HYB-AM process, upon further optimization, has the capability of processing high quality aluminum alloy components.

Keywords: Additive manufacturing, Solid-state bonding, Aluminium alloys, HYB-AM

Declarations of interest: none

---

[*] Corresponding author
Email address: `jorgen.blindheim@ntnu.no` (Jørgen Blindheim)

Preprint submitted to Journal of Materials Processing Technology *September 2, 2019*

1. Introduction

Over the past years, additive manufacturing (AM) of metals has seen massive research interest along with a gradual adoption by the industry. The use of AM-technology enables new design freedom and opens for mass customization of near net-shape or net-shape parts at reduced energy consumption and with less material waste compared to traditional subtractive processes. A variety of AM processes exists, each with its individual characteristics when it comes to parameters like feedstock materials, part complexity, deposition rates, form of feedstock material (powder, wire, sheet), source of fusion (e.g. electron beam, laser, ultrasound) or state of fusion (solid-state, melted-state). The latter parameter – state of fusion – is of particular interest regarding processing of aluminium alloys.

In the melted-state category, the use of aluminium has been limited to a few alloys due to the resulting "as-cast" microstructure inherited from the melting involved. Only recently, Martin et al. (2017), demonstrated that this problem can be overcome by the addition of nanoparticles acting as nucleation sites for new grains upon processing of AA7075 and AA6061, resulting in material strengths comparable to those of wrought materials. Still, many melted-state processes suffer from reduced deposition rate due to limitations in the melt pool size. In addition, the contractions occurring during solidification and subsequent cooling can lead to a build-up of residual stresses in the structure, hence, causing global deformations and distortions.

Solid-state processes, on the other hand, have no such limitations in deposition rates, as long as the processing temperature is kept below the melting temperature of the material. This makes solid-state processes attractive for manufacturing of larger components. Moreover, it enables the use of the advanced aluminium alloys.

In the solid-state category, processes based on ultrasonic consolidation of sheets and foils are found, as first demonstrated by White (2003). Lately, ultrasound has also been used for joining of wire feedstock material (Deshpande

& Hsu, 2018). Another solid-state process used for AM purposes is Friction stir welding (FSW), which has been demonstrated for joining of stacked metal plates (Palanivel et al., 2015). Also, a modified FSW process, where the feedstock is added through a rotating stirring tool, has been developed by Aeroprobe (Schultz & Creehan, 2014). In addition, a process based on friction welding has been developed, where the material is deposited onto the substrate using a rotating consumable rod (Dilip et al., 2011).

In this work, the Hybrid Metal Extrusion & Bonding Additive Manufacturing (HYB-AM) process is presented in its current development stage, along with an investigation of the mechanical integrity of samples produced from AA6082. HYB-AM is a new solid-state process using metal feedstock wire to deposit material in a stringer-by-stringer manner to form layers and eventually a near net-shape structure. Subsequent to deposition, the part is finished by means of subtractive machining to achieve the desired net-shape, as depicted in Fig. 1. The potentials of this AM-process has previously been discussed by Blindheim et al. (2018).

For new manufacturing technology to be attractive to the industry, it needs to provide increased value compared to the currently available and proven manufacturing methods. A prerequisite, however, is that the mechanical integrity of the deposited material can compete with that of established production methods. In the case of HYB-AM, the bond strength between the individual stringers is considered to be the most critical quality requirement, and hence it has been the main objective of the study presented herein. Moreover, a new method for fabrication of specimens for tensile testing have been developed and applied for evaluation of the layer-to-layer bond strength.

The following section provides an introduction to the working principles of the HYB-AM process, whereas Section 3 covers the experimental setup. Section 4 presents the results and discusses the outcome based on the objective for this study. Finally, the conclusions are given in Section 5.

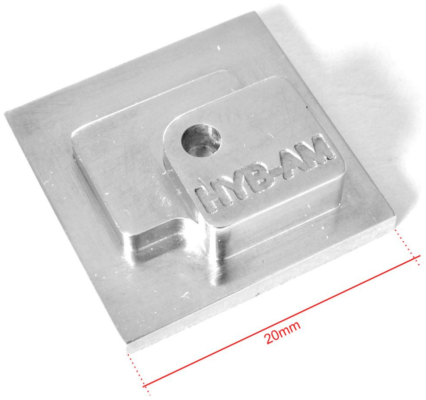

Figure 1: A demo-part in aluminium produced by the HYB-AM process. Three layers are deposited on a substrate plate, and subsequent subtractive machining is used to obtain the final net-shape.

2. The HYB-AM process

The material flow in the HYB-AM process is based on the principle of continuous rotary extrusion, also known as Conform extrusion (Green, 1972). The extrusion step serves a dual purpose in this new AM process: First, the feedstock is heavily deformed in the extruder and oxides present on the feedstock surface are dispersed into the extrudate. Secondly, the extruder provides the required pressure to obtain bonding at the interface between the extrudate and the underlying structure. Following the illustration in Fig. 2a, the extrusion pressure is created by the frictional force between the feedstock wire and the tapered groove of the rotating wheel. The wheel is sealed by a stationary housing provided with an abutment and a die. The feedstock is firmly pressed into the groove and driven forward by the rotation of the wheel. Subsequently, the feedstock wire is blocked by the abutment and an axial compression is induced, causing the material to yield and fill the entire cross-section. This, in turn,

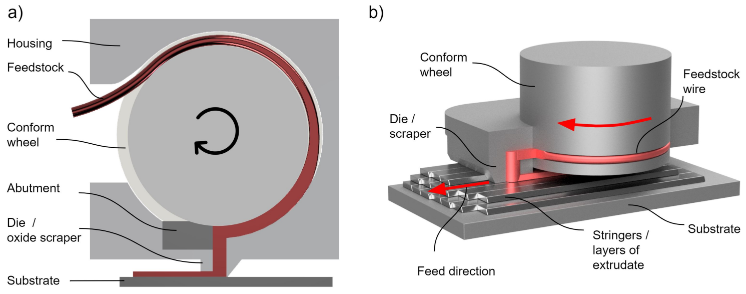

Figure 2: Principal illustrations of the HYB-AM extruder; (a) The extruder consists of a wheel with a groove surrounded by a stationary housing. The feedstock wire is pressed into the groove, and upon rotation the extrusion pressure is built up as the material is blocked by an abutment close to the die. The die also act as a scraper in order to remove oxides from the substrate prior to bonding with the extrudate; (b) Rendering of the extruder and a deposited structure.

increases the contact surface and friction, leading to further pressure build-up, ultimately causing the material to flow out of the die.

Fig. 2b illustrates the HYB-AM deposition sequence. A blank of aluminium is fixed onto a heated bed to act as a substrate upon which the material is deposited. The extruder adds material as it moves in the direction of deposition, placing stringers side-by-side to form a layer, allowing new layers to be added on top of each other. As deposition proceeds, the die-outlet is simultaneously scraping the top of the underlying layer and the side wall of the adjacent stringer to remove the oxide layer. This creates the required conditions for bonding with the extrudate to occur. The scraped material is accumulated on the die outlet and needs to be removed during processing. This accumulated material is considered loss and the scraping depth should therefore be minimized. The metal flow and the bonding mechanisms in the HYB-AM process are similar to those observed in longitudinal seam welds of porthole-die extrusions, where welds are formed under high pressure as material streams merge after flowing around the

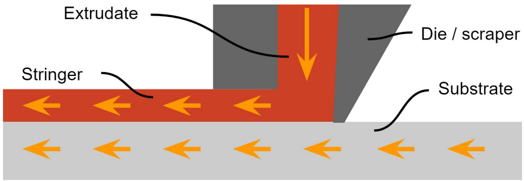

Figure 3: In HYB-AM bonding is achieved as the metal streams of the oxide free extrudate and the scraped substrate merges at pressures exceeding the flow stress of the materials.

die-bridges, as reviewed by Akeret (1992) and later by Valberg (2002). However, in the case of HYB-AM, the merging metal streams should be considered as mating streams of extrudate and substrate, as illustrated in Fig 3. For an HYB-AM deposited structure, the weld quality is crucial in order for the structure to be able to withstand tensile loads across layers. Hence, in the current development stage of the process it is of interest to further assess the bond strength.

3. Experimental

3.1. Equipment

The individual components of the extruder were produced from hardened Uddeholm Orvar Supreme tool steel. The extruder is depicted in Fig. 4. A Sieg SX3 CNC milling machine was used to control the speed and position of the extruder head. The rotation of the wheel is provided by a 1.8 kW servo motor connected to a gearbox with a gear reduction of 30. A PID-controller is used in combination with Nichrome heat-cartridges and a K-type thermocouple to control the temperature of the heated bed during deposition. The extruder house is, by the same means, pre-heated to reduce the flow stress of the feedstock material during extrusion. The experimental setup is depicted in Fig. 5 and some key data for the extruder are listed in Table 1.

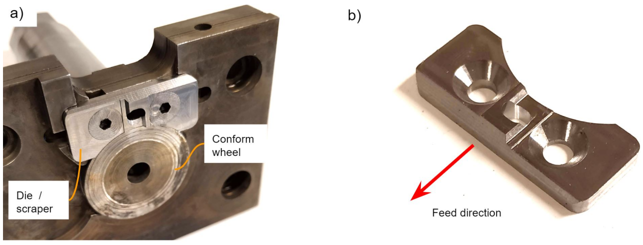
a)
Conform wheel
Die / scraper
b)
Feed direction

Figure 4: The current version of the extruder; (a) As seen from underneath; (b) The die that also is used to scrape the under-laying surfaces.

Table 1: Specifications for the HYB-AM extruder.

Parameter	Value
Wire diameter	1.6 mm
Max deposition rate	2150 g/h at 100 RPM
Outlet dimensions (w x h)	4 mm x 1 mm
Extruder wheel outer diameter	28 mm

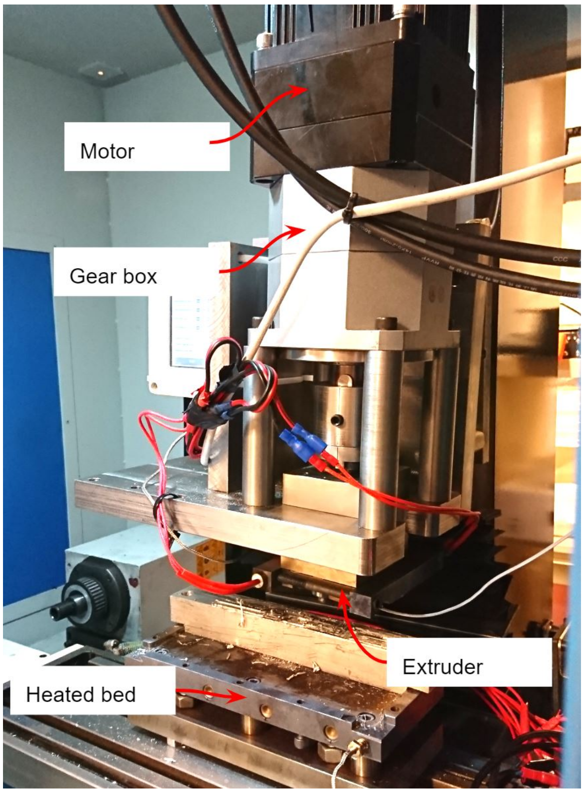
Motor
Gear box
Extruder
Heated bed

Figure 5: The extruder assembly attached to the CNC machine. A heated bed is used to control the temperature of the deposited structure.

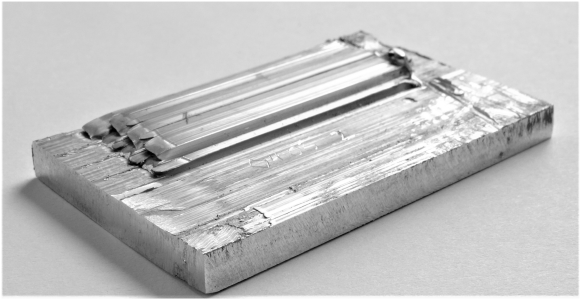

Figure 6: Photograph of a two-layered sample of AA6082 (4 + 3 stringers).

3.2. Materials and process parameters

Fig. 6 shows a two-layered structure deposited on a substrate material. The operational conditions are summarized in Table 2. The feedstock material was a Ø1.6 mm wire of the AA6082-T4 type, produced by HyBond AS. The wire was made from a DC cast billet, which was homogenized, hot extruded, cold drawn and shaved to the final diameter. 4 mm rolled plates of AA6082-T6 were used as substrate material. The rolling direction of the plate is parallel to the deposition direction. Table 3 gives the chemical composition of the AA6082 feedstock material and the substrate material.

Upon finished deposition, the samples were removed from the hot machine bed and immediately quenched in water. The samples were naturally aged at room temperature for two weeks to reach the relatively stable T4 condition prior to mechanical testing.

3.3. Mechanical testing

In order to sample the bond strength between the individual layers, a novel way of producing specimens for tensile testing was developed and applied. By using a single cutting thread mill, miniature specimens with a length constituting the height of two stringers could be machined into the sample. This allows

Table 2: Parameters used in the experimental setup.

Parameter	Value
Wheel rotation speed	4.0 RPM
Feed rate	185 mm/min
Deposition rate	110 g/h
Wheel torque	220 Nm
Extruder pre-heating temperature	300°C
Deposition temperature	500°C

Table 3: Chemical compositions of AA6082 feedstock wire (F) and substrate plate (S).

	Si	Mg	Cu	Fe	Mn	Cr	Zn	Ti	Zr	B	Other	Al
F	1.11	0.61	0.002	0.20	0.51	0.14	-	0.043	0.13	0.006	0.029	Balance
S	0.9	0.8	0.06	0.45	0.42	0.02	0.05	0.02	-	-	0.03	Balance

the bonding interface to be located in the region of the reduced section of the specimen, as depicted in Fig. 7. The number of tested specimens are shown in Table 4, while the locations are indicated in Fig 8a. The reduced section of the specimens has a length and a diameter of 1.0 mm and Ø0.52 mm, respectively, and a total length of 1.8 mm. A specifically designed split collar was used to grip the head of the specimens, while keeping the sample clamped to the lower section of the test machine, as shown in Fig7a. The total displacement and the load was measured on a MTS Criterion Model 42 ball screw universal testing machine, at a cross-head speed of 1 mm/min and a sampling frequency of 10 Hz.

Hardness measurements were made using a Mitutoyo Micro (HM200 series) Vickers hardness testing machine at a constant load of 1 kg. Six individual randomly located measurements were carried out for both the substrate and the extrudate for both sample sections.

The samples used for microstructural analyses were prepared according to standard preparation procedures. To reveal the macrostructure, the samples were immersed in a solution of 1% sodium hydroxide and water for 4 minutes.

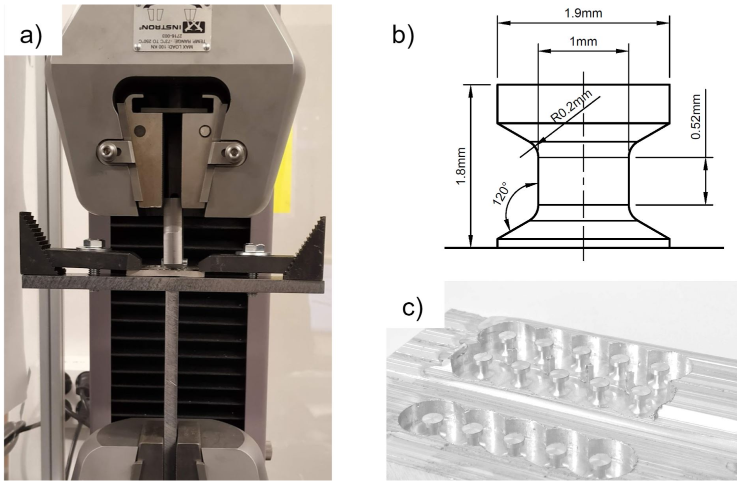

Figure 7: Tensile testing; (a) The tensile testing machine with a sample; (b) The geometry of a specimen; (c) Specimens used for testing of the substrate material and the layered structure.

Table 4: Overview of test samples and number of tests conducted.

	Description	No.
Sample 1	Tensile specimens, substrate	3
	Tensile specimens, layer interface	4
	Vickers hardness, deposited material	6
	Vickers hardness, substrate	6
Sample 2	Tensile specimens, substrate	4
	Tensile specimens, layer interface	4
	Vickers hardness, deposited material	6
	Vickers hardness, substrate	6

Macrographs were captured using an Olympus BX35M light microscope and an Alicona Confocal Microscope. Finally, fractographs were captured by a Quanta FEG 450 scanning electron microscope (SEM). The fracture surface examination was performed at an acceleration voltage of 20 kV.

4. Results and Discussion

The macrostructure of a transverse section of a sample is shown in Fig. 8. The interface between the substrate and the extrudate is clearly visible after etching, showing that the mating interfaces have merged into a fully dense material. Still, the etched section reveals some defects in the form of cracks, as depicted in Fig 8c and d, indicating variable bonding quality. Two possible reason for the crack formation can be: (1) Too low contact pressure during deposition, prohibiting full metallic contact between the merging interfaces, or: (2) Oxide formation on the interfaces during deposition due to exposure to oxygen. The latter being similar to that observed in longitudinal seam welds in porthole die extrusion when a gas pocket is present behind the bridge, as reported by Yu & Zhao (2018).

The mean tensile properties of all specimens are graphically presented in Fig. 9, showing that there is no significant difference in the ultimate tensile strength (UTS) of the layered material as opposed to the substrate material. Still, when considering the stress vs. displacement curve for one of the samples (Fig. 11), it is obvious that the elongation, and thus, the ductility is lower for the specimens covering the layer interface.

Fractographs of representative specimens (Fig. 10) furthermore confirms this behaviour. Fig. 10a clearly shows regions with lack of bonding. Fig. 10b represents the specimen with the highest elongation prior to fracture, and also here, regions of kissing-bond formation are visible. Still, extensive dimple formation is observed, indicating that metallic bonding is obtained (Fig. 10d and e).

Fig. 10c shows the comparable fractograph from a specimen made from the substrate material. The dimple formation (f) is similar to that observed for the

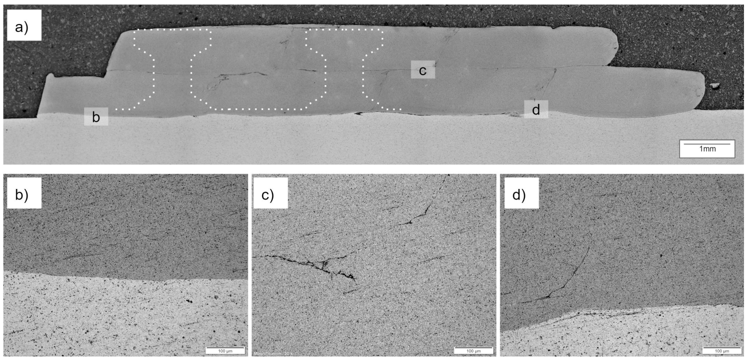

Figure 8: Optical micrographs of; (a) Section of a deposited structure along with the superimposed contours of the tensile specimens; (b) The bonding interface between the substrate and the first layer; (c) and (d) Voids observed at the interface between two stringers.

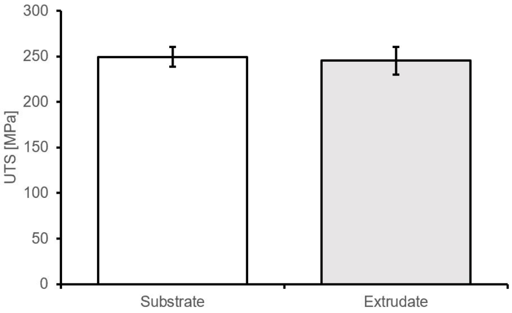

Figure 9: Ultimate tensile strength of the substrate material(n=7) and the bonded layers (n=8). The error bars represent the standard deviation of the measurements.

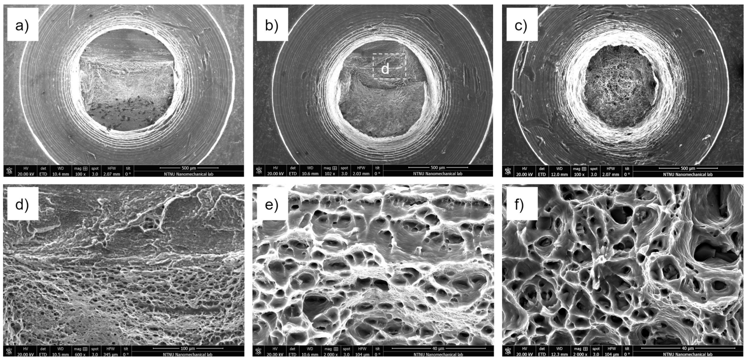

Figure 10: SEM fractographs of fracture surfaces from three broken specimens. The corresponding tensile test results are plotted in Fig. 11; (a) Fracture surface of specimen B3; (b) Fracture surface of specimen B4; (c) Fracture surface of substrate specimen S1; (d) Mixed region with kissing-bond and dimple formation in specimen B4; (e) Dimpled fracture surface observed in specimen B3, and; (f) Dimpled fracture surface observed in specimen S3.

layer interface. The difference in cross-section is also noticeable, reflecting a more ductile response of the substrate specimens, as shown by the tensile test data in Fig. 11.

The results from the transverse hardness measurements are presented in Fig 12. As can be seen from the figure, the hardness values are ∼12% lower for the substrate material compared to the extruded material. The higher hardness of the extruded material is believed to be the result of the high silisium content of the extruded material, which contributes to significant solid solution hardening, as pointed out by Callister et al. (2013). In addition, the extrudate contains the dispersoid-forming elements Mn, Cr and Zr. These elements prevent recrystallization during deposition and therefore facilitate the formation of a substructure in the bonded layers with a high dislocation density and thus higher hardness than that of the substrate material (Hatch, 1984).

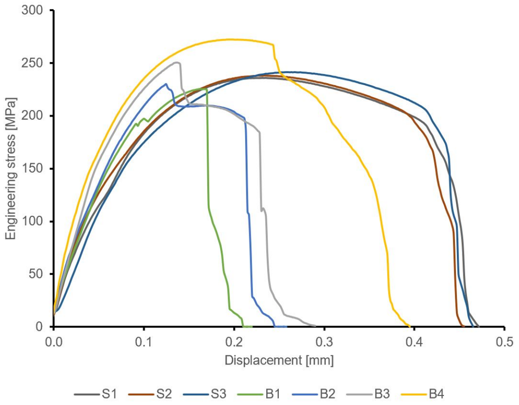

Figure 11: Engineering stress vs. displacement curves for different tensile specimens. Four specimens, B1-B4, crossing two bonded layers, and three specimens representing the substrate material, S1-S3.

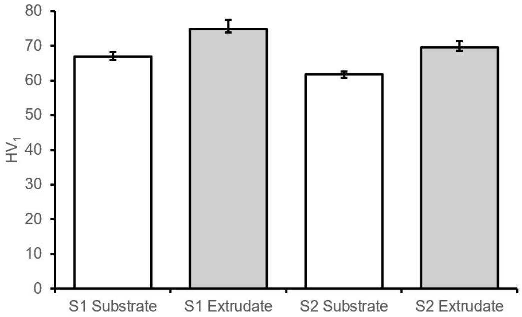

Figure 12: Measured Vickers hardness of different samples.

5. Conclusions

The main objective of this study has been to assess the bond strength between the individual stringers of a structure deposited by the HYM-AM process. In order to assess the layer-to-layer bond strength, a novel method for fabrication of tensile specimens has been developed and applied. The method allows miniature specimens to be cut into the sample with the layer interface located in the reduced section of the specimens. For this work the method allowed the strength between the layers to be tested in pure tension. The method is applicable for for other small sized samples where it is challenging to isolate specimens by other means, and future research should further assess this potential.

The results from the mechanical testing display an ultimate tensile strength of the bonded layers approaching that of the substrate material, yet at lower elongation prior to fracture. Moreover, inspections of the fracture surfaces showed evidence of extensive dimple formation, indicating that metallic bonding is achieved between the layers.

Through this work the technical feasibility of the HYB-AM process has been conclusively demonstrated in producing mechanically sound 3D structures. However, regions of kissing-bonds and lack of bonding are also present, thus calling for further process optimization.

Acknowledgements

The authors acknowledge the financial support from NTNU, NAPIC (NTNU Aluminium Product Innovation Center) and the KPN project Value sponsored by Research Council of Norway, Hydro and Alcoa.

References

Akeret, R. (1992). Extrusion welds-quality aspects are now center stage. In *Proceedings of the 5th International Aluminium Extrusion Technology Seminar, 1992*.

Blindheim, J., Grong, ., Aakenes, U. R., Welo, T., & Steinert, M. (2018). Hybrid Metal Extrusion & Bonding (HYB) - a new technology for solid-state additive manufacturing of aluminium components. *Procedia Manufacturing*, *26*, 782–789. URL: `https://linkinghub.elsevier.com/retrieve/pii/S2351978918307637`. doi:`10.1016/j.promfg.2018.07.092`.

Callister, W. D., Rethwisch, D. G., & others (2013). *Materials science and engineering: an introduction* volume 9.

Deshpande, A., & Hsu, K. (2018). Acoustoplastic metal direct-write: Towards solid aluminum 3d printing in ambient conditions. *Additive Manufacturing*, *19*, 73–80. URL: `https://linkinghub.elsevier.com/retrieve/pii/S2214860417300234`. doi:`10.1016/j.addma.2017.11.006`.

Dilip, J. J. S., Rafi, H. K., & Ram, G. J. (2011). A new additive manufacturing process based on friction deposition. *Transactions of the Indian Institute of Metals*, *64*, 27.

Green, D. (1972). Continuous extrusion-forming of wire sections. *J INST MET*, *100*, 295–300.

Hatch, J. (1984). *Aluminum: properties and physical metallurgy*. Materials Park (OH): American Society for Metals.

Martin, J. H., Yahata, B. D., Hundley, J. M., Mayer, J. A., Schaedler, T. A., & Pollock, T. M. (2017). 3d printing of high-strength aluminium alloys. *Nature*, *549*, 365–369. doi:`10.1038/nature23894`.

Palanivel, S., Nelaturu, P., Glass, B., & Mishra, R. (2015). Friction stir additive manufacturing for high structural performance through microstructural control in an Mg based WE43 alloy. *Materials & Design (1980-2015)*, *65*, 934–952. doi:`10.1016/j.matdes.2014.09.082`.

Schultz, J., & Creehan, K. (2014). System for continuous feeding of filler material for friction stir welding, processing and fabrication.

5

Valberg, H. (2002). Extrusion welding in aluminium extrusion. *International Journal of Materials and Product Technology*, *17*, 497–556.

White, D. R. (2003). *Ultrasonic consolidation of aluminum tooling* volume 161. ASM International.

Yu, J., & Zhao, G. (2018). Interfacial structure and bonding mechanism of weld seams during porthole die extrusion of aluminum alloy profiles. *Materials Characterization*, *138*, 56–66. doi:`10.1016/j.matchar.2018.01.052`.

Paper 6

metals

MDPI

Article

Investigating the Mechanics of Hybrid Metal Extrusion and Bonding Additive Manufacturing by FEA

Jørgen Blindheim *, **Torgeir Welo and Martin Steinert**

Department of Mechanical and Industrial Engineering, Norwegian University of Science and Technology, 7491 Trondheim, Norway
* Correspondence: jorgen.blindheim@ntnu.no; Tel.: +47-905-02-216

Received: 21 June 2019; Accepted: 18 July 2019; Published: 24 July 2019

Abstract: Hybrid Metal Extrusion & Bonding Additive Manufacturing (HYB-AM) is a hybrid manufacturing technology for the deposition of layered metal structures. This new deposition process is a complex metal forming operation, yet there is significant lack of knowledge regarding the governing mechanisms. In this work, we have used finite element analysis (FEA) to study material flow in the extruder, as well as the conditions at the interfaces of the deposited extrudate and the substrate, aiming to identify and characterize the process parameters involved. Analysis of the material flow shows that the extrusion pressure is virtually independent of the deposition rate. Furthermore, from the simulations of the material deposition sequence, it is clearly visible how the contact pressure at the interface will drop below the bonding threshold if the feed speed is too high relative to the material flow through the die. The reduced pressure also leads to the formation of a 'gas-pocket' inside the die, thus further degrading the conditions for bonding. The analyses of the process have provided valuable insights for the further development and industrialization of the process.

Keywords: additive manufacturing; conform extrusion; HYB-AM; aluminium alloys

1. Introduction

Hybrid Metal Extrusion and Bonding Additive Manufacturing (HYB-AM) is a new solid-state additive manufacturing process for the fabrication of layered 3D metal structures [1,2]. The process operates in the solid-state, meaning that defects associated with melting of the feedstock material are avoided. Furthermore, the low heat input enables high deposition rates when compared to the melted-state AM-process. The process is, therefore, particularly suitable for low-volume manufacturing of larger components where subtractive machining becomes inefficient due to low material utilization, or where forming or casting processes are disqualified due to high tooling costs.

In HYB-AM, the feedstock material is processed through a continuous rotary extruder, which serves the purpose of dispersing oxides and providing pressure for bonding to occur between the extrudate and the substrate. During operation, the die is scraping the substrate to remove surface oxides as the feedstock material is deposited in a stringer-by-stringer manner to form layers. The principle is illustrated in Figure 1. After deposition, the part needs to be post-processed by traditional subtractive machining to obtain the desired net-shape. The latest extruder design and samples produced by this process are shown in Figure 2.

Up until now, the research on the HYB-AM process has focused on concept development through physical modelling, along with full-scale experiments using AA6082 feedstock material, an Al-Mg-Si alloy mainly used for hot forming processes. The first full-scale experiments aimed at demonstrating the process on a proof-of-concept level and exploring the potential of the process [3]. More recently, a full-scale experiment was carried out to assess the mechanical integrity of a deposited structure [4]. Microscopy analyses show that fully dense bonding interfaces can be achieved, though some voids can be observed between the individual stringers. Observations of fracture surfaces reveal areas of full metallic bonding; however, regions of kissing-bonds and lack of bonding are also visible. Through these full-scale experiments, the HYB-AM process has demonstrated its proof-of-concept and capability for processing advanced aluminium alloys. Nevertheless, this process is a complex metal forming operation, and the governing mechanisms need to be better understood in order to optimize the process towards industrialization.

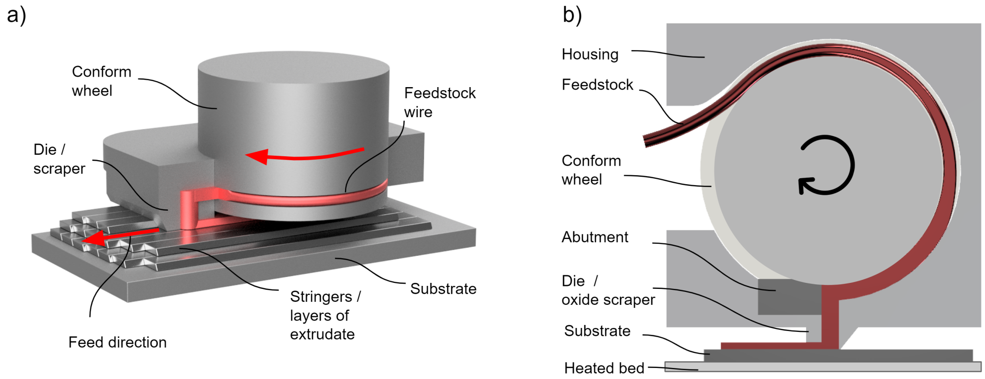

Figure 1. The extruder consists of a wheel with a groove surrounded by a stationary housing. The feedstock wire is pressed into the groove, and upon rotation the extrusion pressure is built up as the material is blocked by an abutment close to the die. The die also acts as a scraper in order to remove oxides from the substrate prior to bonding with the extrudate. (**a**) principal illustrations of the hybrid metal extrusion & bonding additive manufacturing (HYB-AM) extruder; (**b**) rendering of the extruder and a deposited structure.

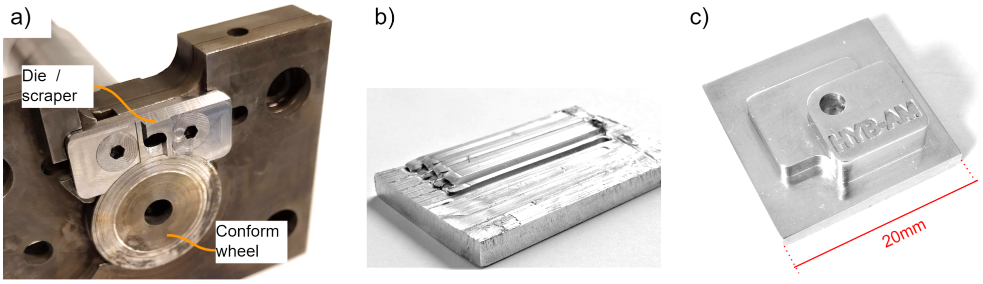

Figure 2. Full-scale demonstration of the HYB-AM process. (**a**) the extruder prototype; (**b**) two layers (4 + 3 stringers) of AA6082 deposited on a substrate of the same alloy; (**c**) net-shape demo sample after post-processing by subtractive machining.

In this study, we have applied finite element analysis (FEA) using commercially available Deform 3D software to analyse and interpret some of the governing mechanisms of the process. The following objectives are covered: (1) to study the material flow in the extruder with regard to extrusion grip length, contact pressure, peak temperatures and strain-rates at steady-state for two different deposition rates; (2) to investigate the thermo-mechanical conditions for the bond interface between the extrudate and the substrate with regard to the obtained contact pressure at different ratios between extrusion flow rate and feed speed.

The remainder of this paper is organized as follows: The next section provides an introduction to the working principles of the HYB-AM process. Section 3 presents the FEM-models and simulation parameters used throughout the study. Section 4 presents the results from the simulations, while Section 5 discusses the results. Conclusions are given in Section 6.

2. The HYB-AM Process

The pressure-generating mechanism in the HYB-AM extruder is based on the principle of continuous rotary extrusion (CRE), also known as Conform extrusion [5,6]. Over the past several decades, the CRE process has been subjected to multiple studies, covering the range of Al, Cu, Mg and Ti alloys [7–11]. More recently, as FEM-modelling has become a viable tool for this type of problems, several studies have validated the relationships between simulations and full-scale experiments. Kim et al. [12] used numerical simulation to identify optimal process parameters for CRE. Hodek and Zemko [13] studied CRE of titanium through experiments and simulations. Valberg et al. [14] have used FEA to study the early stages of CRE using aluminium feedstock, while Rajendran et al. have simulated processing of AA3003 [15] and magnesium alloy AZ91 [16].

Following the illustration in Figure 1b, the extrusion pressure is created by the frictional force between the feedstock wire and the tapered groove of the rotating wheel. The wheel is sealed by a stationary housing provided with an abutment and a die. The feedstock is firmly pressed into the groove and driven forward by the rotation of the wheel. Subsequently, the feedstock wire is blocked by the abutment and axial compression is induced, causing the material to yield and fill the entire cross-section. This, in turn, increases the contact surface and friction, leading to further pressure build-up, ultimately causing the material to flow out of the die.

Figure 1a illustrates the HYB-AM deposition sequence. A blank of aluminium is fixed on a heated bed to act as a substrate upon which the material is deposited. The extruder adds material as it moves in the direction of deposition, placing stringers side-by-side to form a layer, and allowing new layers to be added on top of each other. As deposition proceeds, the die-outlet is simultaneously scraping the underlying layer and the side wall of the adjacent stringer to remove the oxide layer. This creates the required conditions for bonding with the extrudate to occur. The metal flow and the bonding mechanisms in the HYB-AM process are similar to those observed in longitudinal seam welds of porthole-die extrusions, where welds are formed under high pressure as material streams merge after flowing around the die-bridges [17–20]. However, unlike porthole-die extrusions, in the case of HYB-AM, the merging metal streams should be considered as mating streams of extrudate and substrate.

3. Materials and Methods

3.1. FEM-Models

The CAD files for the FEM-models were prepared in Fusion 360 (V2.0, Autodesk, San Rafael, CA, USA). The overall design is similar to that of the parts used for the full-scale experiments (Figure 2), except for the geometry being modified such that an interference is added between all moving parts to prevent loss of nodes during simulations. The FEM analysis is conducted in Deform 3D software (V11.3, Scientific Forming Technologies Corporation, Columbus, OH, USA).

Full-scale experiments on the HYB-AM process have been conducted on AA6082 feedstock material. For the FEM-analysis, the flow stress data for AA6082, as a function of strain and temperature for various strain rates, were obtained from the material library in the software, which is based on [21]. Figure 3 presents the flow stress curves for the temperature range 300 °C to 500 °C for strain rates of 0.3 s^{-1}, 10 s^{-1}and 100 s^{-1}.

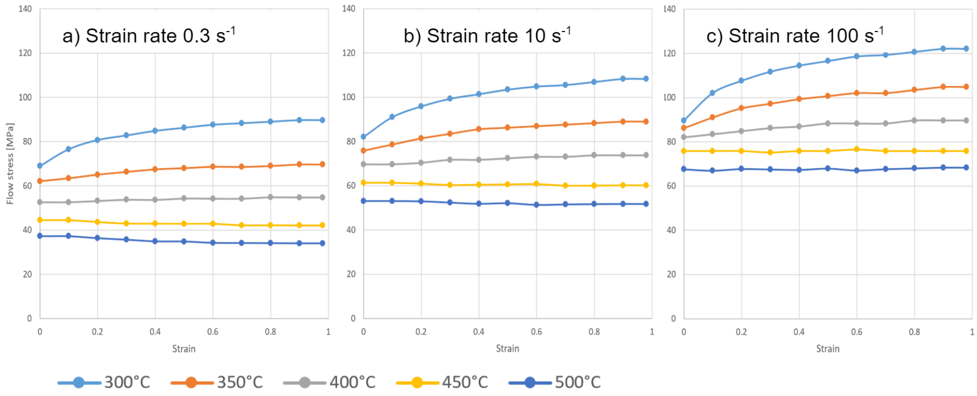

Figure 3. Material data for AA6082 at in the range 300°C to 500°C for strain rates: (**a**) $0.3s^{-1}$, (**b**) $0.3s^{-1}$ and (**c**) $100s^{-1}$. Data is obtained from Deform 3D material library based on [21].

3.2. Model 1: Extrusion Pressure Generating Mechanism

The numerical model of the extruder consists of the housing, the conform wheel and the feedstock material, as depicted in Figure 4. The abutment and the die geometry is merged with the housing to simplify meshing of the FEM-model.

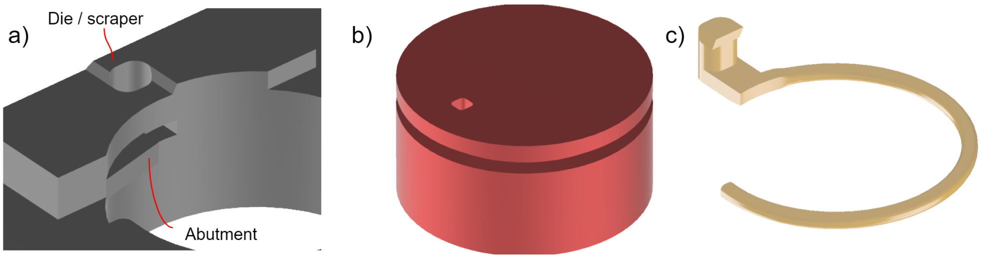

Figure 4. The geometry used for finite element method (FEM) model 1 as seen from below. (**a**) the housing, merged with the die and the abutment; (**b**) the conform wheel; (**c**) the feedstock wire.

Referring to the first objective (1), our investigations aim to observe the material flow at steady-state conditions. The simulations were, therefore, initiated with a filled chamber and die, but with the extrusion grip length shorter than what expected to be seen at steady-state. The feedstock wire is partially formed to the shape of the groove in the wheel, yet it has the same cross-section as that of the Ø1.6 mm feedstock wire, see Figure 5a. The surface area in contact with the groove walls and the wall of the housing is shown in Figure 5b. A rigid surface is modeled to represent the substrate at the die outlet in order to obtain extrusion pressures at the same magnitude as that achieved during deposition.

Two different simulations have been carried out for model 1, where the angular velocity of the wheel is the only parameter subjected to change. The Tresca friction model is used for modelling contact friction; $\tau = m \cdot k$, [22], where τ is the frictional stress, m is the friction factor and k is the shear yield stress. The friction factor between the feedstock material and the tooling was kept arbitrary high, $m = 2$, to ensure sticking friction condition with no sliding. The feedstock is modelled as a rigid-plastic material and the tooling is modelled as a rigid surface. A heat transfer coefficient of 11(N/s)/(mm/c) is applied for the contact between the feedstock and the tool parts. The meshes are shown in Figure 6 and the complete set of simulation parameters can be found in Table 1.

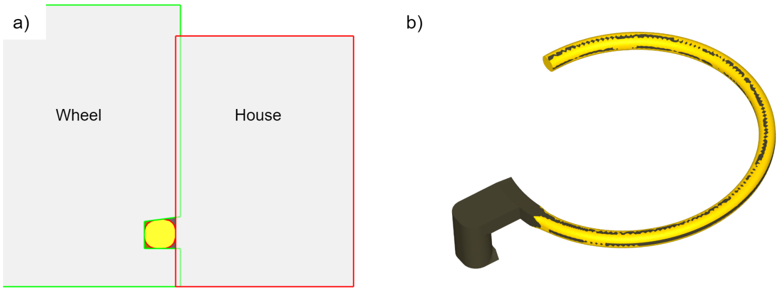

Figure 5. The initial contact between the feedstock material and the tooling for model 1. (**a**) section through the wheel and housing; (**b**) the feedstock with indication of contact points.

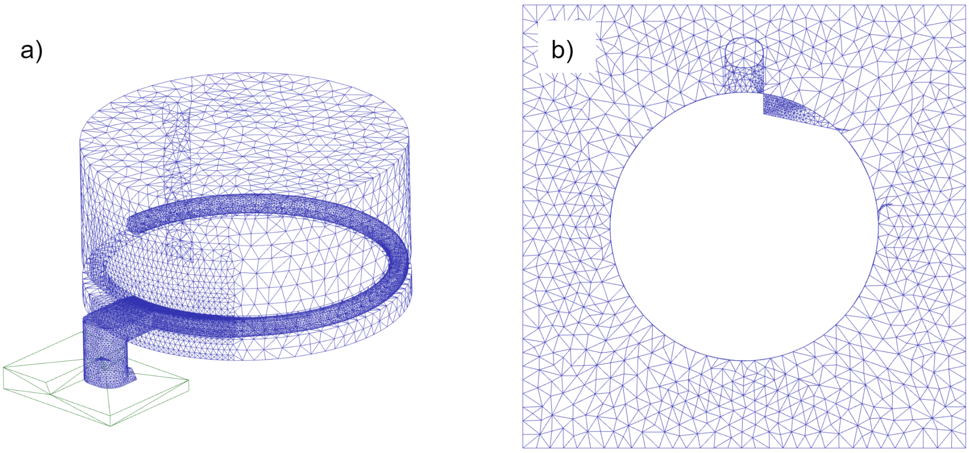

Figure 6. The meshes used for model 1. The meshes are refined in the plastic zone where the strain rates are at the highest. (**a**) the wheel and the feedstock material; (**b**) the housing.

3.3. Model 2: Stringer Deposition Sequence

A separate model has been made to study the material flow and normal pressure at the interface between the die outlet and the substrate. In this model, both the substrate and the feedstock are modelled using a rigid-plastic material representation. The components used in this model are shown in Figure 7, and the simulation parameters are listed in Table 2. The material supply in this model is simplified by the direct extrusion principle where a billet of feedstock is placed in a container and a ram is used to generate the material flow. The substrate model resembles the shape of multiple preceding layers and some stringers of the current layer. The substrate is fixed on a rigid bed, which can move along the feed axis. For the two simulations carried out for model 2, the feed speed is kept constant while the speed of the ram is altered.

Table 1. Parameters used in finite element method (FEM)-model 1.

Parameter	Parameter	Value
General	Pin diameter	28 mm
	Feedstock wire diameter	1.6 mm
	Heat transfer coefficient feedstock/tooling	11(N/s)/(mm/c)
	Simulation type	Lagrangian Deformation & Heat transfer
	Mesh type	Tetrahedral
House	Initial temperature	300 °C
	Material	AISI-H13
	Friction factor against feedstock, m	2
	Initial mesh elements/nodes	48,031/10,844
	Mesh refinement in plastic zone	0.07
	Mesh refinement die	0.25
Wheel	Initial temperature	300 °C
	Material	AISI-H13
	Friction factor against feedstock, m	2
	Initial mesh elements/nodes	29,690/6734
	Mesh refinement in plastic zone	0.1
	Rotational speed	4 RPM/50 RPM
Feedstock	Initial temperature	300 °C
	Material	AA6082
	Initial mesh elements/nodes	124,837/28,375
	Mesh refinement in plastic zone	0.5
	Friction factor against feedstock, m	2
Substrate	Initial temperature	300 °C
	Material	AISI-H13
	Friction factor against feedstock, m	0

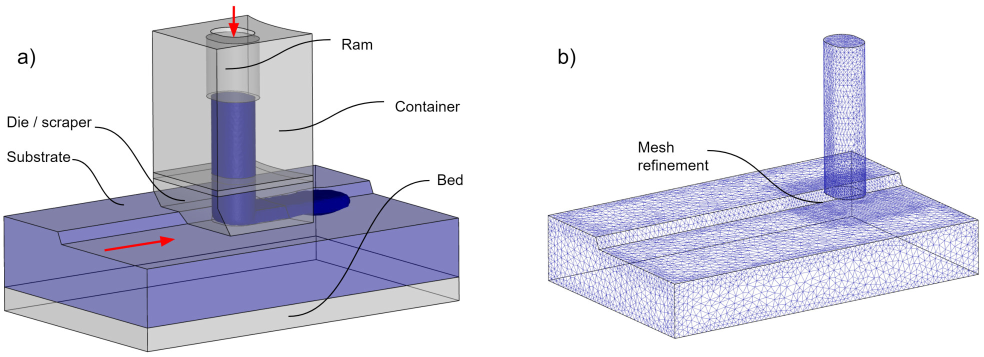

Figure 7. FEM model 2. (**a**) the material deposition is controlled by the ram speed and the horizontal movement of the substrate; (**b**) the initial mesh of the feedstock and the substrate with mesh refinement at the joining interface.

Table 2. Parameters used in FEM-model 2.

Parameter	Parameter	Value
General	Simulation type Mesh type	Lagrangian Deformation Tetrahedral
Feedstock	Material Temperature Initial mesh elements/nodes Mesh refinement	AA6082 500 °C 33,261/7379 0.2
Substrate	Material Temperature Initial mesh elements/nodes Mesh refinement Contact condition feedstock Friction factor against feedstock, m	AA6082 500 °C 79,710/17,714 0.35 non-separable 2
Die	Friction factor against feedstock, m Friction factor substrate, m Inlet cross-section area Outlet cross-section area	2 0 10.5 mm^2 3.5 mm^2
Ram	Speed, Balanced/High	1.0/1.2 mm/s
Container	Friction factor against feedstock, m	0
Bed	Friction factor substrate, m Feed delay Speed in feed direction	2 1 s 3.0 mm/s

4. Results

4.1. Model 1

Simulations for model 1 have been carried out at two different rotational speeds of the extruder, 4 RPM and 50 RPM, where the former being the setting used for prior full-scale experiments [4].

Figure 8 shows the length of the extrusion grip zone for the initial condition (a) and for steady-state for the two rotational speeds considered in the study (b and c). In the primary grip zone of CRE, the wire should be firmly fixed in the groove in order to induce compressive stresses, leading to upsetting of the material and thus establishment of the extrusion grip zone. Despite the difference in rotational speed, the extrusion grip lengths are of the same magnitude for Figure 8b,c. Figure 9 shows the total velocity of the feedstock material and the wheel, confirming that the wire has the same velocity as the wheel in the primary grip zone.

A contour plot of the strain-rates is shown in Figure 10 for both rotational speeds subjected to analysis. At 50 RPM, the flow stress is expected to increase due to the increased strain-rates; however, the temperature also increases, as depicted in Figure 11. It is observed that at 4 RPM the temperature peaks at 330 °C, while at 50 RPM the temperature reaches 550 °C.

Figure 12 illustrates the contact pressure between the feedstock material and the walls of the groove and the housing. For both rotational speeds, the contact pressure is at the same level, despite the difference in flow rate.

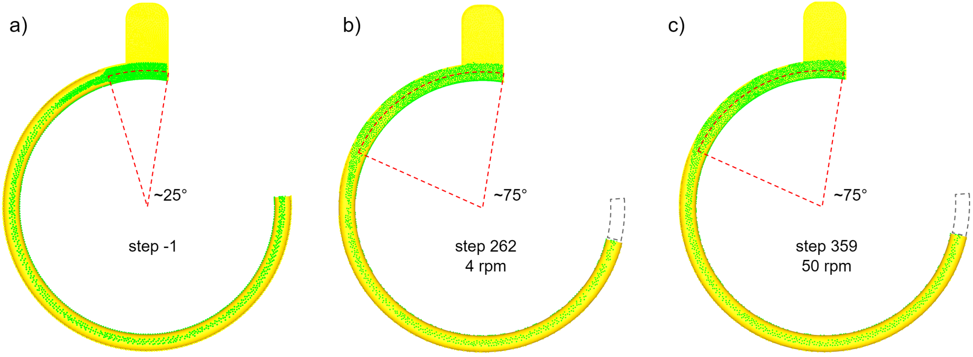
a)
~25°
step -1
b)
~75°
step 262
4 rpm
c)
~75°
step 359
50 rpm

Figure 8. The feedstock material and the nodal contact points at steady-state for different rotational speeds. (**a**) the initial extrusion grip length in the extruder; (**b**) extrusion grip length at 4 RPM; (**c**) extrusion grip length at 50 RPM is similar to that of 4 RPM.

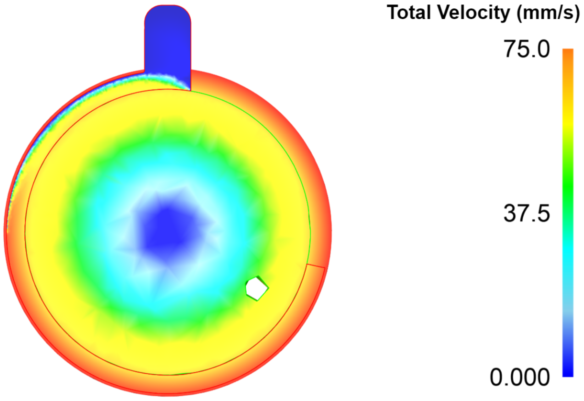

Figure 9. Section through the groove of the conform wheel displaying maximum element velocity at 50 RPM. The feedstock wire has the same velocity as the wheel in the primary grip zone. In the extrusion grip zone, the feedstock is stationary as it sticks to the wall of the housing, whereas at the inner wall of the groove the material has the velocity of the wheel.

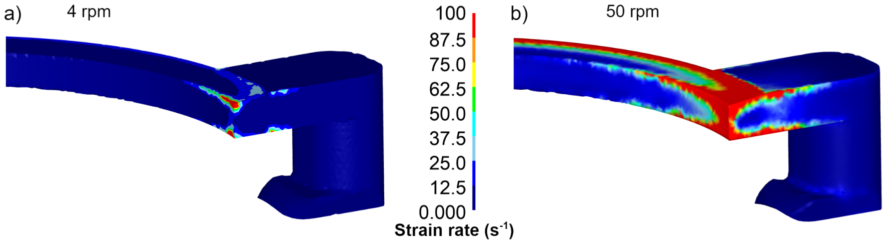
a)
4 rpm
100
87.5
75.0
62.5
50.0
37.5
25.0
12.5
0.000
Strain rate (s^{-1})
b)
50 rpm

Figure 10. Strain rates in the extrusion grip zone. (**a**) rotational speed 4 RPM; (**b**) rotational speed 50 RPM.

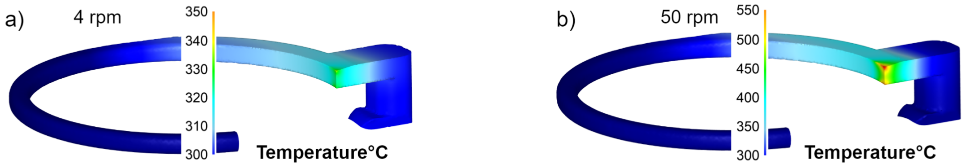

Figure 11. Temperature level in the extrusion grip zone. (**a**) rotational speed 4 RPM; (**b**) rotational speed 50 RPM.

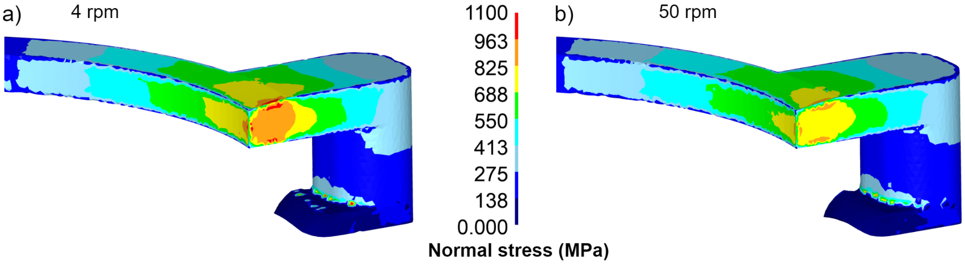

Figure 12. Normal pressure in the extrusion grip zone. (**a**) rotational speed 4 RPM; (**b**) rotational speed 50 RPM.

4.2. Model 2

The only parameter subjected to change in model 2 is the ratio between the ram speed and the feed speed. At a balanced ratio, the volumetric flows at both the inlet and the outlet (the rear opening between the substrate and the die) are equal, whereas at high speed the inlet flow is increased by 20% through increased ram speed. In the simulations, the ram is moved for one second to have the extrudate fill the die cavity prior to moving the bed.

Figure 13 illustrates the effective stress for the balanced and high ratios of ram vs. feed speed, respectively. For the balanced ratio, it can be seen that after 1.2 s the section of the die cavity is completely filled (Figure 13a). However, as deposition proceeds, a pocket is formed in the front part of the die (Figure 13b). For the high ratio (Figure 13c,d), the plastic region of the substrate is higher than for the balanced ratio after 1.2 s, and the stress levels have further increased after 5 s.

For solid-state bonding to occur in the absence of surface oxides, the normal stress at the bonding interface must exceed the instantaneous flow stress of the material. Referring to Figure 14, the strain rate of the extrudate in contact with the substrate is in the range of 0 to 7 s^{-1}. For the actual temperatures and strain rates, the flow stress of the material is less than 50 MPa (Figure 3). When adding a margin of 10%, the bonding threshold can be estimated to 55 MPa.

Figure 15 illustrates the normal stress in a section through the die, perpendicular to the deposition direction. For the balanced speed ratio, the normal stresses exceed 55 MPa only in the centre part of the die, whereas, for the high ratio, the full width of the stringer is subjected to contact stresses above the estimated bonding threshold.

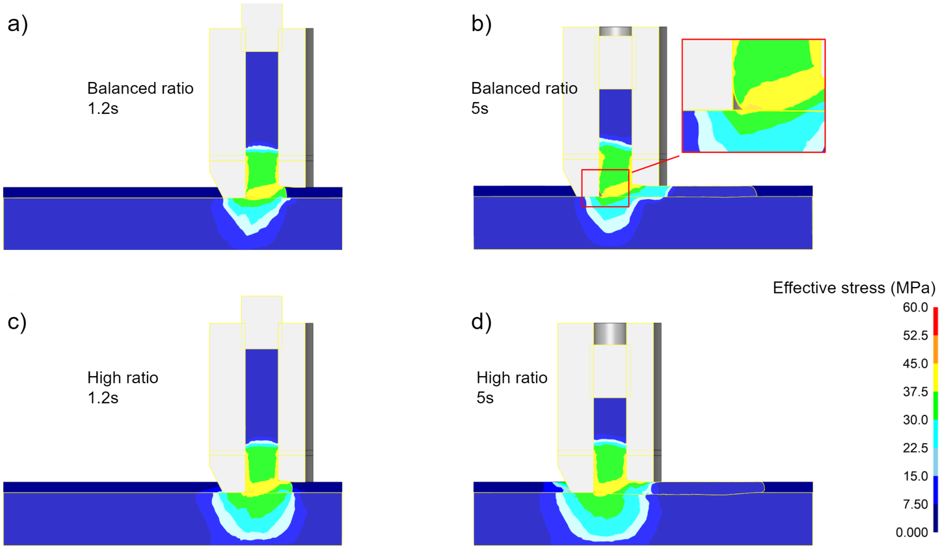
a)
Balanced ratio
1.2s
b)
Balanced ratio
5s
c)
High ratio
1.2s
d)
High ratio
5s
Effective stress (MPa)
60.0
52.5
45.0
37.5
30.0
22.5
15.0
7.50
0.000

Figure 13. Effective stress during deposition at 500 °C. (**a**) balanced ratio; after 1.2 s the die cavity is filled and the feeding has started; (**b**) balanced ratio; after 5 s a pocket is formed in the front section of the die; (**c**) high ratio; after 1.2 s, the die cavity is filled; (**d**) high ratio; after 5 s, the die cavity is still full and the effective stress has increased.

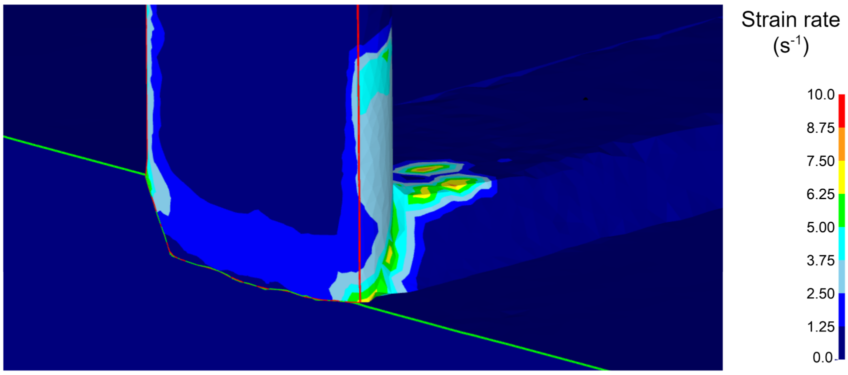
Strain rate
(s-1)
10.0
8.75
7.50
6.25
5.00
3.75
2.50
1.25
0.0

Figure 14. Strain rate at the bonding interface. The strain rates are in the range of 0 to 7 s^{-1}.

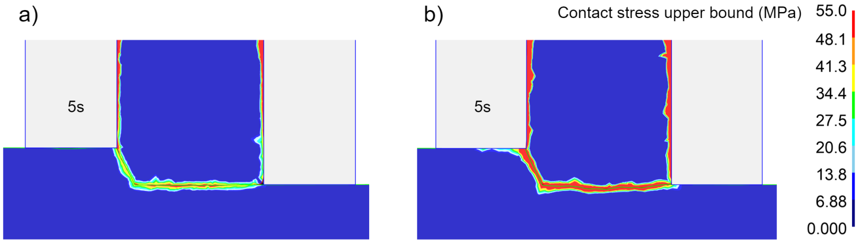
a)
5s
b)
Contact stress upper bound (MPa)
5s
55.0
48.1
41.3
34.4
27.5
20.6
13.8
6.88
0.000

Figure 15. Normal pressure in a section through the die transverse to the feed direction. (**a**) balanced speed ratio; (**b**) high speed ratio, 20% over-extrusion.

5. Discussion

Through the simulations presented herein, new knowledge and understanding of the HYB-AM process have been gained. These new insights will be valuable in the further development and industrialization of the process.

For the pressure-generating mechanism, it is observed that the strain rates in the plastic zone increase at high rotational speeds. However, the temperatures also increase as a result of (adiabatic) heating due to deformation work. This temperature increase, in turn, reduces the flow stress of the material, and, despite the higher strain-rate, the length of the extrusion grip zone remains virtually unchanged. Furthermore, from the provided results, it is clear that there is no significant increase in contact pressures at higher deposition rates. This means that future experiments can utilize higher flow rates without putting excessive loads on the extruder.

Moreover, it is of interest to observe that the wheel diameter; i.e., the length of the Conform slot can be considered sufficiently long for any extrusion speed. Still, the current extruder design has a limitation in the maximum allowable flow rate due to high peak temperatures in the plastic zone. The simulations show that the temperature increases from the initial pre-heating temperature of 300 °C up to 550 °C in the plastic zone.

From model 1, it is seen how the extrusion grip zone is established. When using feedstock material with a smaller cross-sectional area than that of the groove, the length of the extrusion grip zone will vary depending on the extrusion pressure. A change in the conditions at the die outlet will call for a change in pressure, and, thus, the extrusion grip length will have to adapt accordingly. Since the feedstock material is supplied at a constant speed, the flow rate out of the die will be subjected to reduced flow while the extrusion grip length is increased. This implies that the process is vulnerable to fluctuations in the flow rate and pressures. However, by filling the entire cross-section in the grip zone by means of a coining wheel, the process will respond better to changes in pressures. This can also be beneficial in terms of reduced heat generation, as the slip in the extrusion grip zone will be reduced similarly.

The aim of the simulations carried out in this study has been to analyse and interpret some of the governing mechanisms of the process that are difficult to observe through physical experiments. The relationships between FEA and full-scale experiments for the CRE process have previously been validated through numerous studies by others. Hence, these results provide reliable input for the further process development. For the bonding interface between the extrudate and the substrate, future experiments need to be conducted to further validate the results. However, when briefly comparing to the observations from the prior full-scale experiments, it was observed that the material deposition sequence has been modelled adequately. Figure 16 represents a section of the sample depicted in Figure 2b and is included for reference. This sample was deposited at a rotational speed of 4 RPM and the same feed speed as that used in the simulations presented. For the first stringer, the volumetric flow was set at a level corresponding to that of the high ratio, whereas a balanced ratio was used for the subsequent stringers. Defects in the form of cracks and pores are visible on this sample and indicate substandard bond quality. The FEA results clearly show the importance of using a correct deposition rate vs. feed speed. If the extruder fails to deliver the correct volumetric flow, the contact pressure at the interface will drop below the bonding threshold, resulting in substandard samples. From the simulations, it is also visible that a ’gas-pocket’ is formed inside the die in this case. When the scraped surface of the substrate is exposed to the conditions inside this pocket, a new oxide layer can be formed, thus reducing the layer bonding quality.

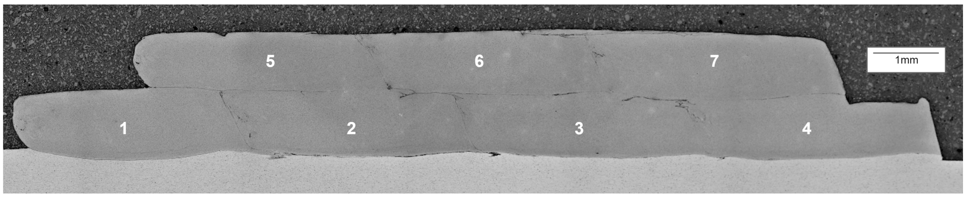

Figure 16. Section through the sample shown in Figure 2b with deposition order of the individual stringers indicated. The structure is almost fully dense, yet some pores and areas with lack of bonding are present.

6. Conclusions

Based on the FEA results obtained in this study, the following conclusion can be made for the pressure-generating mechanism:

1. Increased angular velocity of the wheel both increases the strain rates and the heat generation due to the higher deformation work.
2. The simulations show that the contact pressure inside the plastic zone is virtually similar at 4 RPM and 50 RPM. For the current design, the maximum deposition rate will be 1 kg/h when the extruder, as well as the substrate material, is pre-heated to 300 °C.
3. The length of the extrusion grip zone is not affected by an increased deposition rate.

Furthermore, from interpretations of the FEA models for the bonding interface between the substrate and the extrudate, the following conclusions can be drawn:

4. In order to obtain sufficient contact pressure for bonding to occur across the full stringer width, the input flow rate needs to be higher than the actual flow out of the rear opening of the die.
5. When the feed speed becomes too high relative to the material flow through the die, a gas pocket is formed in the outlet. This gas pocket can cause oxidation of the scraped surface with reduced bonding quality as a consequence.

Author Contributions: Formal analysis, J.B.; Methodology, J.B. and T.W.; Project administration, M.S.; Supervision, T.W. and M.S.; Visualization, J.B.; Writing—original draft, J.B., T.W. and M.S.

Funding: This research was funded by the KPN project Value, sponsored by the Research Council of Norway, Hydro and Alcoa.

Acknowledgments: The authors acknowledge the support from NAPIC (NTNU Aluminium Product Innovation Center). They are also indebted to Henry Valberg for valuable assistance.

Conflicts of Interest: The authors declare no conflict of interest.

Abbreviations

The following abbreviations are used in this manuscript:

AM	Additive Manufacturing
CRE	Continuous Rotary Extrusion
FEM	Finite Element Method
FEA	Finite Element Analysis

References

1. Blindheim, J.; Grong, Ø.; Aakenes, U.R.; Welo, T.; Steinert, M. Hybrid Metal Extrusion & Bonding (HYB)—A new technology for solid-state additive manufacturing of aluminium components. *Procedia Manuf.* **2018**, *26*, 782–789. [CrossRef]
2. Blindheim, J.; Welo, T.; Steinert, M. Rapid prototyping and physical modelling in the development of a new additive manufacturing process for aluminium alloys. *Procedia Manuf.* **2019**, *34*, 489–496. [CrossRef]

3. Blindheim, J.; Welo, T.; Steinert, M. First demonstration of a new additive manufacturing process based on metal extrusion and solid-state bonding. *Int. J. Adv. Manuf. Tech.* **2019**, under review.
4. Blindheim, J.; Grong, Ø.; Welo, T.; Steinert, M. On the mechanical integrity of AA6082 3D structures deposited by hybrid metal extrusion & bonding additive manufacturing. *J. Mater. Process. Technol.* **2019**, under review.
5. Green, D. Continuous extrusion-forming of wire sections. *J. INST MET* **1972**, *100*, 295–300.
6. Etherington, C. Conform—A new concept for the continuous extrusion forming of metals. *J. Eng. Ind.* **1974**, *96*, 893–900. [CrossRef]
7. Song, L.; Yuan, Y.; Yin, Z. Microstructural Evolution in Cu-Mg Alloy Processed by Conform. *Int. J. Nonferrous Metall.* **2013**, *2*, 100–105. [CrossRef]
8. Thomas, B.M.; Derguti, F.; Jackson, M. Continuous extrusion of a commercially pure titanium powder via the Conform process. *Mater. Sci. Technol.* **2017**, *33*, 899–903. [CrossRef]
9. Mitka, M.; Misiolek, W.Z.; Lech-Grega, M.; Gawlik, M.; Bigaj, M.; Szymanski, W. Continuous rotary extrusion of magnesium alloy AZ 91. In Proceedings of the Conference: Materials Science & Technology 2015, Columbus, OH, USA, 4–8 October 2015; p. 7.
10. Mitka, M.; Gawlik, M.; Bigaj, M.; Szymanski, W. Continuous Rotary Extrusion (CRE) of Flat Sections from 6063 Alloy. *Key Eng. Mater.* **2015**, *641*, 183–189. [CrossRef]
11. Ji, X.; Zhang, H.; Luo, S.; Jiang, F.; Fu, D. Microstructures and properties of Al–Mg–SI alloy overhead conductor by horizontal continuous casting and continuous extrusion forming process. *Mater. Sci. Eng. A* **2016**, *649*, 128–134. [CrossRef]
12. Kim, Y.H.; Cho, J.R.; Jeong, H.S.; Kim, K.S.; Yoon, S.S. A study on optimal design for CONFORM process. *J. Mater. Process. Technol.* **1998**, *80*, 671–675. [CrossRef]
13. Hodek, J.; Zemko, M. FEM Model of Continuous Extrusion of Titanium in DEFORM Software. In Proceedings of the 2nd International Conference on Recent Trends in Structural Materials, Parkhotel Plzen, Czech Republic, 21–22 November 2012; p. 7. Available online: http://comat2014.tanger.cz/files/proceedings/11/reports/1326.pdf (accessed on 5 May 2019).
14. Valberg, H.; Rajendran, N.; Misiolek, W. The Mechanics of the Continuous Rotary Extrusion Process Investigated by FEM analysis. In Proceedings of the Eighth International Conference On Advances in Mechanical, Aeronautical and Production Techniques-MAPT 2018, Kuala Lumpur, Malaysia, 3–4 February 2018; pp. 1–7. [CrossRef]
15. Rajendran, N.; Valberg, H.; Misiolek, W.Z. The FEM simulation of continuous rotary extrusion (CRE) of aluminum alloy AA3003. *Aip Conf. Proc.* **2017**, 050004. [CrossRef]
16. Rajendran, N.; Mitka, M.; Lech-Grega, M.; Misiolek, W.Z. Effect of tool geometry on the velocity and strain rate fields in continuous rotary extrusion of magnesium AZ91 alloy. *Procedia Manuf.* **2018**, *15*, 264–271. [CrossRef]
17. Akeret, R. Extrusion welds-quality aspects are now center stage. In Proceedings of the 5th International Aluminium Extrusion Technology Seminar, Chicago, IL, USA, 19–22 May 1992.
18. Valberg, H. Extrusion welding in aluminium extrusion. *Int. J. Mater. Prod. Technol.* **2002**, *17*, 497–556. [CrossRef]
19. Yu, J.; Zhao, G. Interfacial structure and bonding mechanism of weld seams during porthole die extrusion of aluminum alloy profiles. *Mater. Charact.* **2018**, *138*, 56–66. [CrossRef]
20. Yu, J.; Zhao, G.; Chen, L. Analysis of longitudinal weld seam defects and investigation of solid-state bonding criteria in porthole die extrusion process of aluminum alloy profiles. *J. Mater. Process. Technol.* **2016**, *237*, 31–47. [CrossRef]
21. Heinemann, H. Flow Stress of Different Aluminum and Copper Alloys for High Strain Rates and Temperature. Ph.D. Thesis, TH Aachen, Aachen, Germany, 1961.
22. Valberg, H.S. *Applied Metal Forming*; Cambridge University Press: Cambridge, UK, 2006.

© 2019 by the authors. Licensee MDPI, Basel, Switzerland. This article is an open access article distributed under the terms and conditions of the Creative Commons Attribution (CC BY) license (http://creativecommons.org/licenses/by/4.0/).